THEORETICAL STUDY OF
HEAT DISTRIBUTION AND SURFACE TEMPERATURES
GENERATED IN OSCILLATING CONTACT

by

Ser Jee Foo

Thesis submitted to the Faculty of the

Virginia Polytechnic Institute and State University

in partial fulfillment of the requirements for the degree of

Master of Science

in

Mechanical Engineering

APPROVED:

Brian Vick, Chairman

Michael J. Furey

Douglas J. Nelson

January 1990

Blacksburg, Virginia

THEORETICAL STUDY OF HEAT DISTRIBUTION AND SURFACE TEMPERATURES GENERATED IN OSCILLATING CONTACT

by

Ser Jee Foo

Brian Vick, Chairman

Mechanical Engineering

(ABSTRACT)

The objective of this study was to formulate a theoretical model and to develop an efficient and accurate solution method to predict the distribution of frictional heat and resulting temperature rise for simple systems with sliding contact. The solution method developed is a variation of the boundary integral equation method (BIEM) in which a moving, full-space Green's function is used as the fundamental solution. The numerical characteristics and limitations for the solution method are presented, as well as the physical parameters that affect the surface temperature rise. The analysis includes an arbitrary sliding velocity, with special focus on oscillating and unidirectional motion. Since the real contact area is extremely important, the theoretical analysis has the flexibility to handle any arbitrary contact area. Results are presented which display the effect of velocity or Peclet number, the frequency and amplitude of oscillation, and thermal properties. Also, results showing the effect of the number, spacing and orientation of the contact patches are presented. Finally, theoretical calculations corresponding to experiments involving a ball on an oscillating sapphire disk are presented and are found to correlate well with experimental data.

Acknowledgements

The author would like to give special thanks to his advisor Dr. Brian Vick, who recently became a father, for his invaluable advice and constant guidance throughout the duration of this work. The author also expresses much thanks to Dr. M. J. Furey and Dr. D. J. Nelson for serving on his committee and offering helpful suggestions, Brian Weick for providing much needed experimental data from his research work, and the National Science Foundation Tribology Program for a year (1988-1989) of assistantship funding.

The author also would like to thank his fellow graduate students for all the help and wonderful times over the past year.

Finally, the author wishes to thank his family and Siew Huey in Malaysia for their constant support, understanding, and encouragement, which made this graduate study possible.

Table of Contents

List of Illustrations

List of Tables

Nomenclature

a	half length of rectangular contact area in x-direction (m)
A	Peclet number in X-direction ($\frac{a\, v_r}{\alpha_2}$)
b	half length of rectangular contact area in y-direction (m)
B	Peclet number in Y-direction ($\frac{b\, v_r}{\alpha_2}$)
A_c	contact area
D	dimensionless distance between contact patches
f	frequency (Hz)
f(I)	one dimension matrix
G	Green's function
$\overline{G}, \overline{\overline{G}}, \overline{\overline{\overline{G}}}$	X, Y, Z transform of Green function, respectively
GI	integral of Green function
GI(I,K)	two dimension matrix of Green function
G1I, G2I	integral of Green function for region-1 and region-2
i	region indicator, stationary region (1), moving region (2)
IDT	number of time step per quarter cycle
j, jj	number of contact patches counter.
k_i	thermal conductivity ($watts/m\ K$)
K_1	ratio of thermal conductivity ($\frac{k_1}{k_2}$)
l	half length of square contact area use in Jaeger [4] (m)
L	Peclet number use in Jaeger [4] ($\frac{l\, v}{\alpha}$)

m, mm	the spatial element counter in X direction
ma	number of element in X direction
n, nn	the spatial element counter in Y direction
N, ncon	number of contact areas
nb	number of element in Y direction
p, pp	the time step counter
P, P_m	pressure (N/m^2)
q	frictional heat flux ($watts/m^2$)
q1(I)	one dimension matrix
Q	dimensionless heat flux
$Q1^p_{mn}$	heat distributed to region-2 evaluate at m, n, and time p
QS^p_{mn}	heat generated in the contact evaluate at m, n, and time p
R_i	region (i= 1, 2)
S_i	surface (i= 1, 2)
t	time (second)
T	temperature (K)
T_o	initial temperature (K)
v	velocity (m/s)
v_m	maximum velocity in oscillating motion (m/s)
V	dimensionless velocity
x, y, z	position in coordinate system (m)
X, Y, Z	dimensionless form of x, y, z, respectively
x_m	amplitude of oscillation (m)
X_c	center location of contact area due to motion

Greek Letters

α_i	thermal diffusivity (m^2/s)

$\delta_x, \delta_y, \delta_z, \delta$	thermal affected zone
$\delta(X - X_o)$	Dirac delta function
θ_i	dimensionless temperature rise for region i
θ_m	mean surface temperature rise
θ_s	surface temperature rise
λ	a constant, equal to 1/2 (at surface) or 1 (in the region)
Λ_i	ratio of thermal diffusivity $(\frac{\alpha_1}{\alpha_2})$
μ	coefficient of friction
π	3.141592654
$\Delta\tau$	size of dimensionless time step
τ	dimensionless time
τ_o	dimensionless time when the initial impulse occur
ω	frequency (rad/s)
Ω	dimensionless frequency

Superscripts

+	indicates a value that is slightly greater than the original value
p	time step counter
i	region indicator (i = 1, 2)

Subscripts

1	region-1
2	region-2
i	region indicator (i = 1, 2)
m	element counter in the X direction
n	element counter in Y direction
o	initial impulse

p, pp	time step counter
r	reference
s	surface

Chapter 1

INTRODUCTION

RATIONALE FOR THE RESEARCH

The surface temperature rise involving two sliding contacts is frequently important in tribology processes, as in bearings, brakes, cams, gears, sliding electrical contacts, the striking of a match, machining and metal working, machinery, and various joints (including human synovial joints.) The theoretical calculation of temperature due to the constant sliding case has been extensively studied; however, the surface temperature rise generated by friction in oscillating contact or fretting condition is still an unknown.

Energy conversion and transmission involve moving surfaces in contact. Friction and wear are the result of this sliding of one solid body over another. High surface temperature has many possible consequences, including the following: surface melting of one of the contact bodies; deterioration and increased wear; oxidation and oxidational wear

of metallic sliding components; softening and increased wear of metallic components in non-oxidizing environments; and breakdown of solid and lubricant films. Frictional heating has significant impact on the failure of sliding components, such as thermocracking of brakes and face seals, scuffing in gears, sparking and excessive wear of electrical brushes and wear in a variety of sliding components. Temperature affects the physical and chemical behavior of rubbing solids as well as of the lubricants between these solids. Higher temperature could cause breakdown of lubricant and increase surface wear. On the other hand, the concept of reduction of wear in boundary lubrication [1,2] by the use of particular compounds capable of forming protective polymeric films directly on rubbing surfaces results from the high surface temperature rise in the region of sliding motion. Higher surface temperatures produced by friction in sliding is one of the important factors that cause surface damage.

Fretting is defined as wear and corrosion occurring between two surfaces having oscillating relative motion of small amplitude [3]. Fretting damage is dependent on such factors as amplitude and frequency of vibration, load, material, surface finish, hardness, coatings, lubricants and environment. The surface temperature rise is also dependent on the same factors. Fretting contact occurs in a variety of tribology systems such as mechanical joints, supports, flanges, clutches, and bearings. The thermal effects could aggravate the surface damage and failure of components, increased rate of chemical reaction between the contact and the environment, increased wear, thermal fatigue at the contact surface, and changes of the physical properties of the contacting surface. Thus, the surface temperature plays an important role in these complex tribological processes.

OBJECTIVES OF THE RESEARCH

The objectives of this theoretical research are to develop a theoretical model and efficient solution method to predict the distribution of frictional heat and the resulting surface temperature rise in oscillating contact or fretting. This model has to be general enough to describe real systems observed in practice and the solution method must be efficient and accurate to allow for a systematic study of the physical parameters affecting surface temperature. Limitations and characteristics of the solution method, and the major factors that influence the surface temperature rise in tribological systems are investigated. Also, a comparison of theoretical predictions with the experimental results obtain from the laboratory is made.

SCOPE OF THE RESEARCH

In recent years, several studied have been carried out on fretting as part of the Tribology Program at Virginia Polytechnic Institute and State University (VPI&SU). A theoretical and experimental study of surface temperature generated during the fretting is one of the projects being conducted at VPI&SU and sponsored by the National Science Foundation Tribology program [3, 46]. This study is phase I of the theoretical part of the project.

A general real world oscillating contact system, in which one body rubs against another, is modeled. The heat is generated at the area of true contact, and is then conducted

away into the bulk of the rubbing members. The distribution of the total frictional heat is determined by solving the energy equations, and matching the single region solutions using the criteria that the surface temperatures over the contact region match and that energy is conserved. The magnitude and distribution of the temperatures in real systems can then be determined.

The simple model used in this study allows for careful examination of the effect of sliding velocity of the moving region, the size, the distribution and orientation of the area of contact, and the thermal properties of the two regions. In the model, the frictional heat source is treated as an arbitrary function of the velocity. The velocity input is arbitrary, which could be oscillating, or constant velocity. The study of oscillating velocity is concentrated on the effect of frequency and amplitude in the oscillating motion. This model could handle any combination of geometry and multiple contacts. The distribution of heat between the two regions , which has never been carefully and effectively studied, is also investigated in the present research.

Solution methodology: Boundary Integral Equation Method

The boundary integral equation method or boundary element method is a relatively new technique based on the combination of classical integral equations and finite element concepts. The boundary integral equation method (BIEM) used in this study utilizes the full-space moving Green's Function, which is the solution to a concentrated pulsed heat source in a moving region. In the boundary integral equation method, the general solution is evaluated at the exposed surfaces, as elements are only defined on the external surface; internal unknowns are not required as the problem has been mathematically

reduced into a boundary solution. Thus, the method leads to an integral equation for the unknown boundary data. The transient heat conduction requires time as well as space integrals. The time integral is handled in a similar manner to the space integrals. The end result is a system of integral equations which requires evaluation only over the boundaries. Once all the boundary data are known, one can calculate any internal variables as functions of the boundary values. Unlike finite differences and finite elements, there is no need to construct a mesh over the entire volume. This reduction in dimensionality greatly reduces the required computation time and storage, and is a major advantage in using BIEM. Other advantages of this technique include the simplicity of the input data required to run it, and the fact that the time step used by BIEM can be much larger than those required by finite difference or finite element methods.

Chapter 2

LITERATURE REVIEW

The theoretical prediction of surface temperatures resulting from frictional heating was initiated with the pioneering works of Blok [4] and Jaeger [5]. Both of these works employ the analytical solution for the temperature distribution due to a point source over a single contact patch on the surface of a semi-infinite medium. In order to partition the frictional heat between sliding bodies, Blok [4] first calculated the temperature distribution for stationary and moving sources subject to a uniform heat flux. The total heat flux was then partitioned such that the maximum temperatures on the two surfaces were the same. This method shows significant inaccuracies at high sliding velocity. Jaeger [5], instead of matching maximum temperatures, matched the average temperatures of the two surfaces to determine the division of frictional heat. Another approximation was suggested by Archard [6] who proposed that the average interfacial temperature rise is half of the harmonic mean of the average rises if each surface received all the heat flux. The formulation was recently extended to allow an estimation of temperature distribution both at the surface and in subsurface regions [7].

In order to eliminate the need to approximate the division of frictional heat, Ling [8,9] evoked the condition that all points of intimate contact must have the same surface temperature. This leads to a singular integral equation for the heat partition function and shows that the correct partitioning function is not constant but varies with both position within the real contact area and with velocity. The technique suggested by Ling has been extended to problems with finite geometry for some practical situations involving rotating disks [10] and bearings [11,12]. Analytical solutions using the integral transform technique were developed for these problems in finite regions with a single area of contact.

The effect of multiple contacts has been studied by several investigators. A stochastic approach [13,14] was used in which a number of small contact spots were generated in a random manner over a nominal contact area. The resulting flash temperatures at the contact spots were found to be much higher than those elsewhere on the surface. Marscher [15] studied the effect of multiple interacting heat sources in a one-region problem. The problem of two solids with different bulk temperatures and multiple contacts was investigated Barber [16] who used Jaeger's point heat source method and approximation for the partition of frictional heat.

The analytical treatment of surface temperatures has also been extended to include the effect of lubricants and third-body layers between the sliding surfaces. Lai and Cheng [17] considered lubricated sliding with rough contact where the surface roughness was generated numerically. The results show that scuffing is correlated with high temperature asperities which are above the material softening temperature. Other studies [18, 19] that used the energy-based friction model of Rigney [20] show that nearly all frictional energy is dissipated as heat, primarily within the top few microns of the con-

tacting bodies. Another interesting analysis was performed by Ryhming [21] who assumed that all frictional heat was produced within a third-body layer between the two sliding bodies. Furthermore, the surface temperature rise has been found to depend on sliding velocity, and/or contact pressure from experimental data by using the dynamic thermalcouple [22].

A variety of other analyses have employed analytical techniques [23 – 25] to study effects such as convective cooling from the noncontacting portions of the surface [23] and the effect of a Hertzian distribution of heat flux over a contact patch [24].

Numerical methods have also been used for the analysis of surface temperatures, especially for sliding bodies of complex shape. Both finite differences [26 – 28] and finite elements [18,29 – 31] have been employed. In order to accurately calculate the large temperature gradients in the vicinity of contact areas, the finite difference technique requires an excessively fine grid, resulting in long computer times and storage. As a result, the finite element technique seems more suited to these types of problems using a fine mesh in the region of contact and a coarser mesh elsewhere. Despite the general applicability of the finite element technique, problems with numerical oscillations and inaccuracies can occur if the Peclet number is too high [31].

The finite element technique was applied by Kennedy et al [18,29 – 32] to analyze a variety of situations of interest, including disk brakes, bearings, and gas seals. The work of Rashid and Seireg [28] models the sliding bodies. The results show that both these effects can significantly influence surface temperatures. Recently, Kennedy and coworkers [32] also used a finite element technique [31] to predict contact temperatures in an oscillating sliding contact with low frequency and high amplitude.

Since both analytical and numerical techniques have advantages and disadvantages, an interesting hybrid technique has been proposed by Colon and Floquet [33]. It makes use of a finite element method in only the stationary component, which is usually the member of most complex geometry, and uses the integral transform technique in the simpler-shaped moving component. The initial results with the method are quite promising. A comparison of analytical and numerical methods was presented by Floquet [34]. He points out that analytical techniques can present substantial advantages over numerical methods in accuracy and computational time but analytical methods are difficult to apply to complex geometry.

As a whole, these surface temperature analyses have shown that the most important factors governing surface temperature magnitudes are the rate of heat generation, sliding velocity, thermal properties of the contacting materials, and the true nature of the real area of contact. The first three of these factors can generally be specified. However, the size, shape,and distribution of the actual contact spots and the influence of any third bodies, including oxide films and wear debris, is seldom known with certainty. All these factors and their complicated relationship with surface temperature require more study. In particular, the influence of an oscillating sliding velocity, especially fretting, has not been investigated since almost every study considers a constant velocity [3].

The boundary integral equation method is a relatively new numerical technique for the analysis of thermal problems. The BIEM was first applied by Rizzo and Shippy [35] for the solution of transient heat conduction problems. They used the Laplace transform in a time variable. Another approach was proposed by Chang et al. [36] and Shaw [37]. They used a time-dependent fundamental solution of the governing linear heat equation. Many researchers [38,39] have discussed the computer implementation of

numerical procedures for application in engineering problems. Geometrically singular problems and infinite domain problems were considered by Kuroki et al. [40]. Non-linear problems were tackled by Skerget and Brebbia [41] by using a Kirchkoff transform. Non-linear transient heat transfer problems were considered by Onishi and Kuroki [42] by using Green's function.

Chapter 3

THEORETICAL MODEL

In this chapter a theoretical model for frictional heating between two semi-infinite regions with sliding contact is formulated in the rectangular coordinate system. The thermal properties and hardness of the two regions are assumed constant. This model only considers the simple system of two pure contact regions with no loss of heat from the noncontacting portion of the surface, no surface film, no oxide formation, no chemical reaction on the surface, and no lubrication.

GENERAL GOVERNING EQUATIONS

The general schematic and coordinate system are depicted in figure 1. The problem is analyzed by fixing the coordinate system to the center of the contact area and letting the

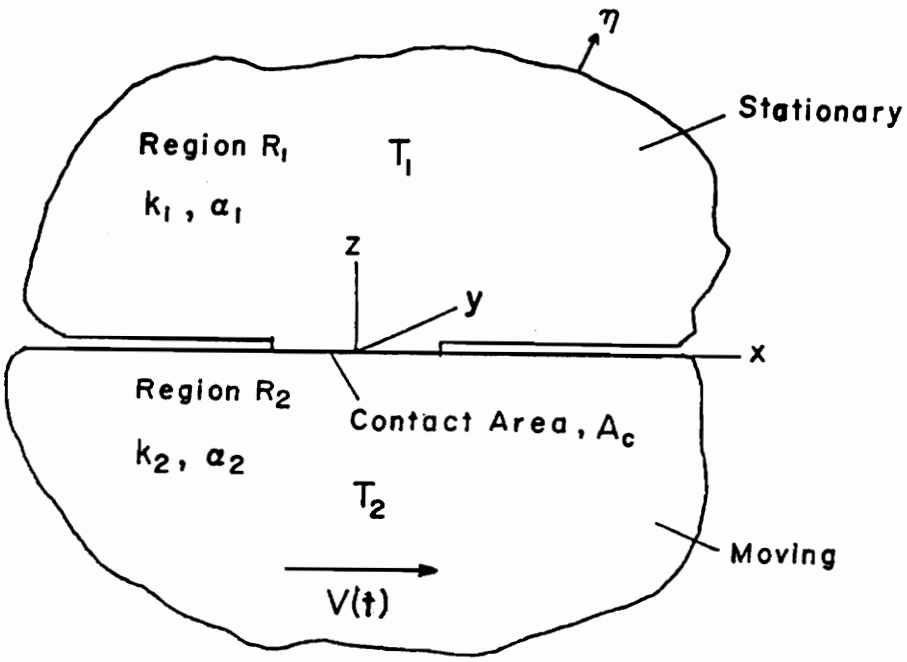

Figure 1. TWO REGION PROBLEM – A stationary region on a moving region.

region-2 move with velocity, v(t) in the x-direction. Thus, the governing energy equations include a convection term, and become

$$\frac{\partial T_i}{\partial t} + v_i(t) \frac{\partial T_i}{\partial x} = \alpha_i \nabla^2 T_i \tag{3.1a}$$

where i = 1 or 2, and

$$\begin{aligned} v_i(t) &= 0, \qquad i = 1 \\ &= v(t) \qquad i = 2 \end{aligned} \tag{3.1b}$$

The boundary and initial conditions for region i are,

$$T_i = T_o, \qquad at \ t = 0 \tag{3.1c}$$

$$T_i \rightarrow T_o, \qquad x,y,z \rightarrow \pm \infty \tag{3.1d}$$

The coupling conditions on the contact area, $A_c(x,y)$ are based on the assumptions that surface temperatures of both regions on the contact area must be equal and the energy is conserved, thus

$$T_1 = T_2 \tag{3.2a}$$

$$\begin{aligned} q_s'' &= -k_1 \frac{\partial T_1}{\partial z} + k_2 \frac{\partial T_2}{\partial z} \\ &= q_1'' + q_2'' \ , \quad \text{on contact area } A_c \end{aligned} \tag{3.2b}$$

On the noncontacting portions of the surface, negligible heat loss is assumed, thus

$$\frac{\partial T_i}{\partial z} = 0, \qquad \text{noncontacting portion of } z = 0 \tag{3.2c}$$

The total frictional heat flux, $q_s''(x,y,t)$, in equation (3.2b) is generally known; however, the distribution of this frictional heat to each region,

$$q_i''(x,y,t) = \begin{cases} (-1)^i k_i \dfrac{\partial T_i}{\partial z}, & \text{on contact area } A_c \\ 0 & \text{on noncontacting surfaces} \end{cases}$$

is unknown. The total frictional heat is due to the conversion of mechanical energy into heat and is given by

$$q_s'' = \mu P \, | v(t) |$$

where both the coefficient of the friction, μ, and pressure, P, may vary over the contact area and over time.

The velocity term (see also "APPENDIX C: Oscillating contact: Velocity, Position, and Heat Source" on page 107) in the governing equations can be arbitrary. The two most common and important cases, namely unidirectional and oscillating velocity, are

$$v(t) = \begin{cases} v, & \text{unidirectional velocity} \\ v_m \cos(\omega t), & \text{oscillating velocity} \end{cases} \tag{3.3}$$

In the oscillating velocity case the maximum velocity, v_m, is given by

$$v_m = x_m \omega \tag{3.4}$$

where ω is the frequency and x_m is the amplitude of oscillation. The contact area $A_c(x,y)$ is treated as N rectangular patches, where each patch has dimension 2a by 2b.

SCALE ANALYSIS

Scale analysis is often used to determine relevant reference quantities such as the length scale, time scale, temperature scale, and so on. It also produces order-of magnitude estimates for quantities of interest and suggests logical dimensionless variables. The governing equation (3.1a) for moving region-2 is scaled in the following manner.

$$\frac{\Delta T}{\delta_x^2} + \frac{\Delta T}{\delta_y^2} + \frac{\Delta T}{\delta_z^2} \sim \frac{1}{\alpha_2}\frac{\Delta T}{t} + \frac{v_m}{\alpha_2}\frac{\Delta T}{\delta_x}$$

where the symbol " $\sim$" indicates order of magnitude. If the thermal affected zones are equal,

$$\delta_x \cong \delta_y \cong \delta_y \cong \delta$$

the above equation becomes

$$\frac{1}{\delta^2} \sim \frac{1}{\alpha_2 t} + \frac{v_m}{\alpha_2 \delta}$$

When $t \rightarrow \infty$,

$$\frac{1}{\delta^2} \sim \frac{v_m}{\alpha_2 \delta}$$

$$\delta \sim \frac{\alpha_2}{v_m} \qquad (3.5a)$$

which gives an appropriate length scale.

When $t \rightarrow 0$,

$$\frac{1}{\alpha_2 t} \sim \frac{v_m}{\alpha_2 \delta}, \qquad \text{or}$$

$$t \sim \frac{\delta}{v_m} \sim \frac{\alpha_2}{v_m^2} \tag{3.5b}$$

which defines a meaningful time scale. The temperature scaling is determined using equation (3.2b) as following:

$$k_2 \frac{\Delta T}{\delta} \sim q_s''$$

$$\Delta T \sim \frac{q_s'' \delta}{k_2} \sim \frac{q_s'' \alpha_2}{k_2 v_m} \tag{3.5c}$$

DIMENSIONLESS VARIABLES

Based on the previous scaling arguments, reference quantities are defined as following,

- Length scale $= \frac{\alpha_2}{v_r}$
- Time scale $= \frac{\alpha_2}{v_r^2}$
- Temperature scale $= \frac{q_r'' \alpha_2}{k_2 v_r}$

where v_r and q_r'' are the characteristic velocity and heat flux. For unidirectional and oscillating velocity, the following reference velocity and heat flux are used,

$$v_r = \begin{cases} v, & \text{unidirectional velocity} \\ v_m, & \text{oscillating velocity} \end{cases}$$

$$q_r'' = \mu P_r v_r$$

where P_r is the reference pressure. Using these reference quantities, dimensionless parameters can be defined as,

$$X = \frac{v_r x}{\alpha_2}, \quad Y = \frac{v_r y}{\alpha_2}, \quad Z = \frac{v_r z}{\alpha_2}, \quad \tau = \frac{v_r^2 t}{\alpha_2} \tag{3.6a}$$

$$A = \frac{v_r a}{\alpha_2}, \quad B = \frac{v_r b}{\alpha_2} \tag{3.6b}$$

$$\theta = \frac{T_i - T_o}{\frac{q_r'' \alpha_2}{k_2 v_r}}, \quad Q_s'' = \frac{q_s''}{q_r''}, \quad Q_i'' = \frac{q_i''}{q_r''}, \tag{3.6c}$$

$$\Lambda_i = \frac{\alpha_i}{\alpha_2}, \quad K_i = \frac{k_i}{k_2} \tag{3.6d}$$

$$\Omega = \frac{\alpha_2 \omega}{v_r^2}, \quad V_i = \frac{v_i(t)}{v_r} \tag{3.6e}$$

where,

$$i = 1, \text{ or } 2$$

Substitute dimensionless variables defined by equations (3.6) into equation (3.1) and (3.2). The dimensionless form of the governing energy equation for the two region problem becomes,

$$\frac{\partial \theta_i}{\partial \tau} + V_i(\tau) \frac{\partial \theta_i}{\partial x} = \Lambda_i \nabla^2 \theta_i \tag{3.7a}$$

The boundary conditions for region i are,

$$\theta_i = 0, \qquad at \ \tau = 0 \tag{3.7b}$$

$$\theta_i \to 0, \qquad X,Y,Z \to \pm \infty \tag{3.7c}$$

The dimensionless coupling boundary conditions of equation (3.2) become,

$$\theta_1 = \theta_2 \tag{3.8a}$$

$$\begin{aligned} Q_s'' &= -K_1 \frac{\partial \theta_1}{\partial Z} + \frac{\partial \theta_2}{\partial Z} \\ &= Q_1'' + Q_2'', \qquad \text{on contact area } A_c \end{aligned} \tag{3.8b}$$

$$\frac{\partial \theta_i}{\partial Z} = 0, \qquad Z = 0, \ \text{noncontacting areas} \tag{3.8c}$$

where,

$$i = 1, \text{ or } 2$$

The total frictional heat, Q_s'', is unknown, and the solution must yield the division of this frictional heat,

$$Q_i'' = \begin{cases} (-1)^i K_i \left(\frac{\partial \theta_i}{\partial Z} \right)_{z=0} & \text{contact area } A_c \\ 0 & \text{noncontacting portion} \end{cases}$$

PHYSICAL PARAMETERS

The physical parameters involved in this problem include: dimension of contact areas (a,b), thermal properties of both regions (k_1, k_2, α_1, α_2), and velocity (v) for unidirectional motion or amplitude (x_m) and frequency of oscillating (ω) for oscillating motion. The distribution of frictional heat and the resulting temperature rise will depend on the following dimensionless parameters,

constant velocity:

$$\Lambda_1, K_1, A, B, N, \text{spacing, and orientation of contact areas} \tag{3.9a}$$

oscillating velocity:

$$\Lambda_1, K_1, A, B, \Omega, N, \text{spacing and orientation of contact areas} \tag{3.9b}$$

where N is number of contacts.

Chapter 4

SOLUTION USING BOUNDARY INTEGRAL EQUATION METHOD

The boundary integral equation method (BIEM) is used to solve the governing equations in chapter 3 by using a moving or convecting Green's function (GF). Satisfaction of boundary conditions produces a system of equations which can be solved to find the boundary unknowns. Once all values on the boundary are known, temperature anywhere can be calculated as function of the boundary values. The use of a moving Green's function distinguishes this analysis from the standard BIEM which uses the classical stationary diffusion GF.

MOVING GREEN'S FUNCTION

Let $G_i(X,Y,Z,\tau,|X_o, Y_o, Z_o, \tau_o)$ or G_i denote the fundamental full-space moving Green's function in region i. The full-space moving GF is governing by

$$\frac{\partial G_i}{\partial \tau} + V_i(\tau)\frac{\partial G_i}{\partial X} = \Lambda_i \nabla^2 G_i + \delta(X - X_o)\,\delta(Y - Y_o)\,\delta(Z - Z_o)\,\delta(\tau - \tau_o) \qquad \text{for all } X,Y,Z,\tau \tag{4.1a}$$

$$G_i \to 0, \qquad X, Y, Z \to \pm\infty \tag{4.1b}$$

$$G_i = 0, \qquad \tau < \tau_o \tag{4.1c}$$

where

$$i = 1, 2$$

and δ is the Dirac delta function. The details of the solution for the GF using the Fourier transform method are shown in "APPENDIX A: Fourier Transform Method for Moving Green's Function" on page 94. The solution for the Green's function is

$$\begin{aligned} G_i &= G_i(X, Y, Z, \tau\,|\,X_o, Y_o, Z_o, \tau_o) \\ &= \frac{1}{[4\pi\Lambda_i(\tau - \tau_o)]^{3/2}} \\ &\times \mathrm{EXP}\left[-\frac{(X - X_o - X_c)^2 + (Y - Y_o)^2 + (Z - Z_o)^2}{4\Lambda_i(\tau - \tau_o)} \right] \end{aligned} \tag{4.2}$$

where,

$$X_c = \int_{\tau' = \tau_o}^{\tau} V_i(\tau')d\tau'$$

Equation (4.2) is similar to the classical solution of GF, except for the term X_c, which represents the effect of the convection term in equation (4.1a)

GENERAL SOLUTION IN TERMS OF THE MOVING GREEN'S FUNCTION

Express equation (3.7a) in the (X_o, Y_o, Z_o, τ_o) variables and perform the following operation.

$$\int_{\tau_o=0}^{\tau} \int \int \int_{R_i} \left[\Lambda_i \nabla_o^2 \theta_i - \frac{\partial \theta_i}{\partial \tau_o} - V_i(\tau_o) \frac{\partial \theta_i}{\partial X_o} \right] G_i dX_o dY_o dZ_o d\tau_o = 0 \qquad (4.3)$$

When i = 1, the Z integral ranges from 0 to ∞, when i = 2, the Z integral ranges from 0 to $-\infty$, and the volume integral represents integration over the entire region,

$$\int \int \int_{R_i} \equiv \int_{X_o=-\infty}^{\infty} \int_{Y_o=-\infty}^{\infty} \int_{Z_o=0}^{\pm\infty}$$

According to Green's theorem, the first term of equation (4.3) becomes

$$\int_{\tau_o=0}^{\tau}\int\int\int_{R_i}[\Lambda_i G_i \nabla_o^2 \theta_i]dX_o dY_o dZ_o d\tau_o$$

$$=\int_{\tau_o=0}^{\tau}\int\int_{S_i}\Lambda_i\left[(G_i\frac{\partial\theta_i}{\partial\eta})_{Z_o=0}-(\frac{\partial G_i}{\partial\eta}\theta_i)_{Z_o=0}\right]dX_o dY_o d\tau_o$$

$$+\int_{\tau_o=0}^{\tau}\int\int\int_{R_i}[\Lambda_i\theta_i\nabla_o^2 G_i]dX_o dY_o dZ_o d\tau_o$$

$$=\int_{\tau_o=0}^{\tau}\int\int_{S_i}\Lambda_i[G_i\frac{Q_i''}{K_i}-(-1)^i\frac{\partial G_i}{\partial Z_o}\theta_i]_{Z_o=0}dX_o dY_o d\tau_o$$

$$+\int_{\tau_o=0}^{\tau}\int\int\int_{R_i}[\Lambda_i\theta_i\nabla_o^2 G_i]dX_o dY_o dZ_o d\tau_o \qquad (4.4a)$$

where the surface integration is,

$$\int\int_{S_i}\equiv\int_{X_o=-\infty}^{\infty}\int_{Y_o=-\infty}^{\infty}$$

The following identities have been used,

$$\frac{\partial G_i}{\partial \eta} \Big|_{Z_o=0} = (-1)^i \frac{\partial G_i}{\partial Z_o}$$

$$\frac{\partial \theta_i}{\partial \eta} \Big|_{Z_o=0} = (-1)^i \frac{\partial \theta_i}{\partial Z} = \frac{Q_i''}{K_i}$$

Here η represents the outward normal derivative.

The second term of equation (4.3) can be integrated by parts in the time variable to get

$$\int_{\tau_o=0}^{\tau} \int\int\int_{R_i} \left[\frac{\partial \theta_i}{\partial \tau_o} G_i \right] dX_o dY_o dZ_o d\tau_o$$

$$= \int\int\int_{R_i} \left[(\theta_i G_i) \Big|_{\tau_o=0}^{\tau^+} - \int_{\tau_o=0}^{\tau} \theta_i \frac{\partial G_i}{\partial \tau_o} d\tau_o \right] dX_o dY_o dZ_o$$

$$= - \int_{\tau_o=0}^{\tau} \int\int\int_{R_i} \left[\theta_i \frac{\partial G_i}{\partial \tau_o} \right] dX_o dY_o dZ_o d\tau_o \qquad (4.4b)$$

At $\tau_o = 0$, θ_i is equal to zero. At τ^+, G_i is also equal to zero by the definition of GF equation (4.1c), because the time for the effect is earlier than the time for impulse.

The third term of equation (4.3) can be integrated by parts in the X-direction to get

$$\int_{\tau_o=0}^{\tau}\int\int\int_{R_i}\left[V_i(\tau_o)\frac{\partial\theta_i}{\partial X_o}\right]G_i dX_o dY_o dZ_o d\tau_o$$

$$=\int_{\tau_o=0}^{\tau}\int_{Y_o}\int_{Z_o}\left[(V_i\theta_i G_i)\Big|_{X_o=-\infty}^{\infty}\right]dY_o dZ_o\tau_o-\int_{\tau_o=0}^{\tau}\int\int\int_{R_i}\left[V_i\theta_i\frac{\partial G_i}{\partial X_o}\right]dX_o dY_o dZ_o\tau_o$$

$$=-\int_{\tau_o=0}^{\tau}\int\int\int_{R_i}\left[V_i\theta_i\frac{\partial G_i}{\partial X_o}\right]dX_o dY_o dZ_o\tau_o \qquad (4.4c)$$

In the above expression, the boundary condition (4.1b), has been used. Substitute equations (4.4) back into equation (4.3)

$$\int_{\tau_o=0}^{\tau}\int\int\int_{R_i}\theta_i\left[\Lambda_i\nabla_o^2 G_i+\frac{\partial G_i}{\partial\tau_o}+V_i\frac{\partial G_i}{\partial X_o}\right]dX_o dY_o dZ_o d\tau_o$$

$$+\int_{\tau_o=0}^{\tau}\int\int_{S_i}\Lambda_i\left[G_i\frac{Q_i''}{K_i}-(-1)^i\frac{\partial G_i}{\partial Z_o}\theta_i\right]_{Z_o=0}dX_o dY_o d\tau_o=0 \qquad (4.5)$$

The Green's function $G(X,Y,Z,\tau\,|\,X_o, Y_o, Z_o, \tau_o)$ satisfying the equation (4.1) must obey the following reciprocity relation [43]

$$\left[\begin{array}{l}\text{Response at } (X,Y,Z,\tau) \text{ due to an impulse} \\ \text{at } (X_o, Y_o, Z_o, \tau_o) \text{ with velocity } V_i(\tau)\end{array}\right]$$

$$\equiv$$

$$\left[\begin{array}{l}\text{Response at } (X_o, Y_o, Z_o, -\tau_o) \text{due to an impulse} \\ \text{at } (X,Y,Z,-\tau) \text{ with velocity } \quad -V_i(\tau_o)\end{array}\right]$$

Therefore, the Green's function must obey the following equations,

$$\begin{aligned}&\Lambda_i \nabla_o^2 G_i + \frac{\partial G_i}{\partial \tau_o} + V_i(\tau_o)\frac{\partial G}{\partial X_o} \\ &= -\delta(X - X_o)\,\delta(Y - Y_o)\,\delta(Z - Z_o)\,\delta(\tau - \tau_o)\end{aligned} \tag{4.6a}$$

$$G_i \to 0, \qquad X, Y, Z \to \pm\infty \tag{4.6b}$$

$$G_i = 0, \qquad \tau_o > \tau \tag{4.6c}$$

The solution to equations (4.1) and (4.6) are identical and are given by equation (4.2). Substitute equation (4.6a) into the first integral in equation (4.5) and use the following property of δ function

$$\int_{\tau_o=0}^{\tau}\int_{X_o=-\infty}^{\infty}\int_{Y_o=-\infty}^{\infty}\int_{Z_o=0}^{\infty}\theta_i[\delta(X - X_o)\,\delta(Y - Y_o)\,\delta(Z - Z_o)\,\delta(\tau - \tau_o)]dX_o dY_o dZ_o d\tau_o$$

$$= \lambda\,\theta_i(X,Y,Z,\tau)$$

where,

$$\lambda = \frac{1}{2}, \qquad Z = 0$$

$$= 1, \qquad Z \neq 0$$

Equation (4.5) now becomes,

$$\lambda\,\theta_i(X,Y,Z,\tau)$$

$$= \Lambda_i \int_{\tau_o=0}^{\tau} \int\int_{S_i} \left[G_i \frac{Q''_i}{K_i} - (-1)^i \frac{\partial G}{\partial Z_o}\,\theta_i \right]_{Z_o=0} dX_o dY_o d\tau_o \qquad (4.7a)$$

for i = 1 or 2

where

$$Q_i'' = \begin{cases} (-1)^i K_i \left(\dfrac{\partial \theta_i}{\partial Z}\right)_{Z_o=0}, & \text{on contact area } A_c \\ 0, & \text{on noncontacting portion} \end{cases} \qquad (4.7b)$$

The integral equation (4.5) is now reduced to a surface boundary integral equation (4.7a). Since the frictional heating acts only over the area $A_c(X,Y)$, rewrite equation (4.7a) as

$$\lambda\,\theta_i(X,Y,Z,\tau)$$

$$\begin{aligned} &= \Lambda_i \int_{\tau_o=0}^{\tau} \int\int_{A_c} \left[\frac{Q_i''}{K_i} (G)_{Z_o=0} \right] dX_o dY_o d\tau_o \\ &\quad - (-1)^i \Lambda_i \int_{\tau_o=0}^{\tau} \int\int_{S_i} \left[\theta_i \left(\frac{\partial G}{\partial Z_o} \right) \right]_{Z_o=0} dX_o dY_o d\tau_o \end{aligned} \qquad (4.8)$$

Evaluate equation (4.8) at surface (Z = 0) and use

$$\left(\frac{\partial G}{\partial Z_o}\right)_{Z_o=Z=0} = 0$$

to obtain a general solution for surface temperature, $\theta_{s,i}$. Thus,

$$\frac{1}{2}\theta_i(X,Y,0,\tau) = \frac{1}{2}\theta_{s\,i}(X,Y,\tau)$$

$$= \Lambda_i \int_{\tau_o=0}^{\tau} \int\int_{A_c} \left[\frac{Q_i''}{K_i} (G)_{Z_o=Z=0} \right] dX_o dY_o d\tau_o \qquad (4.9)$$

INTEGRAL EQUATION FOR THE DISTRIBUTION OF FRICTIONAL HEAT

The general solution for the surface temperature rise, equation (4.9) has two unknowns. One is the $\theta_{s\,i}$ itself, another one is Q_i''. Thus, use the coupling boundary conditions of equation (3.8a), which states that points of direct contact must have continuity of temperatures,

$$\theta_{s\,1} = \theta_{s\,2} \qquad \text{in } A_c(X, Y)$$

Replacing $\theta_{s\,1}$ and $\theta_{s\,2}$ with the solution given by equation (4.9) gives

$$\Lambda_1 \int_{\tau_o=0}^{\tau} \int\int_{A_c} \left[\frac{Q_1''}{K_1} (G_1)_{Z_o=Z=0} \right] dX_o dY_o d\tau_o$$

$$= \int_{\tau_o=0}^{\tau} \int\int_{A_c} [Q_2''(G_2)_{Z_o=Z=0}] dX_o dY_o d\tau_o \tag{4.10}$$

Now use conservation of energy, given by the boundary condition of equation (3.8b),

$$Q_s'' = Q_1'' + Q_2''$$

to substitute for Q_2'' in equation (4.10), and rewrite the resulting expression as

$$\int_{\tau_o=0}^{\tau} \int\int_{A_c} \left[Q_1''(X_o, Y_o, \tau_o) G(X, Y, \tau \,|\, X_o, Y_o, \tau_o) \right] dX_o dY_o d\tau_o$$
$$= F(X, Y, \tau), \qquad \text{valid for } (X,Y) \text{ on } A_c(X,Y) \tag{4.11}$$

where

$$G(X, Y, \tau \,|\, X_o, Y_o, \tau_o) = \text{ kernel}$$
$$= \frac{\Lambda_1}{K_1} (G_1)_{Z_o=Z=0} + (G_2)_{Z_o=Z=0} \tag{4.12a}$$

$$F(X, Y, \tau) = \int_{\tau_o=0}^{\tau} \int\int_{A_c} [Q_s''(X_o, Y_o, \tau_o)(G_2)_{Z_o=Z=0}] dX_o dY_o d\tau_o \tag{4.12b}$$

Equation (4.11) provides an integral equation for the determination of Q_1'' from which Q_2'' immediately follows from,

$$Q_2'' = Q_s'' - Q_1''$$

NUMERICAL SCHEME AND DISCRETIZATION

Up to this point, the solution for the surface temperature, given by equation (4.9), and heat flux, given by equation (4.11), are exact. However, due to the difficulty of the integration, a numerical integration method is employed to perform the calculations. Two numerical integration rules (trapezoid rule and midpoint rule) have been investigated; but only one (midpoint rule) is presented here in detail.

Trapezoid rule

Use the trapezoid rule to integrate equation (4.11) for time and midpoint rule for space. The unknown heat flux is treated as following

$$Q1_{m,n}^{p} \cong Q_1'', \quad \text{in region} \quad X_m \le X \le X_{m+1}, \quad Y_n \le Y \le Y_{n+1}$$

$$\text{at time} \quad \tau = \tau_p$$

The advantage of using the trapezoid rule is to avoid solving simultaneous equations. But at $\tau = \tau_p$, the Green's Function has a singular point. Another disadvantage of the

trapezoid rule is that it is unstable for integral equations of the first kind [44] , like equation (4.11).

Midpoint rule

Use the midpoint rule to integrate equation (4.11) for time and space. The unknown heat flux is approximated as follows,

$$Q1^{p}_{m,n} \cong Q_1'', \qquad QS^{p}_{m,n} \cong Q_s''$$

$$\text{in region} \quad X_m \le X \le X_{m+1}$$

$$Y_n \le Y \le Y_{n+1}$$

$$\text{in time period} \quad \tau_p \le \tau \le \tau_{p+1}$$

The midpoint rule is stable for first kind integral equations like equation (4.11) [44]; therefore, this method is used for this research study.

Rewrite the distribution of frictional heat equation (4.11) as

$$\int_{\tau_o=0}^{\tau}\int\int_{A_c}\left[Q_1''(X_o, Y_o, \tau_o)G(X, Y, \tau \mid X_o, Y_o, \tau_o)\right]dX_o dY_o d\tau_o$$

$$= \int_{\tau_o=0}^{\tau}\int\int_{A_c}\left[Q_s''(X_o, Y_o, \tau_o)(G_2)_{Z_o=Z=0}\right]dX_o dY_o d\tau_o$$

The above equation is evaluated at time $\tau = \tau_{pp} = pp \times \Delta\tau$ and discretized over time and space with a midpoint rule. The above expression becomes,

$$\sum_{p=0}^{pp-1}\sum_{m}\sum_{n}\int_{\tau_o=\tau_p}^{\tau_{p+1}}\int_{X_o=X_m}^{X_{m+1}}\int_{Y_o=Y_n}^{Y_{n+1}}\left[Q_1''(X_o, Y_o, \tau_o)G(X, Y, \tau \mid X_o, Y_o, \tau_o)\right]dX_o dY_o d\tau_o$$

$$= \sum_{p=0}^{pp-1}\sum_{m}\sum_{n}\int_{\tau_o=\tau_p}^{\tau_{p+1}}\int_{X_o=X_m}^{X_{m+1}}\int_{Y_o=Y_n}^{Y_{n+1}}[Q_s''(X_o, Y_o, \tau_o)(G_2)_{Z_o=Z=0}]dX_o dY_o d\tau_o \tag{4.13}$$

where,

m, n are summed over the elements of the contact area A_c in X, and Y

and

$$\tau = \tau_{pp} = pp \times \Delta\tau = \text{ current time step}$$

Using the midpoint rule to approximate Q_1'' in equation (4.13) provides the following,

$$\sum_{p=0}^{pp-1}\sum_{m}\sum_{n} Q1^{p}_{m\,n} GI^{p}_{m\,n}(X, Y, \tau_{pp})$$

$$= \sum_{p=0}^{pp-1}\sum_{m}\sum_{n} QS^{p}_{m\,n} G2I^{p}_{m\,n}(X, Y, \tau_{pp}) \tag{4.14}$$

$GI^{p}_{m\,n}(X,Y,\tau)$ is the effect of the integral of the Green's Function (see equation (4.12a)) over element (m,n) in time period p, and is defined by,

$$GI^{p}_{m\,n}(X, Y, \tau_{pp}) = \int_{\tau_o=\tau_p}^{\tau_{p+1}}\int_{X_o=X_m}^{X_{m+1}}\int_{Y_o=Y_n}^{Y_{n+1}} G(X, Y, \tau \mid X_o, Y_o, \tau_o)dX_o dY_o d\tau_o \tag{4.15a}$$

where the kernel, G, was defined by equation (4.12a).

Similar to $GI^{p}_{m\,n}(X,Y,\tau)$

$$G2I^{p}_{m\,n}(X, Y, \tau_{pp}) = \int_{\tau_o=\tau_p}^{\tau_{p+1}} \int_{X_o=X_m}^{X_{m+1}} \int_{Y_o=Y_n}^{Y_{n+1}} [G_2]_{Z_o=Z=0} dX_o dY_o d\tau_o \tag{4.15b}$$

(For detailed derivation of $GI^{p}_{m\,n}(X,Y,\tau)$ see "APPENDIX B: Integral of Moving Green's Function" on page 101) The summation over space is valid only in the area of contact $A_c(X,Y)$. The only unknowns in equation (4.14) are the most recent heat flux values, $Q1^{pp-1}_{m\,n}$. Thus, rewrite equation (4.14) as

$$\begin{aligned} &\sum_{m}\sum_{n} Q1^{pp-1}_{m\,n} GI^{pp-1}_{m\,n}(X, Y, \tau_{pp}) \\ &= \sum_{p=0}^{pp-1}\sum_{m}\sum_{n} QS^{p}_{m\,n} G2I^{p}_{m\,n}(X, Y, \tau_{pp}) \\ &\quad - \sum_{p=0}^{pp-2}\sum_{m}\sum_{n} Q1^{p}_{m\,n} GI^{p}_{m\,n}(X, Y, \tau_{pp}) \end{aligned} \tag{4.16}$$

There is one unknown , $Q1^{pp-1}_{m\,n}$, for each element. Thus, evaluate expression (4.16) at the middle of each element. This type of element is always "smooth" as the node is always at the center of the element, hence, the multiplier λ of θ is 1/2 (see equation (4.9)) at the surface. Rewrite equation (4.16) with X, Y evaluated at the center of the elements as,

$$\sum_m \sum_n \mathrm{Q1}^{\mathrm{pp}-1}_{m\,n} \mathrm{GI}^{\mathrm{pp}-1}_{m\,n}(\mathrm{mm}+1/2, \mathrm{nn}+1/2, \mathrm{pp})$$

$$= \sum_{p=0}^{\mathrm{pp}-1} \sum_m \sum_n \mathrm{QS}^p_{m\,n} \mathrm{G2I}^p_{m\,n}(\mathrm{mm}+1/2, \mathrm{nn}+1/2, \mathrm{pp}) \qquad (4.17)$$

$$- \sum_{p=0}^{\mathrm{pp}-2} \sum_m \sum_n \mathrm{Q1}^p_{m\,n} \mathrm{GI}^p_{m\,n}(\mathrm{mm}+1/2, \mathrm{nn}+1/2, \mathrm{pp})$$

The following shorthand notation has been used,

$$(\mathrm{X}, \mathrm{Y}, \tau_{\mathrm{pp}}) = (\mathrm{X}_{mm+1/2}, \mathrm{Y}_{nn+1/2}, \tau_{\mathrm{pp}})$$
$$= (\mathrm{mm}+1/2, \mathrm{nn}+1/2, \mathrm{pp})$$

The contact area is considered to be composed of ncon rectangular patches, each divided into ma elements in X, and nb elements in Y. Thus, the m and n summations in equation (4.17) can be expressed as,

$$\sum_{j=1}^{\text{ncon}} \sum_{m=1}^{\text{ma}} \sum_{n=1}^{\text{nb}} Q1_{j\,m\,n}^{pp-1}\, GI_{j\,m\,n}^{pp-1}(jj, mm + 1/2, nn + 1/2, pp)$$

$$= \sum_{j=1}^{\text{ncon}} \sum_{m=1}^{\text{ma}} \sum_{n=1}^{\text{nb}} QS_{j,m,n}^{pp-1}\, G2I_{j,m,n}^{pp-1}(jj, mm + 1/2, nn + 1/2, pp)$$

$$+ \sum_{p=0}^{pp-2} \sum_{j=1}^{\text{ncon}} \sum_{m=1}^{\text{ma}} \sum_{n=1}^{\text{nb}} [QS_{j,m,n}^{p} G2I_{j,m,n}^{p}(jj, mm + 1/2, nn + 1/2, pp)$$

$$- Q1_{j,m,n}^{p} GI_{j,m,n}^{p}(jj, mm + 1/2, nn + 1/2, pp)] \qquad (4.18)$$

where,

jj = 1, ncon	ncon is the number of contacts
mm = 1, ma	ma is the number of elements per contact in X
nn = 1, nb	nb is the number of elements per contact in Y

Equation (4.18) can be written in matrix form as,

$$\mathbf{GI} \bullet \mathbf{q1} = \mathbf{f} \qquad (4.19)$$

where,

$$q1(I) = \begin{bmatrix} Q1^{pp-1}_{1,1,1} \\ Q1^{pp-1}_{1,1,2} \\ \downarrow \text{increment j, m, n} \\ \bullet \\ \bullet \\ \bullet \\ Q1^{pp-1}_{ncon,\,ma,\,nb} \end{bmatrix} \tag{4.20a}$$

$$GI(I, K) = \begin{bmatrix} \rightarrow \text{increment j, m, n} \\ \downarrow \text{increment jj, mm, nn} \\ \bullet \\ \bullet \\ \bullet \\ GI^{pp-1}_{j\,m\,n}(jj, mm + 1/2, nn + 1/2, pp) \end{bmatrix} \tag{4.20b}$$

$$f(I) = \begin{bmatrix} \downarrow \text{increment jj, mm, nn} \\ \bullet \\ \bullet \\ \bullet \\ f(jj, mm + 1/2, nn + 1/2, pp) \end{bmatrix} \tag{4.20c}$$

The solution of equation (4.18) gives the desired heat flux distribution, $Q1^{pp-1}_{j,m,,n}$. Once the heat distribution is known, the surface temperature can be evaluate in term of $Q1^{pp-1}_{j,m,,n}$. using equation (4.9). Equation (4.9) is discretized with the midpoint rule as follows,

$$\theta_{s\,i}(X, Y, \tau) = \frac{2\,\Lambda_i}{K_i} \int_{\tau_o=0}^{\tau} \iint_{A_c(X,Y)} Q_i''\,(G_i)_{Z_o=Z=0} dX_o dY_o d\tau_o$$

$$= \frac{2\,\Lambda_i}{K_i} \sum_{p=0}^{pp-1} \sum_{j=1}^{ncon} \sum_{m=1}^{ma} \sum_{n=1}^{nb} Qi^{p}_{j,m,n}\, GiI^{p}_{j,m,n}(X, Y, \tau_{pp}) \tag{4.21}$$

where, i = 1 or 2.

Chapter 5

RESULTS AND DISCUSSIONS

NUMERICAL PARAMETERS

Integration rule

A comparison of numerical integration rules is shown in Figure 2 on page 40 for the constant velocity case with A = 1 and 10. In the low Peclet number (A = 1) case, the distribution of frictional heat is divided evenly and both numerical rules predict similar results. However, use of the trapezoidal rule results in numerical oscillation of the distribution of frictional heat for the high Peclet number (A = 10) case. The results of the trapezoidal rule oscillate about the results obtained from the midpoint rule, and are out of the range of this figure after 50 time steps. The temperature rise shows behavior similar to the distribution of frictional heat; therefore, a numerical oscillation of the

temperature also occurs. Since the trapezoidal rule is unstable and shows numerical oscillation for high Peclet number, all the following results are based on the midpoint rule as it is simple and does not exhibit numerical oscillation for high Peclet number.

In order to compare with the existing single region results, a special case of $K_1 = 0$ is input into the BIEM program ("APPENDIX D: Listing of the Program: FRHMID FORTRAN" on page 111). As expected, the distribution of frictional heat, $(\frac{Q_2}{Q_r})$, to the moving region resulting from this case is one. Figure 3 on page 41 shows the temperature rise of the moving region for this special case of unidirectional motion where the moving region gets all the frictional heat, with Peclet number of A = 0.2, 2, 4. These results are indistinguishable from the square contact results of Jaeger [4] , in which his Peclet number is defined as

$$L = \frac{l v_m}{2\alpha} = \frac{1}{2} A$$

where l is the half width of the square contact area. The above comparison validates the BIEM program for the single region case.

Constant velocity

Table 1 on page 43 is a numerical study of the BIEM for constant velocity using the midpoint rule. θ_r and $\frac{Q_2}{Q_r}$, tabulated at the center of contact, are the dimensionless surface temperature rise and the fraction of frictional heat distributed to region-2, respectively. $(\frac{Q_2}{Q_r})_{total}$ is the fraction of total frictional heat distributed to region-2 over the entire contact area. The table clearly shows that the number of the spatial elements has less influence on the numerical accuracy than the size of the time step. Data in

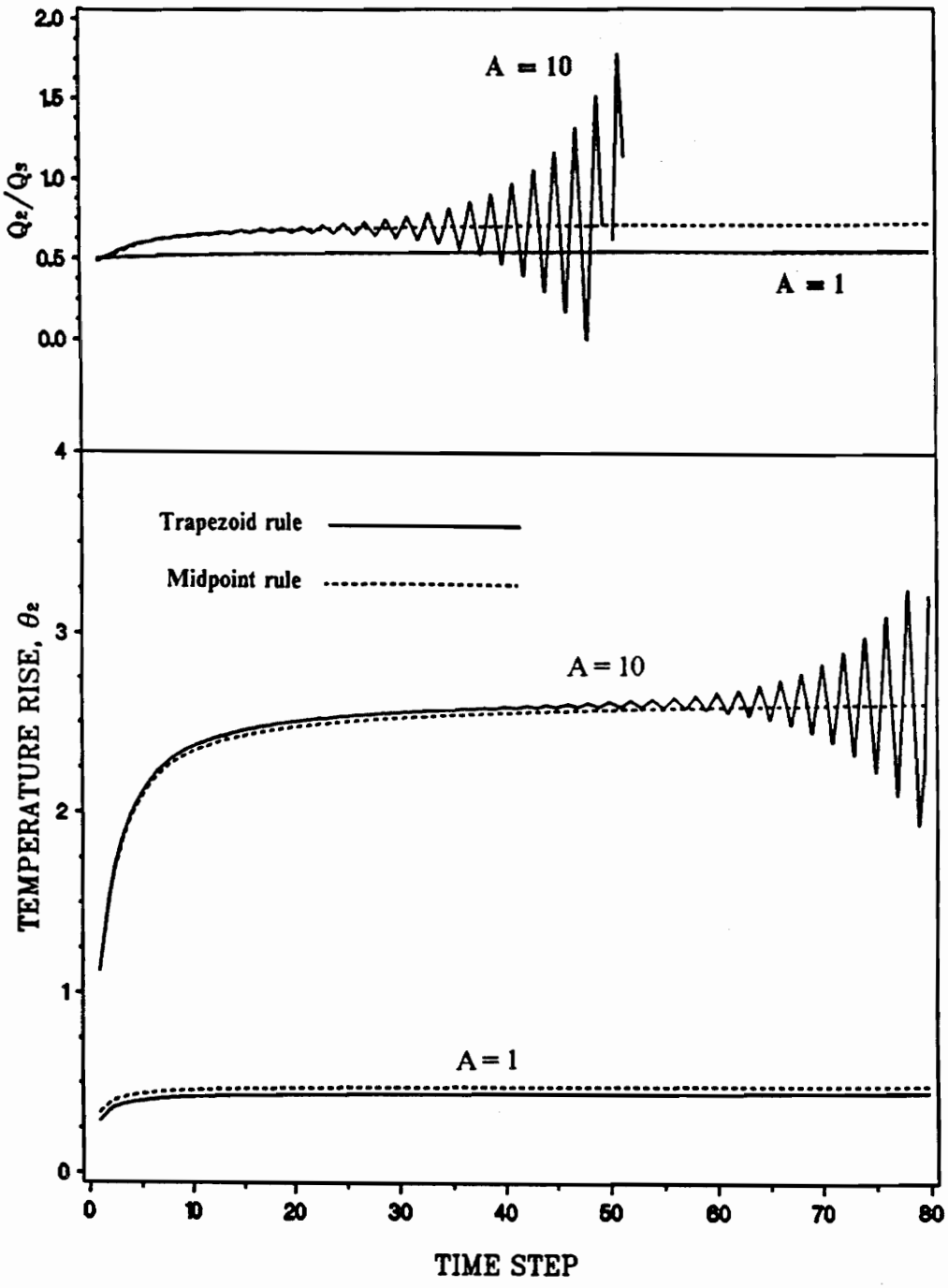

Figure 2. The comparison of numerical integration rules – Trapezoidal and midpoint rules.

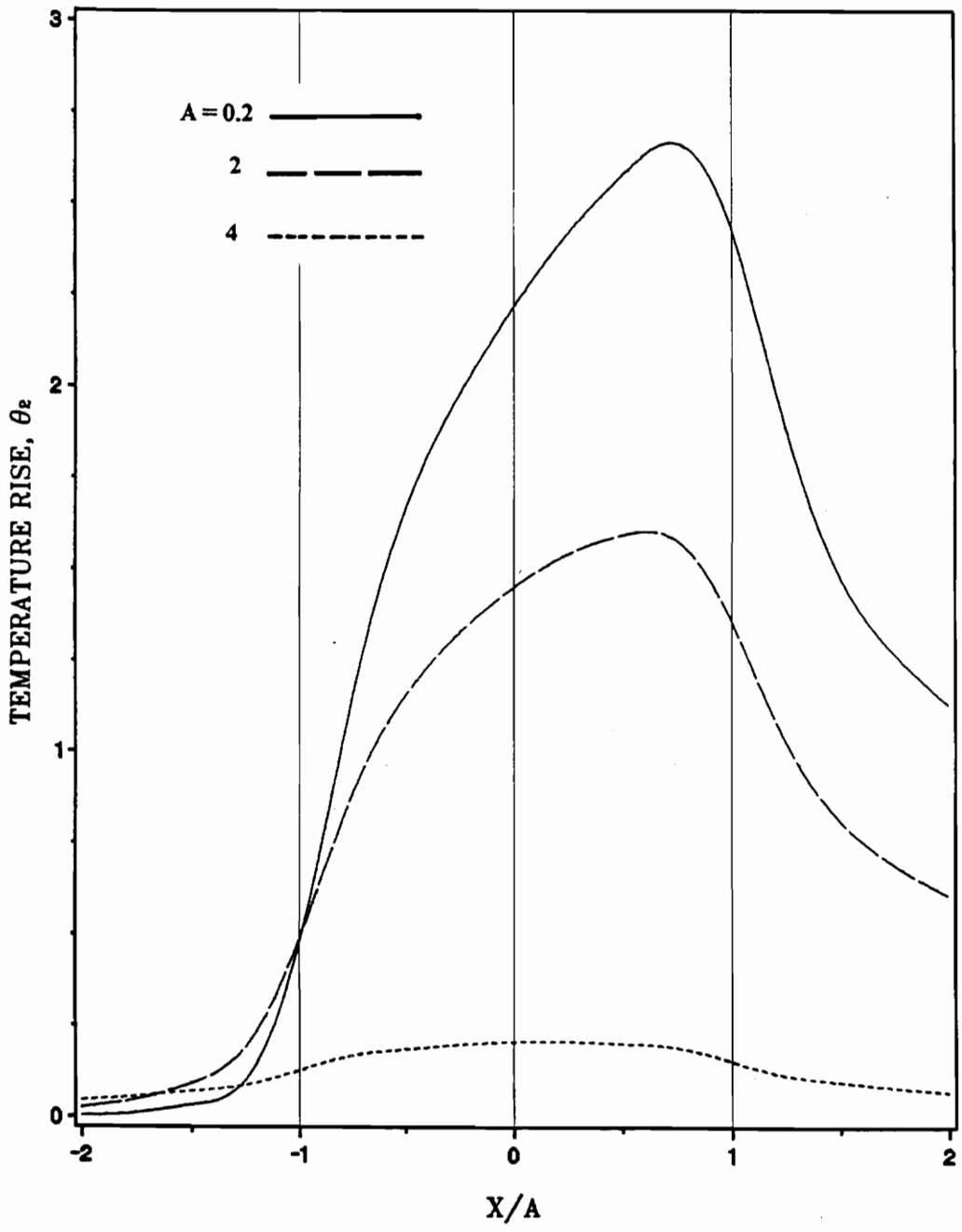

Figure 3. A special case where the moving region receives all the heat for unidirectional motion

Table 1 shows that accurate results can be obtained using the following correlation for the time step

$$\Delta\tau \leq \frac{\pi}{8} A$$

Oscillating velocity

Table 2 on page 44 through Table 5 on page 47 are the numerical studies of the BIEM using the midpoint rule for oscillating velocity. The frictional heat distributions, $\frac{Q_2}{Q_1}$, on Table 5, are greater than one at the zero velocity because the frictional heat, Q_1, at this point is zero. As in the constant velocity case, the number of the spatial elements is less important than the size of time step ($\Delta\tau$). The time step is defined as

$$\Delta\tau = \frac{\pi}{2 \cdot \Omega \cdot IDT}$$

where IDT is the number of steps per quarter cycle. These tables show accurate results for IDT = 4 or higher. Increasing the number of elements does not result in a significant improvement of accuracy but significantly increases cpu time. Thus, increasing the number of elements is not the desired manner for achieving higher accuracy.

Table 1. Numerical study of BIEM for constant velocity case $K_1 = \Lambda_1 = 1.0$: (a) A = 1.0, at $\tau = 20$, (b) A = 10.0, at $\tau = 80$

	ma × nb = 1x1			ma × nb = 3x1			ma × nb = 9x3		
$\Delta\tau$	θ_s	$\frac{Q_2}{Q_s}$	$(\frac{Q_2}{Q_s})$Total	θ_s	$\frac{Q_2}{Q_s}$	$(\frac{Q_2}{Q_s})$Total	θ_s	$\frac{Q_2}{Q_s}$	$(\frac{Q_2}{Q_s})$Total
4.00	0.3534	0.6123	0.6123	0.3583	0.6176	0.5986	0.3587	0.6200	0.5956
2.00	0.4032	0.5858	0.5858	0.4164	0.5870	0.5655	0.4161	0.5874	0.5652
1.00	0.4576	0.5582	0.5582	0.4726	0.5390	0.5454	0.4722	0.5331	0.5479
0.50	0.4815	0.5457	0.5457	0.4917	0.5190	0.5425	0.4913	0.5137	0.5454
0.25	0.4789	0.5437	0.5437	0.4852	0.5280	0.5418	0.4846	0.5299	0.5446
0.10	0.4761	0.5438	0.5438	0.4804	0.5359	0.5415	0.4807	0.5320	0.5444

	ma × nb = 1x1			ma × nb = 3x1			ma × nb = 9x3		
$\Delta\tau$	θ_s	$\frac{Q_2}{Q_s}$	$(\frac{Q_2}{Q_s})Total$	θ_s	$\frac{Q_2}{Q_s}$	$(\frac{Q_2}{Q_s})Total$	θ_s	$\frac{Q_2}{Q_s}$	$(\frac{Q_2}{Q_s})Total$
16.0	2.274	0.7100	0.7100	2.810	0.5701	0.6900	2.758	0.5664	0.6732
8.0	2.449	0.6897	0.6897	2.777	0.6048	0.6776	2.618	0.7297	0.6589
4.0	2.477	0.6873	0.6873	2.625	0.6676	0.6674	2.652	0.6779	0.6548
2.0	2.483	0.6870	0.6870	2.611	0.6758	0.6656	2.636	0.6856	0.6543
1.0	2.484	0.6871	0.6871	2.611	0.6763	0.6656	2.629	0.6850	0.6541
0.5	2.485	0.6872	0.6872	2.611	0.6767	0.6657	2.627	0.6855	0.6541

Table 2. Numerical study of BIEM for oscillating velocity case: $K_1 = \Lambda_1 = 1.0$, $A = 1.0$, $\Omega = 1.0$, $\frac{x_m}{a} = 1.0$

				At $2\frac{1}{4}$ cycles (V = 0)			At $2\frac{1}{2}$ cycles ($V = V_{max}$)		
ma × nb	CPU (sec)	IDT	$\Delta\tau$	θ_s	$\frac{Q_2}{Q_s}$	$(\frac{Q_2}{Q_s})$Total	θ_s	$\frac{Q_2}{Q_s}$	$(\frac{Q_2}{Q_s})$Total
1X1	0.1	1	1.5708	0.3368	0.5104	0.5104	0.3269	0.5322	0.5322
	0.1	2	0.7854	0.2459	0.5091	0.5091	0.4115	0.5164	0.5164
	0.4	4	0.3927	0.1968	0.5196	0.5196	0.4331	0.5087	0.5087
	1.4	8	0.1964	0.1769	0.5356	0.5356	0.4304	0.5081	0.5081
3X1	0.2	1	1.5708	0.3389	0.5103	0.5082	0.3334	0.5317	0.5171
	0.8	2	0.7854	0.2470	0.5094	0.5102	0.4189	0.5033	0.5082
	2.9	4	0.3927	0.1974	0.5192	0.5192	0.4375	0.4965	0.5067
	11.5	8	0.1964	0.1774	0.5381	0.5361	0.4327	0.5028	0.5063
9X3	15.0	1	1.5708	0.3389	0.5102	0.5084	0.3332	0.5339	0.5160
	58.0	2	0.7854	0.2470	0.5074	0.5111	0.4187	0.5041	0.5076
	229.0	4	0.3927	0.1975	0.5158	0.5213	0.4371	0.4984	0.5058
	898.0	8	0.1964	0.1775	0.5329	0.5398	0.4323	0.5064	0.5055

Table 3. Numerical study of BIEM for oscillating velocity case $K_1 = \Lambda_1 = 1.0$, $A = 1.0$, $\Omega = 10.0$, $\frac{x_m}{a} = 0.1$

				At 4 $\frac{3}{4}$ cycles (V = 0)			At 5 cycles ($V = V_{max}$)		
ma × nb	CPU (sec)	IDT	$\Delta\tau$	θ_s	$\frac{Q_2}{Q_s}$	$(\frac{Q_2}{Q_s})$Total	θ_s	$\frac{Q_2}{Q_s}$	$(\frac{Q_2}{Q_s})$Total
1X1	0.1	1	0.15708	0.3239	0.5016	0.5052	0.3261	0.4998	0.4998
	0.4	2	0.07854	0.2752	0.5025	0.5025	0.3253	0.4998	0.4998
	1.0	4	0.03927	0.2580	0.5044	0.5044	0.3248	0.4998	0.4999
	5.0	8	0.01964	0.2519	0.5079	0.5079	0.3245	0.4999	0.4999
3X1	0.8	1	0.15708	0.3241	0.5007	0.5009	0.3263	0.4985	0.5006
	3.0	2	0.07854	0.2753	0.5017	0.5013	0.3253	0.4997	0.5003
	12.0	4	0.03927	0.2580	0.5034	0.5025	0.3247	0.5000	0.5002
	46.0	8	0.01964	0.2519	0.5065	0.5044	0.3244	0.5001	0.5003
9X3	61.0	1	0.15708	0.3241	0.5012	0.5008	0.3262	0.5001	0.5001
	236.0	2	0.07854	0.2753	0.5021	0.5014	0.3253	0.4998	0.5002
	923.0	4	0.03927	0.2580	0.5040	0.5025	0.3247	0.5000	0.5001
	3658.0	8	0.01964	0.2519	0.5075	0.5046	0.3244	0.5001	0.5002

Table 4. Numerical study of BIEM for oscillating velocity case $K_1 = \Lambda_1 = 1.0$, $A = 10.0$, $\Omega = 1.0$, $\frac{x_m}{a} = 0.1$

				At 7 $\frac{1}{4}$ cycles (V = 0)			At 7 $\frac{1}{2}$ cycles (V = V_{max})		
ma × nb	CPU (sec)	IDT	$\Delta\tau$	θ_s	$\frac{Q_2}{Q_s}$	$(\frac{Q_2}{Q_s})$Total	θ_s	$\frac{Q_2}{Q_s}$	$(\frac{Q_2}{Q_s})$Total
1X1	0.3	1	1.5708	2.281	0.5025	0.5025	2.306	0.4988	0.4988
	1.0	2	0.7854	2.033	0.5048	0.5048	2.205	0.4988	0.4988
	3.7	4	0.3927	1.956	0.5093	0.5093	2.180	0.4989	0.4989
	14.3	8	0.1964	1.932	0.5180	0.5180	2.174	0.4990	0.4990
3X1	2.0	1	1.5708	2.279	0.5018	0.5064	2.304	0.4986	0.4973
	7.8	2	0.7854	2.029	0.5048	0.5112	2.202	0.4993	0.4979
	30.8	4	0.3927	1.952	0.5100	0.5207	2.176	0.4996	0.4982
	121.2	8	0.1964	1.927	0.5194	0.5383	2.169	0.4998	0.4985
9X3	151.7	1	1.5708	2.280	0.5018	0.5037	2.305	0.4993	0.5004
	594.9	2	0.7854	2.030	0.5044	0.5064	2.202	0.4995	0.5000
	2344.7	4	0.3927	1.953	0.5087	0.5123	2.172	0.4997	0.4999
	9205.0	8	0.1964	1.928	0.5171	0.5225	2.169	0.4998	0.5001

Table 5. Numerical study of BIEM for oscillating velocity case $K_1 = \Lambda_1 = 1.0$, $A = 10.0$, $\Omega = 0.1$, $\frac{x_m}{a} = 1.0$

				At $4\frac{3}{4}$ cycles (V = 0)			At 5 cycles ($V = V_{max}$)		
ma × nb	CPU (sec)	IDT	$\Delta\tau$	θ_s	$\frac{Q_2}{Q_s}$	$(\frac{Q_2}{Q_s})$Total	θ_s	$\frac{Q_2}{Q_s}$	$(\frac{Q_2}{Q_s})$Total
1X1	2.3	5	3.1416	2.162	0.8254	0.8254	3.093	0.5062	0.5062
	8.6	10	1.5708	2.121	1.082	1.082	3.093	0.5012	0.5012
	33.6	20	0.7854	2.107	1.581	1.581	3.092	0.5157	0.5157
3X1	18.7	5	3.1416	2.217	0.8032	0.7191	3.089	0.5042	0.5190
	74.1	10	1.5708	2.174	1.061	0.8951	3.078	0.5108	0.5216
	294.0	20	0.7854	2.158	1.564	1.235	3.076	0.5137	0.5238
9X1	165.8	5	3.1416	2.224	0.8148	0.7196	3.089	0.5111	0.5145
	657.7	10	1.5708	2.176	1.077	0.8951	3.079	0.5127	0.5173
9X3	1453.0	5	3.1416	2.222	0.8382	0.7197	3.087	0.5119	0.5130
	5780.0	10	1.5708	2.175	1.125	0.9072	3.077	0.5135	0.5152

PHYSICAL PARAMETERS

Constant velocity

Figure 4 on page 49 illustrates the time-space development of the distribution of frictional heat and surface temperature rise for the stationary region and the moving region, θ_1 and θ_2 , respectively. This Figure clearly shows that the temperature rise for the two regions match in the contact area. As the cooler new material, from the negative X region enters the contact area, the negative X region receives a higher fraction of frictional heat distribution than the positive X section. The cold section tends to get more heat than the hotter section. As a result, in the negative X region, $\theta_1 > \theta_2$ while in the positive X region, $\theta_2 > \theta_1$.

The effect of Peclet number (A,B) for unidirectional velocity is shown in Figure 5 on page 50. Since the regions have identical thermal properties, the frictional heat is divided evenly for low Peclet numbers. As Peclet number increases; however, region-2 gets a higher fraction of the frictional heat than region-1 because of the uneven heat and temperature distributions. The surface temperature rise increases proportionally to Peclet number, because as Peclet number increases, the mechanical energy input into the system increases.

The effect of the thermal property ratios for the two regions are also important parameters that influence the surface temperature rise. Figure 6 on page 52 shows the frictional heat distribution and surface temperature rise for unidirectional motion. As the thermal property ratios (Λ_1 and K_1) increase, the thermal conductivity of the region-1

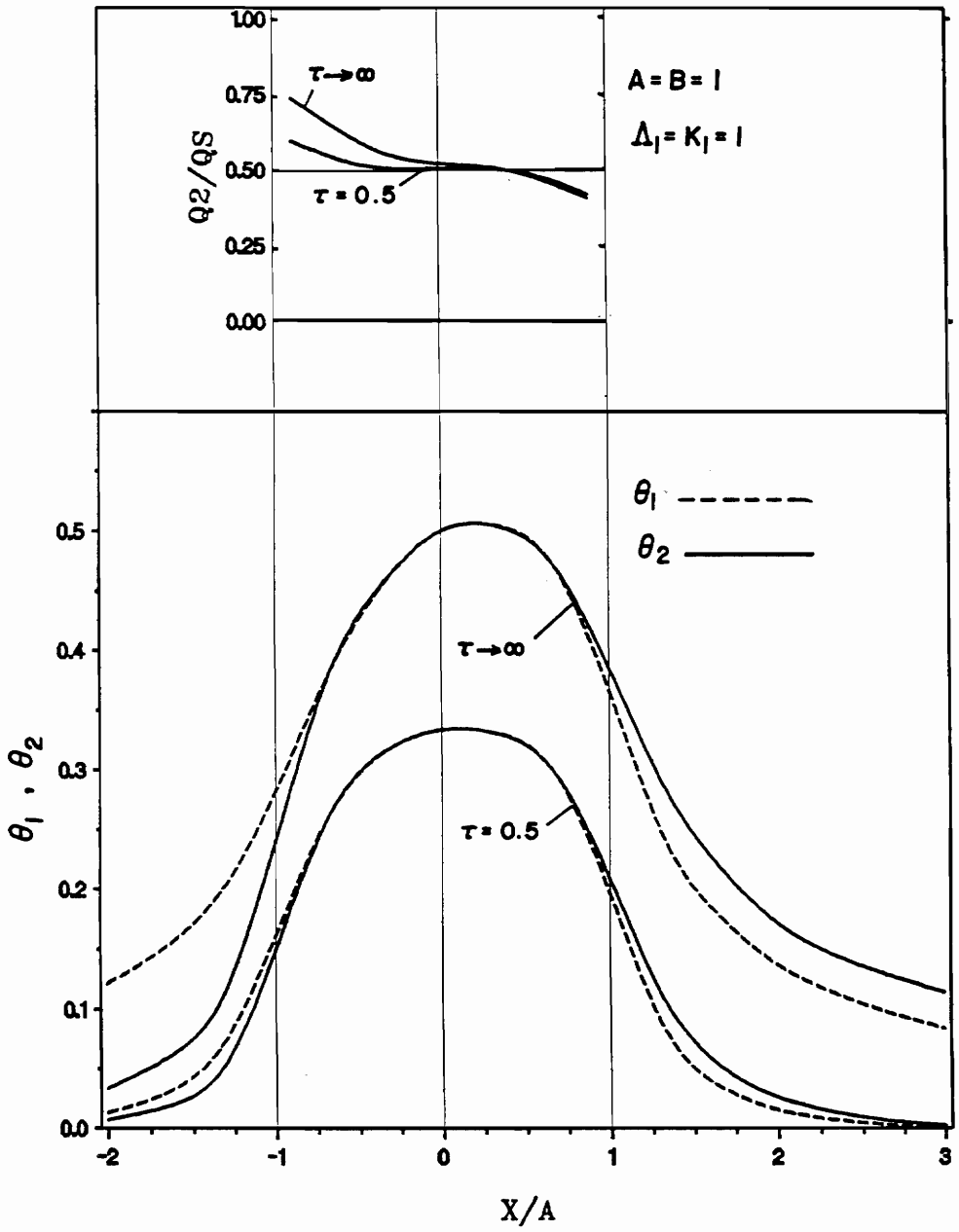

Figure 4. The time-space development of the distribution of frictional heat and surface temperature rise of the two regions with unidirectional motion.

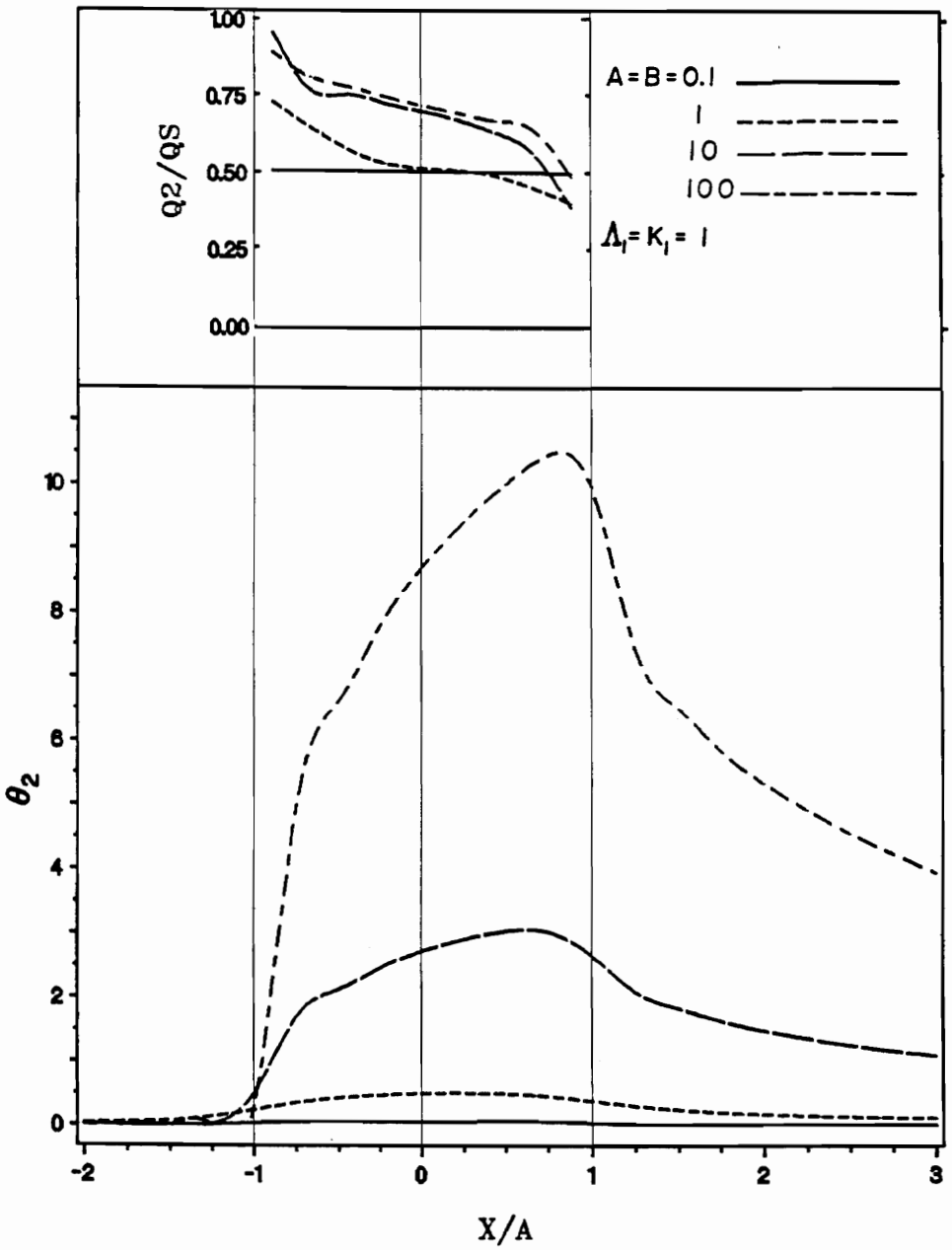

Figure 5. The effect of peclet number on the steady state distribution of frictional heat and surface temperature rise for unidirectional motion.

(k_1) increases with respect to the thermal conductivity of the region-2 (k_2). Region-2 gets the highest distribution of frictional heat for the lowest thermal property ratio, $\Lambda_1 = K_1 = 0.1$, and as a result, produces the highest temperature rise. Thus, the distribution of frictional heat to region-2 decreases as the thermal property ratio increases, and the surface temperature rise increases as the distribution of frictional heat to region-2 increases.

Figure 7 on page 53 shows the effect of multiple contacts and spacing between the contact areas. This figure illustrates that not just the number of contacts is an important factor but also the spacing between the contacts, because one heated area may affect another if the spacing between them is small.

Figure 8 on page 54 and Figure 9 on page 55 further elaborate the effect of multiple contacts for unidirectional motion. The results display the effect of the number of contacts, N, the spacing between the contacts, D, and the orientation of the contacts. The results are referenced to the single square contact case where the total area is a square patch of dimensions 2A by 2A for each case. The vertical axis is the ratio of the mean surface temperature rise, θ_m , to the surface temperature rise of a single square contact, θ_{m1}. Although results for A = B = 10 are displayed, further numerical studies show that the curves in Figures 8 and 9 are virtually unchanged at other values of the Peclet number, A. These figures show that not just the distance and the number of contact areas but also the orientation of contact areas are important factors in determining the mean temperature rise. Figure 8 on page 54 is for divided contact areas oriented in the direction of motion while Figure 9 on page 55 is for patches oriented perpendicular to the direction of motion. The divided contacts oriented along the motion have more heat interaction between patches than the divided areas oriented perpendicular to the motion.

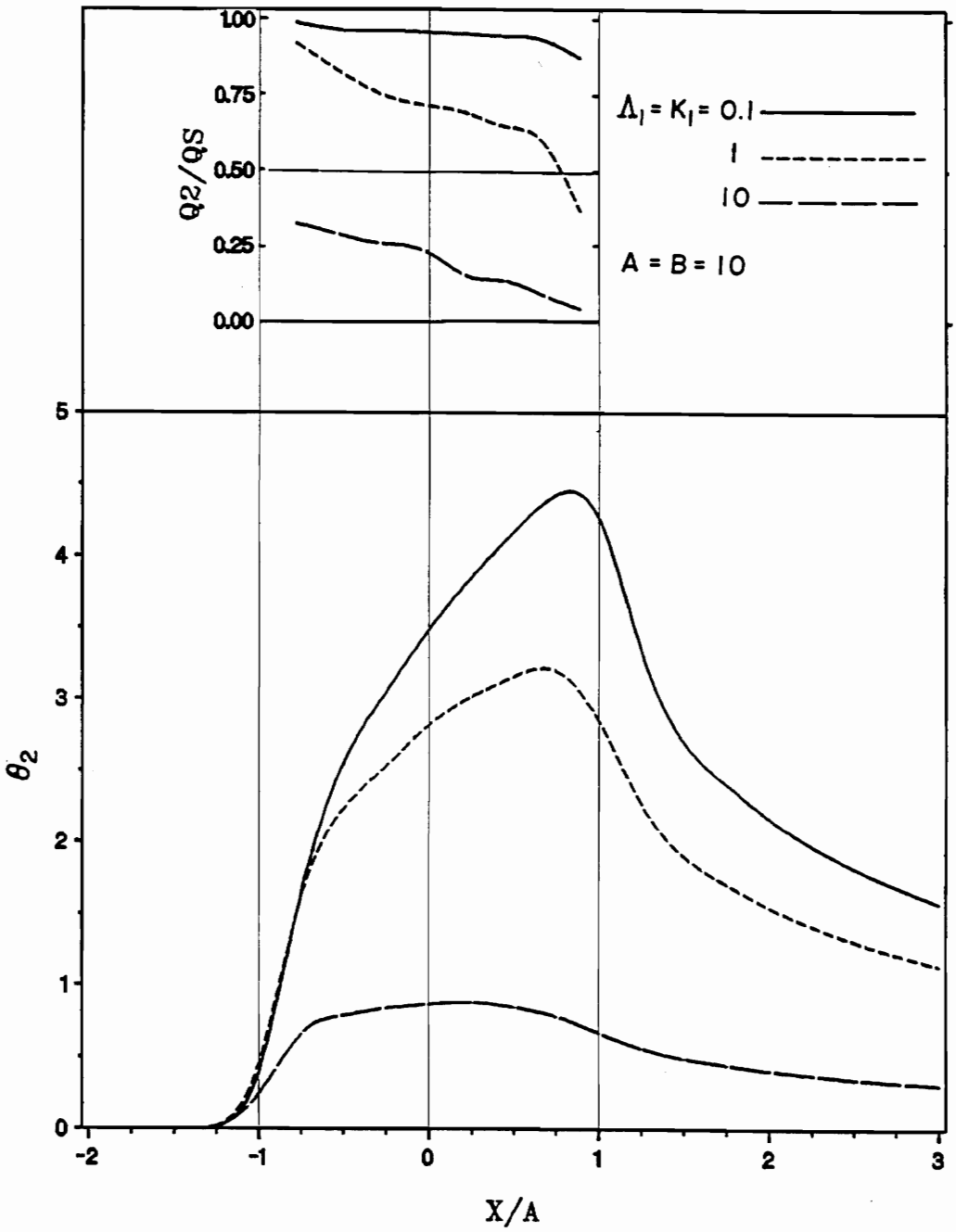

Figure 6. The effect of thermal property ratio on the steady state distribution of frictional heat and surface temperature rise for unidirectional motion.

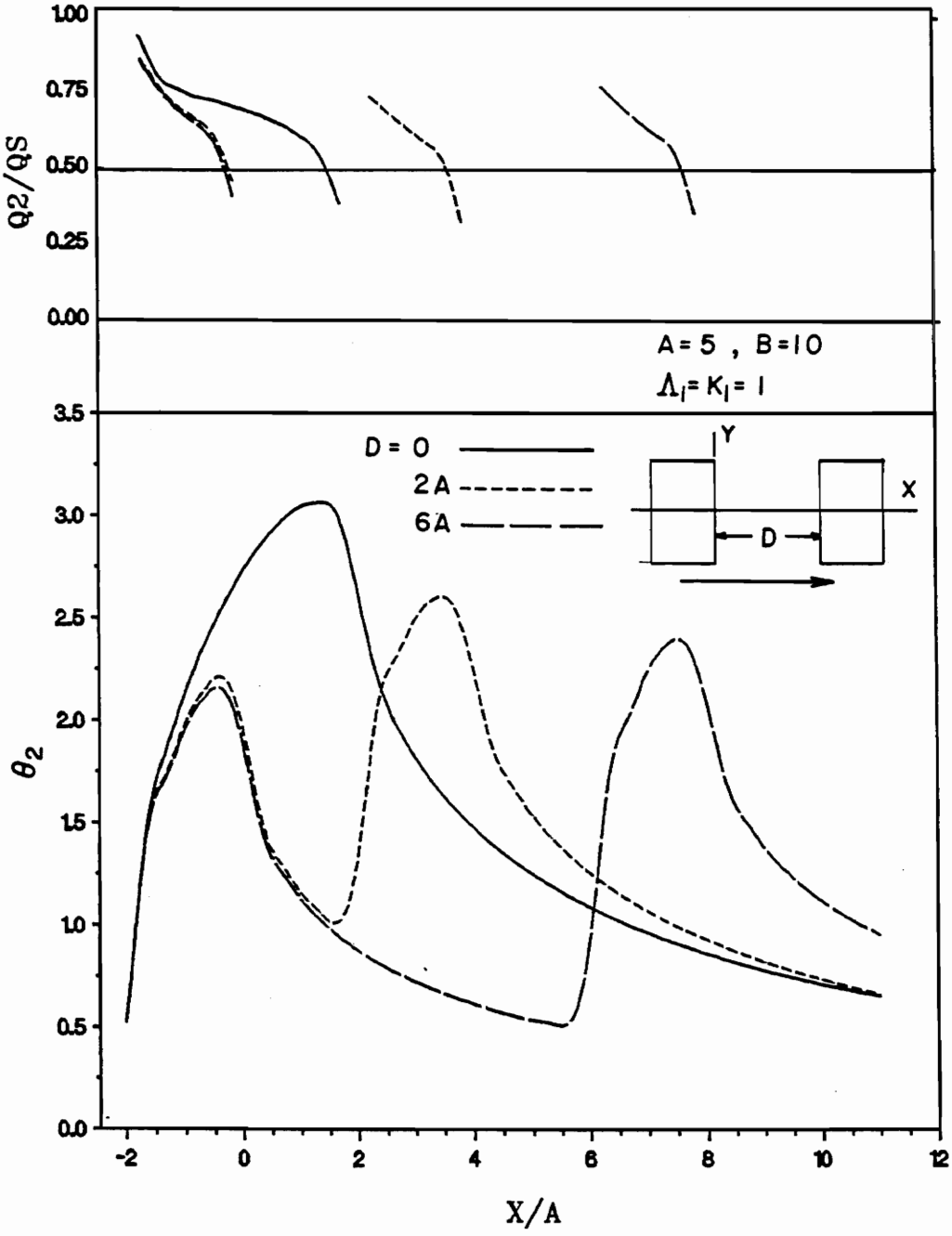

Figure 7. The study of multiple contacts and spacing on the steady state distribution of frictional heat and surface temperature rise for unidirectional motion.

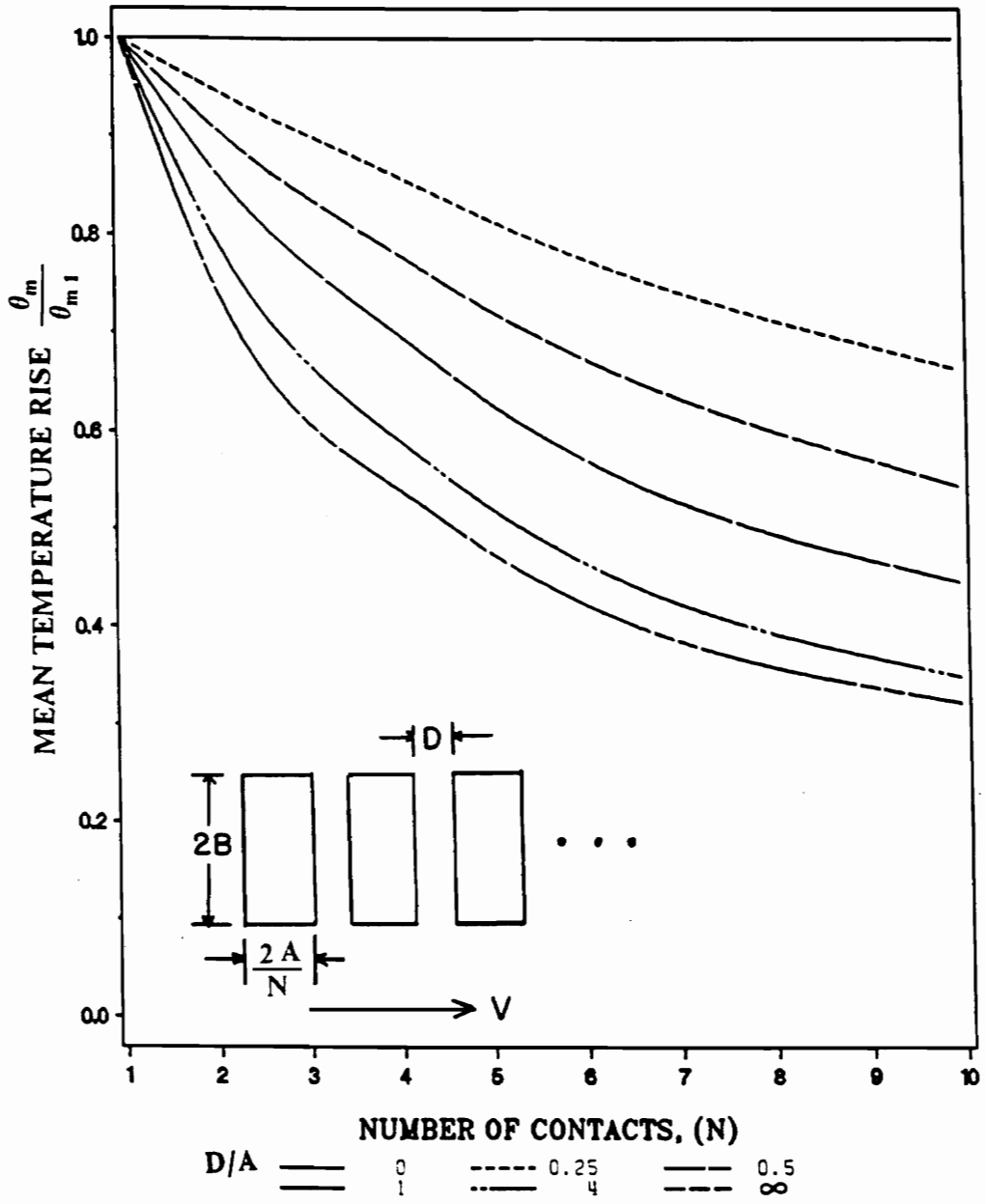

Figure 8. A study of multiple contacts and spacing on the normalized steady state mean surface temperature rise for unidirectional motion with contacts oriented along the direction of motion: $A = 10$, $B = 10$, $K_1 = \Lambda_1 = 1.0$

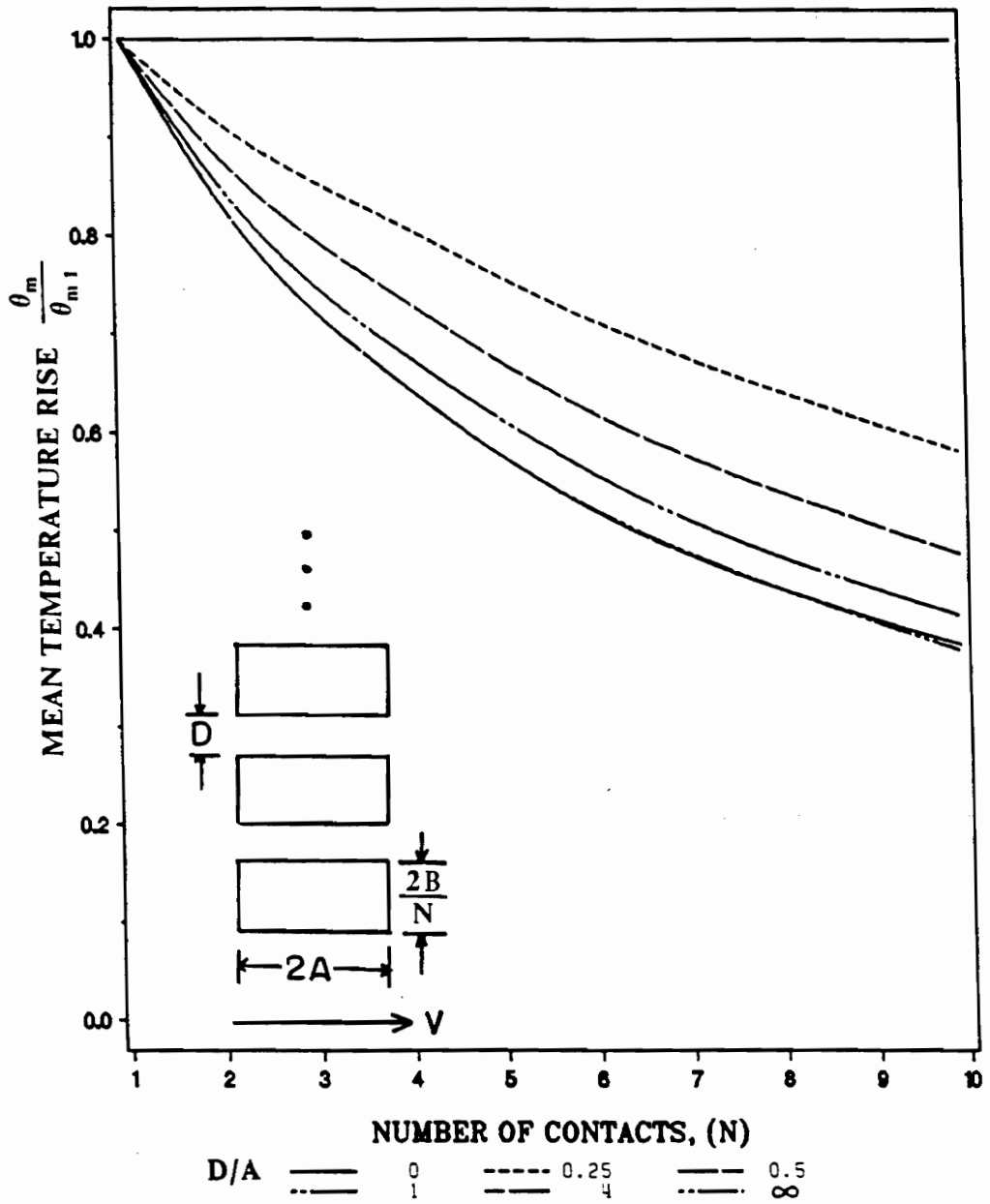

Figure 9. A study of multiple contacts and spacing on the normalized steady state mean surface temperature rise for unidirectional motion with contacts oriented perpendicular to the direction of motion: $A = 10$, $B = 10$, $K_1 = \Lambda_1 = 1.0$

The curves of $D/A \rightarrow \infty$ represent infinite spacing or no thermal interaction between the contact patches. For a spacing of approximately $D/A = 4$ or less, there is significant interaction between the heat patches. A complete thermal analysis, including arbitrary, interacting heat sources, is complex and computationally time consuming compared to simpler approximate analyses such as Archard [5, 6]. However, the results of Figure 8 and 9, which are applicable to all Peclet numbers, can be used in conjunction with a simpler single contact area analyses to refine surface temperature estimates for multiple, interacting heated areas.

Oscillating velocity

Figure 10 on page 58 shows the total energy generated, the total fraction of frictional heat, and the mean surface temperature rise of region-2 versus time for stationary, oscillating, and unidirectional motion. The average energy input for all cases is the same (i.e., for unidirectional motion the velocity is $\frac{2}{\pi} \times v_m$, where $v_m = x_m \times \omega$ is the maximum velocity of the oscillating case). The energy for the stationary case is artificially input into the contact area. The results are for regions with identical material properties. The role of velocity in the distribution of frictional heat and resulting temperature rise can be seen in Figure 10. There is no motion for the stationary heat source case to influence the heat distribution, so each region receives 1/2 of the frictional heat. For the unidirectional motion case, new material continuously enters the contact area which causes the heat to be convected away from the contact area. Thus, the effective thermal resistance in the moving region decreases, and allows the moving region to receive a higher percentage of frictional heat, but, lower temperature rise compared to the sta-

tionary case. For the oscillating case, the heat distribution and surface temperature rise are directly affected by the motion. Figure 10 is for a large amplitude ratio, $\frac{x_m}{a} = 1$, and shows that the peak temperature is higher than both the stationary and unidirectional cases. According to the definition of the dimensionless variables given by equation (3.6), the amplitude ratio is

$$\text{Amplitude ratio} = \frac{1}{A \times \Omega} = \frac{x_m}{a}$$

This quantity represents the ratio of the amplitude of oscillation to the half length of a square contact patch.

Figure 11 on page 59 shows the same comparison as Figure 10 on page 58 in stationary and unidirectional motion but for a lower amplitude ratio, $\frac{x_m}{a} = 0.1$, in the oscillating case. The frictional heat distribution to region-2 for the fretting condition is lower than the high amplitude ratio case; however, the oscillating temperature rise is surprisingly high. The band of temperatures, produced by the oscillating case, oscillates about the temperature rise produced by stationary heat source case. This is because the low amplitude ratio motion is similar to the stationary case, as the amplitude of oscillation is small compared with the area of contact, such as fretting [3].

Figure 12 on page 61 shows the same study as Figure 10 on page 58 but for low Peclet number (A = 1). This figure shows that the distribution of frictional heat to region-2 is lower than in the high Peclet number case, which indicates that the high Peclet number causes higher distribution of frictional heat to the moving region. The temperature rise for the stationary and the unidirectional motion are the same magnitude, which also indicates that the unidirectional motion case temperature calculation can be treated as the stationary case if the Peclet number is low. However, the oscillating case can not be

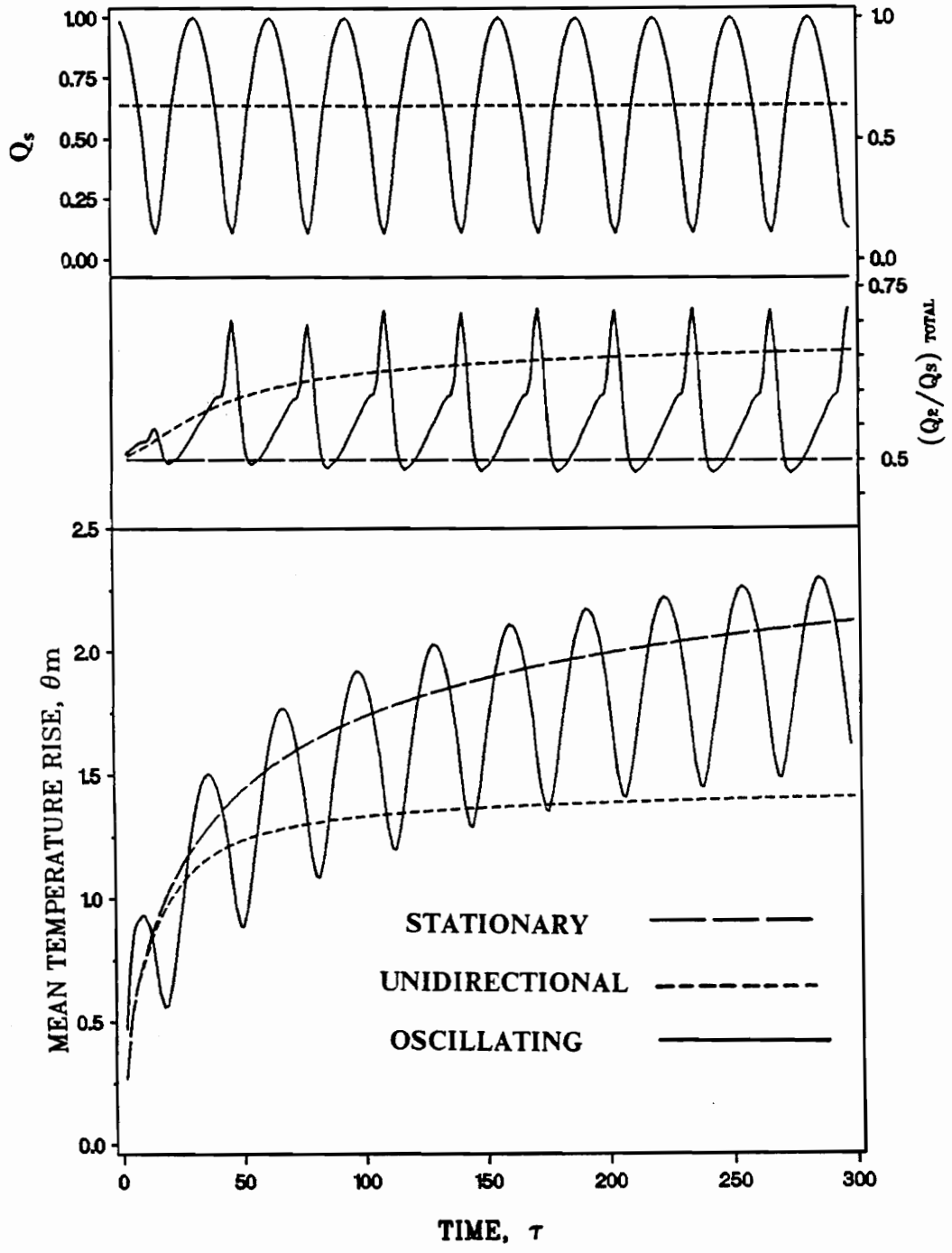

Figure 10. A comparison of total surface frictional heat, distribution of heat, and mean surface temperature rise produced by stationary, oscillating, and unidirectional motion: $x_m/a = 1.0$, $A = 10$, $\Omega = 0.1$, $K_1 = \Lambda_1 = 1.0$

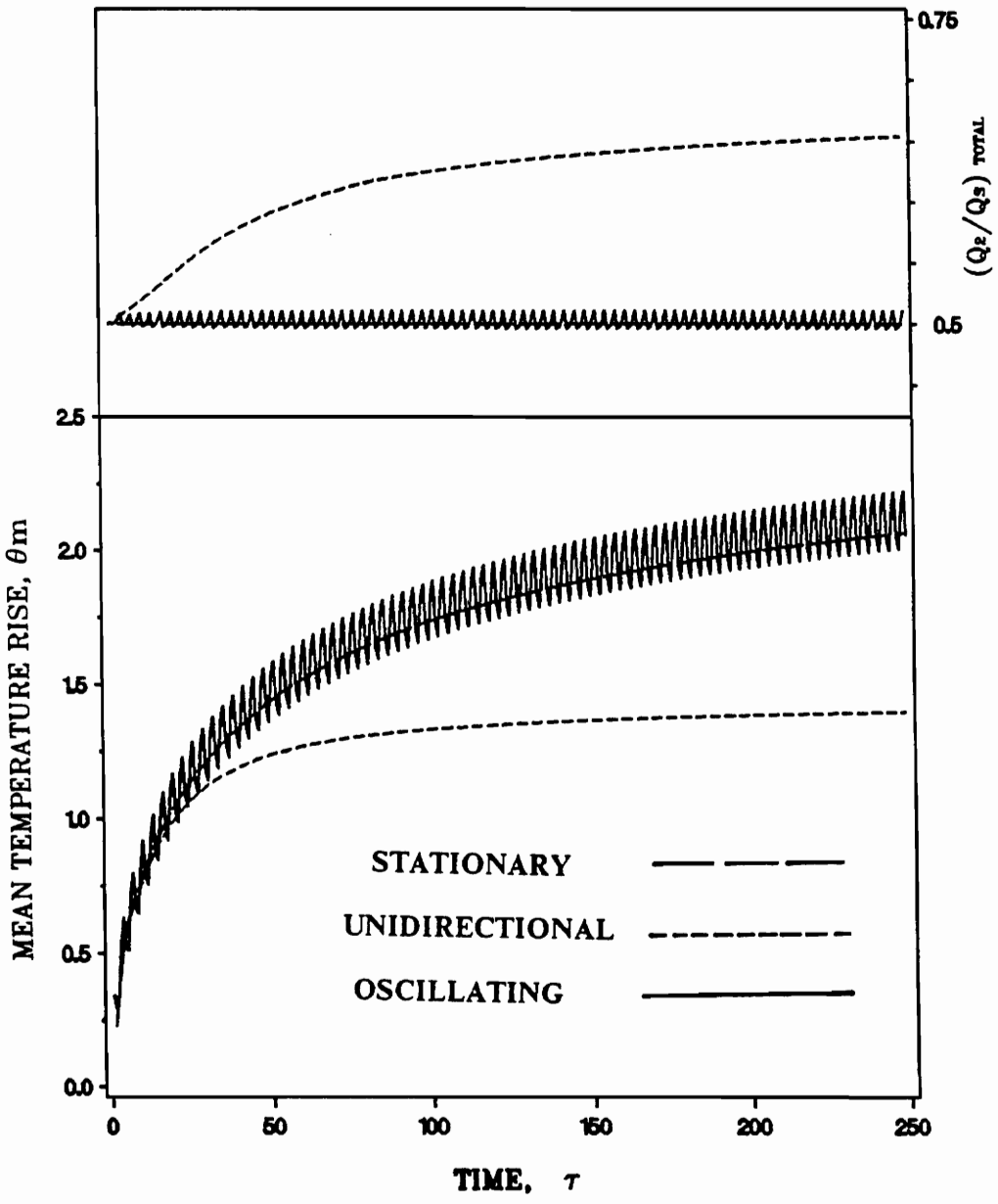

Figure 11. A comparison of total frictional heat distribution, and mean surface temperature rise produced by stationary, oscillating, and unidirectional motion for fretting: $x_m/a = 0.1$, $A = 10$, $\Omega = 1.0$, $K_1 = \Lambda_1 = 1.0$

treated as either the stationary or the unidirectional case; because, the peak temperature of the oscillating case is always higher.

Figure 13 to 15 are detailed studies of the frictional heat distribution and the surface temperature rise in the contact zone. The results are for regions with identical material properties with a single square contact of dimensions 2A by 2B, where A = B = 10, and amplitude ratio ($\frac{x_m}{a}$) = 1. Figure 13 on page 62 shows the distribution of frictional heat and surface temperature rise at the maximum velocity in every cycle. The temperature rises asymptotically in time while the distribution of frictional heat remains almost constant.

Figure 14 on page 63 shows the quasi-steady state distribution of frictional heat and the surface temperature rise at points of zero and maximum velocity during a cycle. The distribution of frictional heat and the surface temperature rise are in a quasi-steady state, because the results repeat every cycle [45]. At positions 1 and 3 the velocities are at a maximum while at positions 2 and 4 the velocities are zero. The rate of frictional heat is assumed to be directly proportional to the absolute velocity; therefore, the temperature rise at the maximum velocity is higher than at the zero velocity. The distribution of frictional heat and temperature rise are mirror images at the same absolute velocities (i.e. the curves at 1 and 3, and at 2 and 4 are mirror images).

Figure 15 on page 65 shows the surface temperature rise at the edges and the center of a square contact area. Peaks in temperature at the edges of contact occur at half the frequency as peaks in the center of contact. This is because when the new material enters the contact area, the temperature at location 1 decreases until it reaches minimum when the velocity is equal to zero. Meanwhile, the temperature at location 3 is continuously increasing as the velocity increases since the point has already been heated for the time

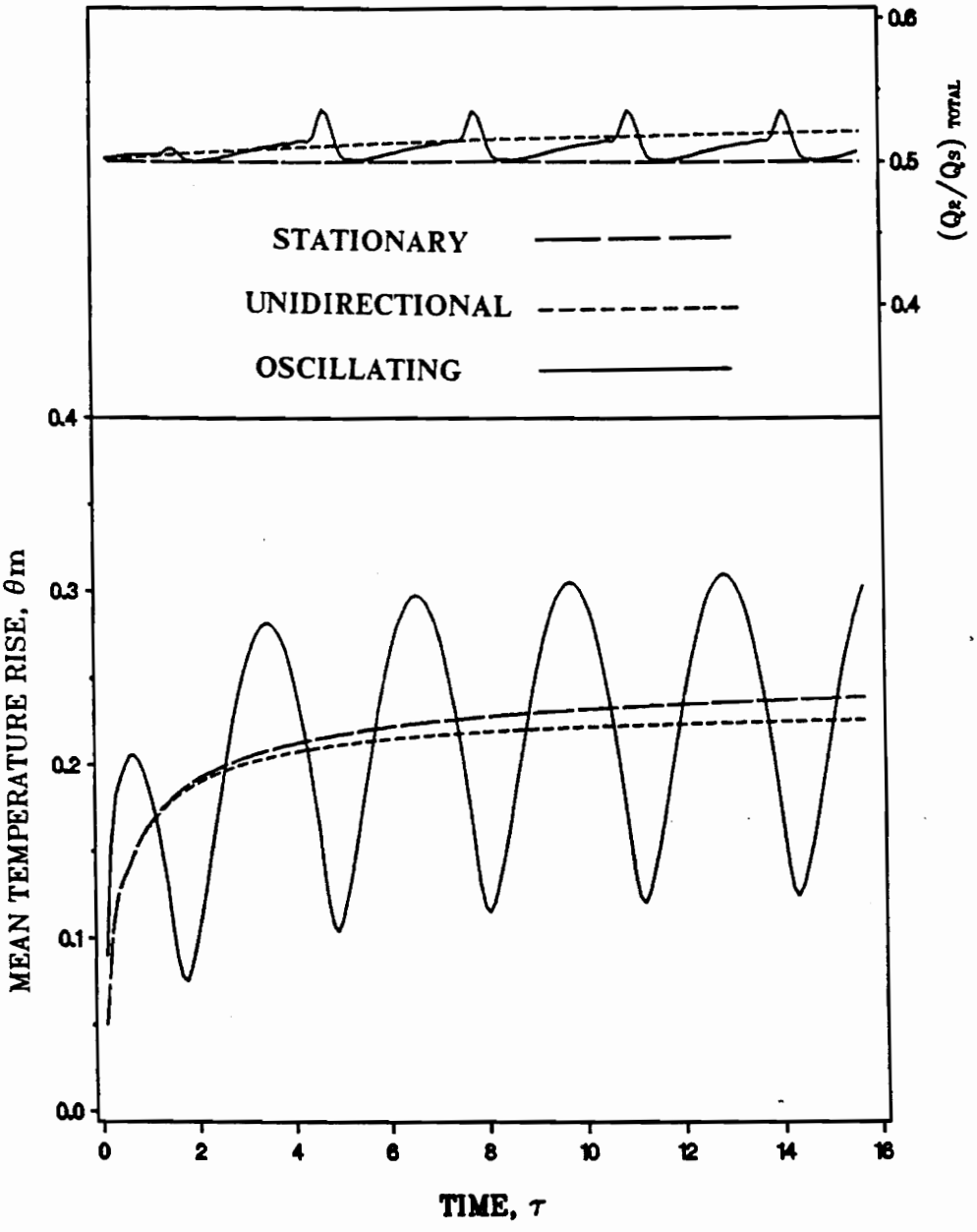

Figure 12. A comparison of distribution of frictional heat, and mean surface temperature rise produced by stationary, oscillating, and unidirectional motion for low Peclet: $x_m/a = 1.0$, $A = 1.0$, $\Omega = 1.0$, $K_1 = \Lambda_1 = 1.0$

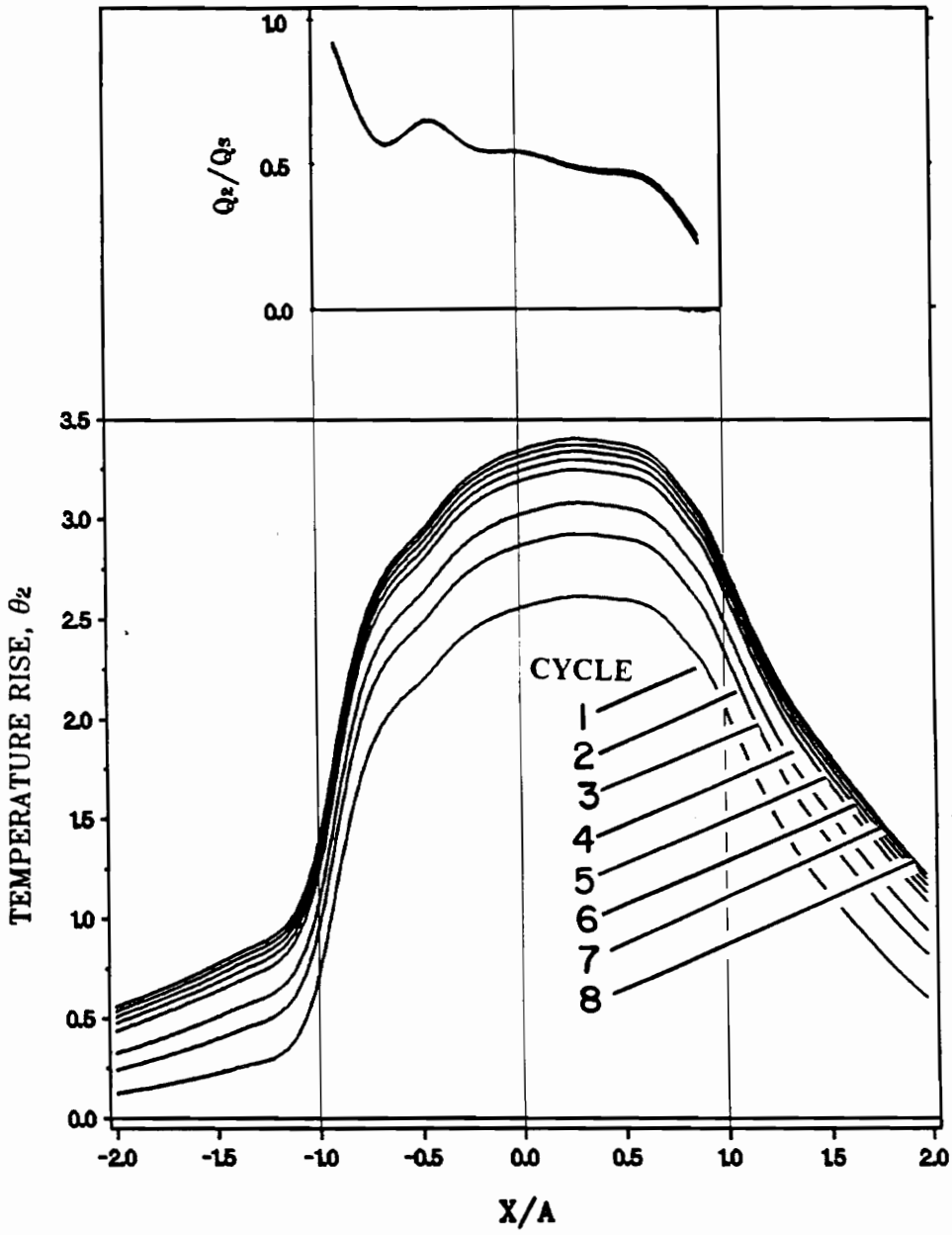

Figure 13. The time-space development of the distribution of frictional heat, and surface temperature rise for oscillating motion: $A = 10$, $\Omega = 0.1$, $K_1 = \Lambda_1 = 1.0$

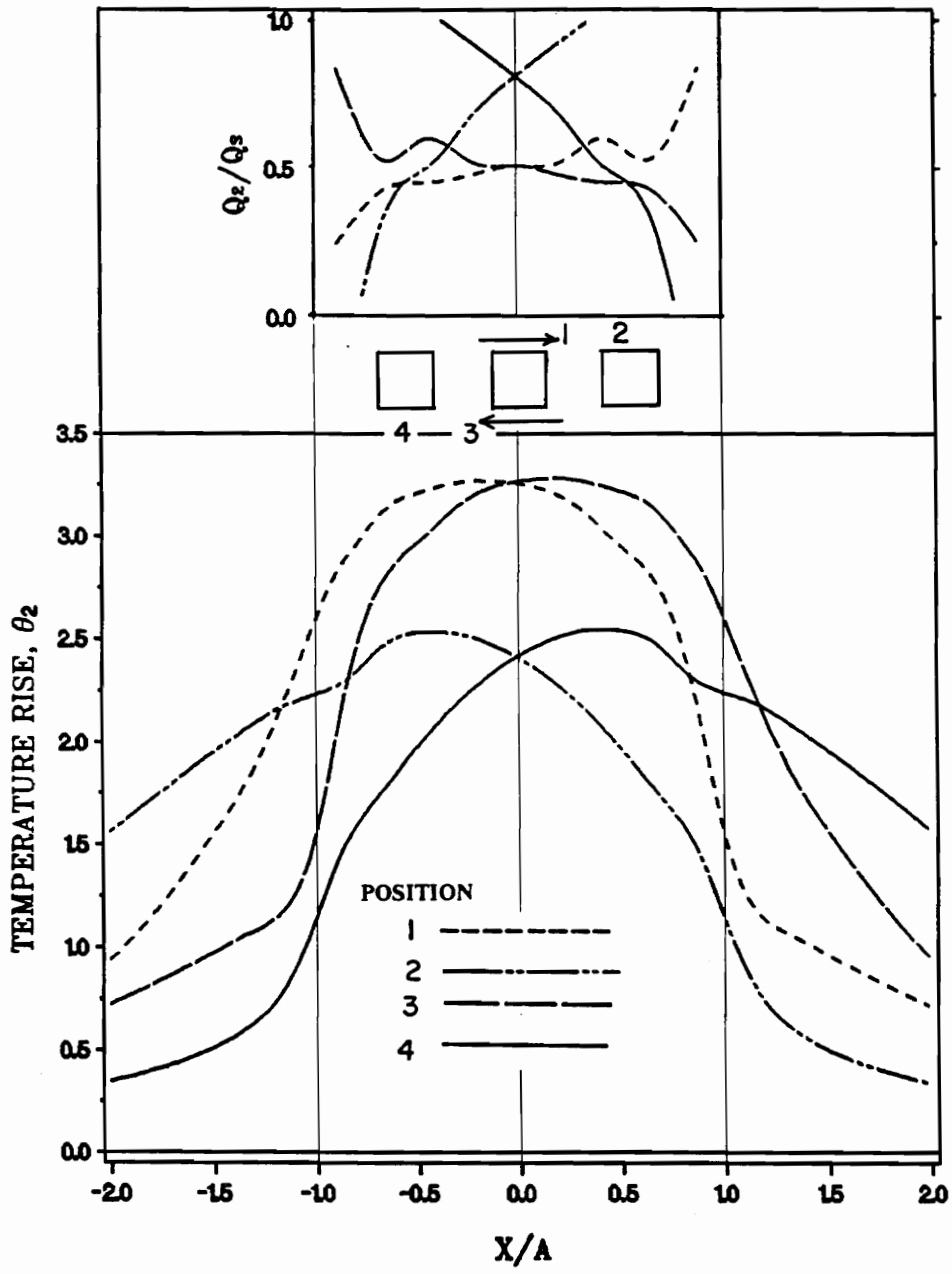

Figure 14. The quasi-steady state distribution of frictional heat, and surface temperature rise for oscillating motion at points of zero and maximum velocity during a cycle: $x_m/a = 1.0$, $A = 10$, $\Omega = 0.1$, $K_1 = \Lambda_1 = 1.0$

required to traveled from location 1 to location 3. When the velocity changes direction, the new material is now entering the contact from location 3, where the point at location 3 would experience the similar temperature changes as the point at location 1, which occurred half a cycle earlier. The temperature oscillation at locations 3 and 1 behave in the same manner but are 90 degrees out of phase, while the temperature at the center of the contact increases proportionally to the absolute value of the velocity.

Figure 16 and 17 show the effect of the Peclet number on the surface temperature rise and heat distribution. The results are for identical material properties of the regions and omega (Ω) = 0.1. Figure 16 on page 66 shows the effect of the Peclet number on the distribution of frictional heat and the mean surface temperature rise. When Peclet number increases, the energy input to the system increases, which produces a high temperature rise, but decreases the amplitude ratio. The distribution of frictional heat for low amplitude ratio is evenly distributed to both regions, and becomes uneven when the amplitude ratio increases. The mean surface temperature rise reaches the quasi-steady state almost instantaneously for the high amplitude ratio, but not for the case of the low amplitude ratio.

Figure 17 on page 67 shows the effect of the Peclet number on the distribution of frictional heat and surface temperature rise at the maximum velocity in the quasi-steady state. The distribution of frictional heat is evenly distributed over the contact area for the low amplitude ratio, and becomes uneven over the contact area as the amplitude ratio increases. The temperature distribution for the low amplitude ratio, A = 100, is symmetric over the contact area, but unsymmetrical when amplitude ratio increases. This displays the role of the amplitude ratio in the temperature distribution over the contact area.

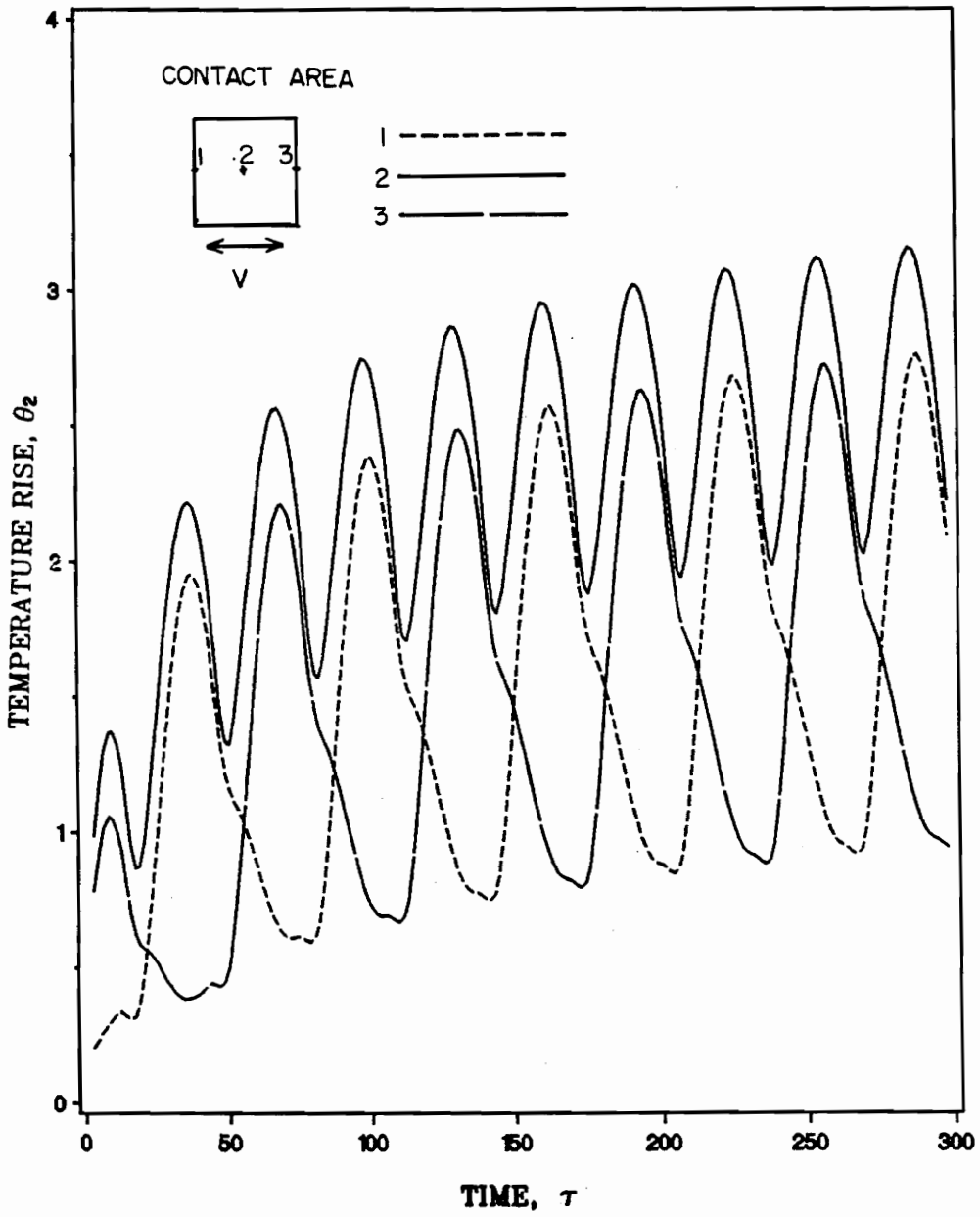

Figure 15. The local surface temperature rise at the edges and center of square contact area for oscillating motion: $x_m/a = 1.0$, $A = 10$, $\Omega = 0.1$, $K_1 = \Lambda_1 = 1.0$

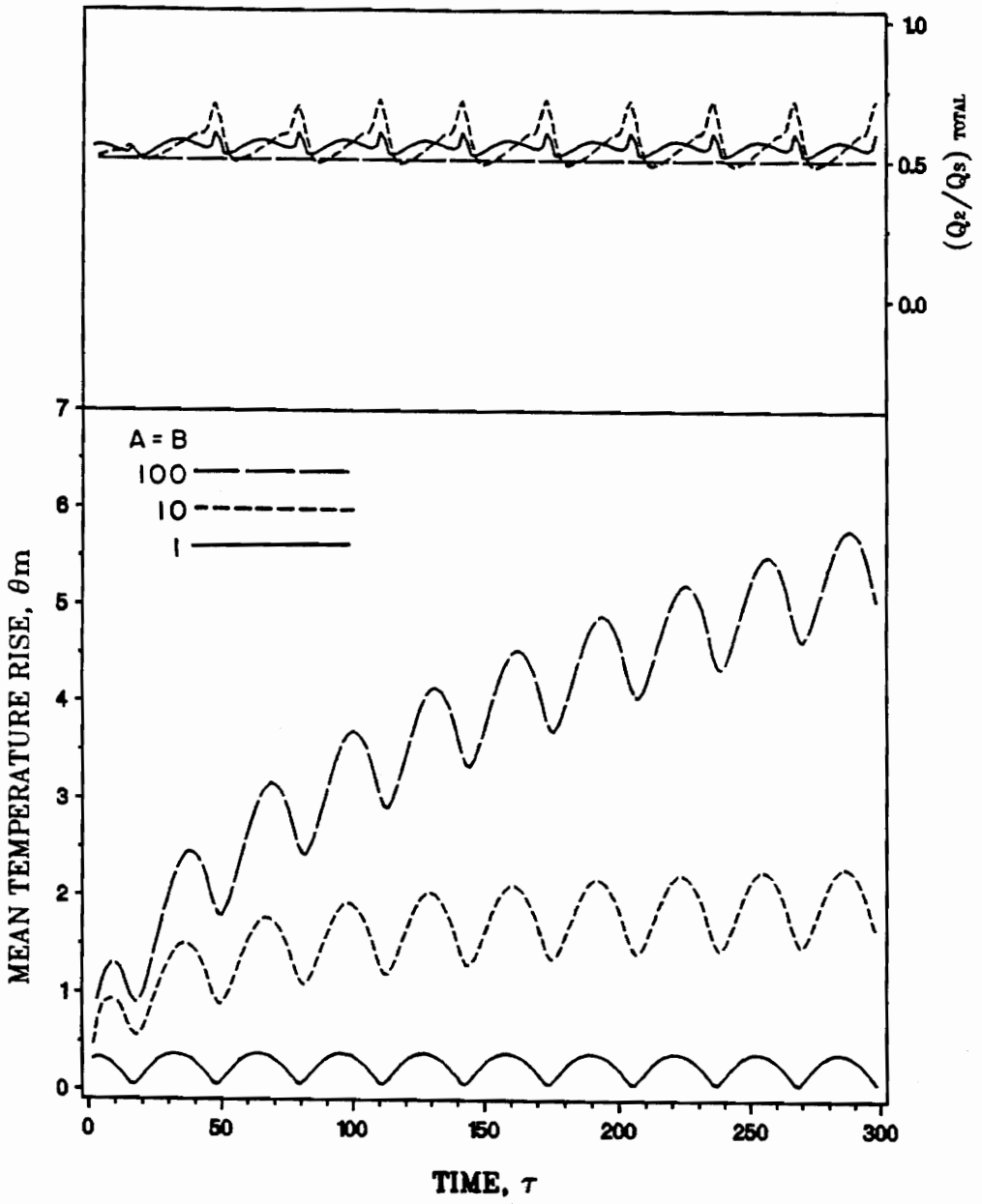

Figure 16. The effect of the Peclet number on distribution of frictional heat and mean surface temperature rise for oscillating motion: $\Omega = 0.1$, $K_1 = \Lambda_1 = 1.0$

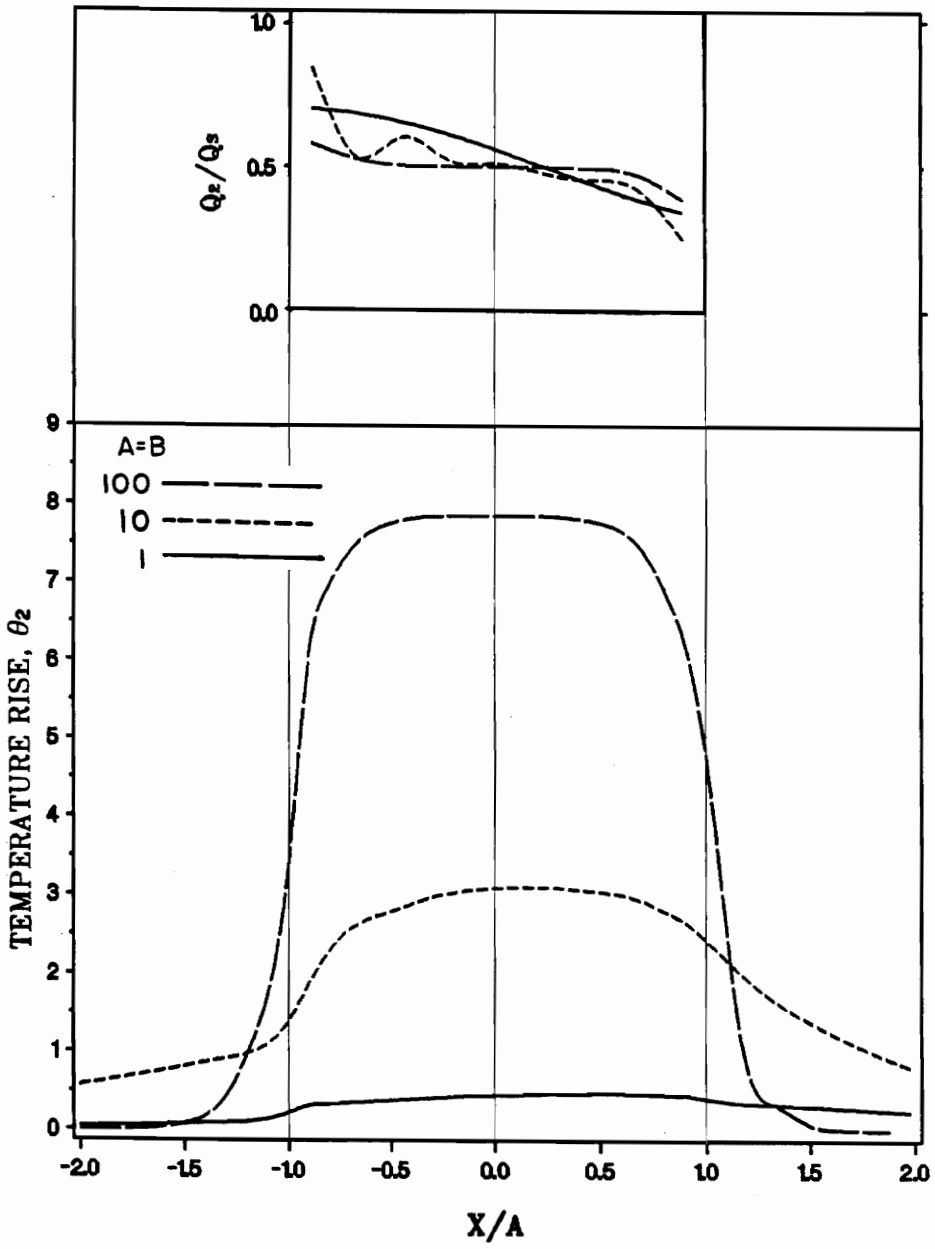

Figure 17. The effect of the Peclet number on the quasi-steady state distribution of frictional heat and surface temperature rise for oscillating motion at the maximum velocity: $\Omega = 0.1$, $K_1 = \Lambda_1 = 1.0$

Figures 18 to 22 are a study of the role of dimensionless frequency (Ω), real amplitude, and real frequency in the distribution of frictional heat and the surface temperature rise. The results are for regions with identical material properties, and A = 10, unless otherwise specified. Figure 18 on page 69 shows the effect of omega on the total distribution of frictional heat and the mean surface temperature rise versus the number of cycle. When all parameters are held constant except omega (Ω), the rate of total energy input to the system is constant and the product of amplitude and frequency is constant. This can be seen by examining the dimensionless variables Ω and A given by equation (3.6)

$$A = \frac{a v_m}{\alpha_2}$$

$$\Omega = \frac{\omega \alpha_2}{v_m^2}$$

$$v_m = x_m \omega$$

Figure 10 shows that the total distribution of frictional heat is evenly distributed for a low amplitude ratio, where $\Omega = 1$ ($\frac{x_m}{a} = \frac{1}{A\,\Omega}$), and becomes uneven for a higher amplitude ratio, where $\Omega = 0.01$.

The effect of the omega on the steady state distribution of frictional heat and the surface temperature rise at the maximum velocity in the quasi-steady state is shown in Figure 19 on page 71. Again, the distribution of frictional heat for the low amplitude ratio is about evenly distributed over the contact area, and the surface temperature rise is symmetric about the center-line of the contact area. Although, the same total energy is input into these cases, the surface temperature rise is different due to the amplitude ratio difference. For a high amplitude ratio, where $\Omega = 0.01$, the temperature distribution is similar to a high Peclet unidirectional case (see Figure 5), where the temperature

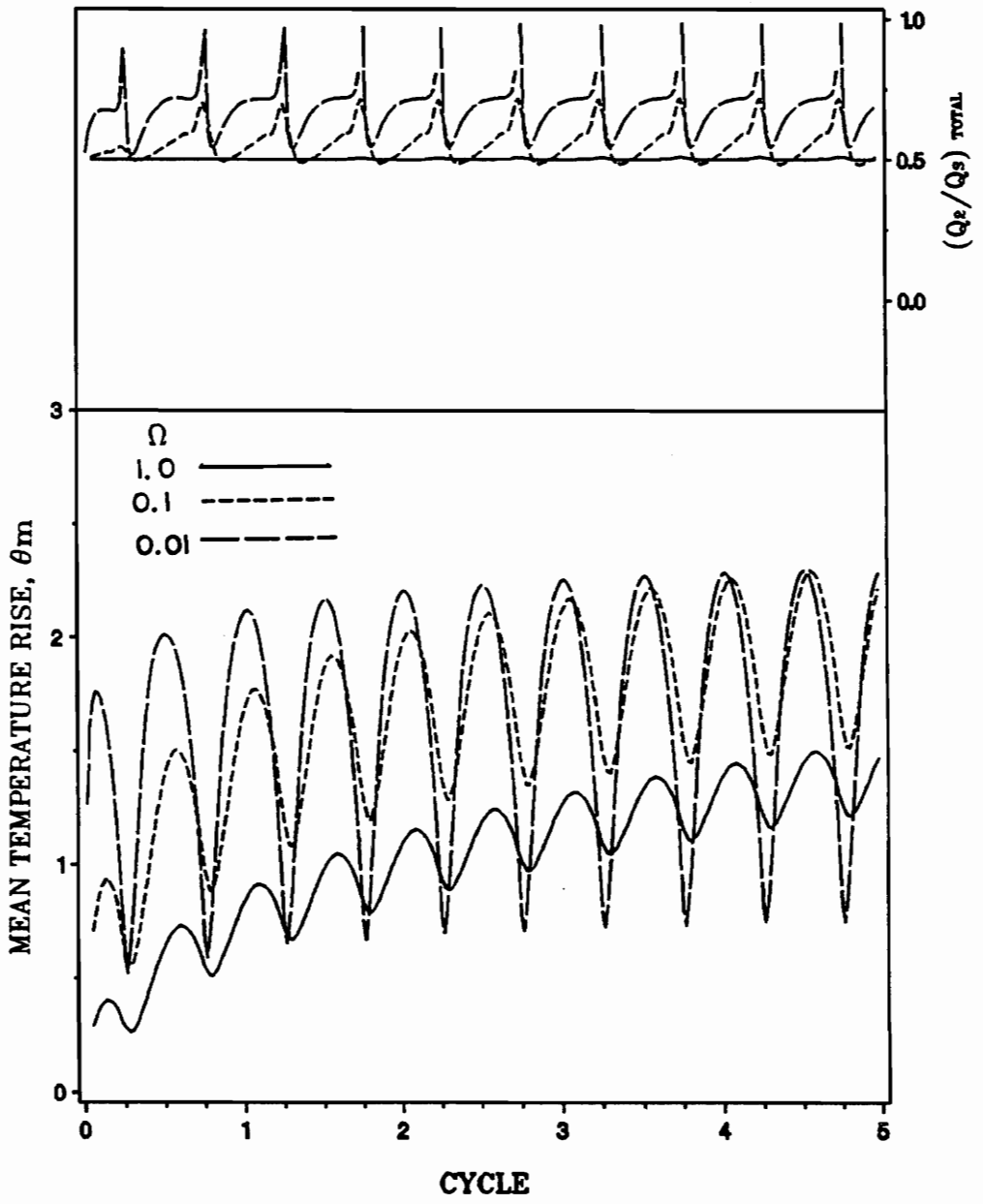

Figure 18. The effect of omega on distribution of frictional heat and mean surface temperature rise for oscillating motion: $A = 10$, $K_1 = \Lambda_1 = 1.0$

rise is unevenly distributed in X direction. The low amplitude ratio case is somewhat similar to a stationary heat source shown in Figure 5.

Figure 20 on page 72 shows the effect of the omega on total distribution of frictional heat and the mean surface temperatures rise as a function of time, τ. This figure also displays the relationship of the real frequency between these oscillating cases, where the product of real frequency and amplitude are constant. The maximum mean surface temperatures reach about the same level at the same time period since the total energy input is the same for all cases.

Figure 21 on page 73 shows the effect of the real frequency (ω) on the distribution of frictional heat and the surface temperature rise at the maximum velocity in the quasi-steady state. In these cases, the amplitude ratio ($\frac{X_m}{a}$) is one. A change in the real frequency (ω) will change both of the dimensionless quantities A and omega (Ω), as shown in the figure. The total energy input is proportional to the real frequency; thus, high frequencies produce high surface temperature rises.

Figure 22 on page 74 shows the effect of the real amplitude (x_m) on the distribution of frictional heat and the surface temperatures rise at the maximum velocity in the quasi-steady state. A change in real amplitude will change both dimensionless quantities A and Ω, which then change the amplitude ratio. As the real amplitude increases, the energy input to the system is also increases; thus, the fraction of frictional heat distributed to region-2 increases and gives a higher surface temperature rise.

Figure 23 on page 76 shows the effect of the thermal property ratio on the quasi-steady state distribution of frictional heat and the surface temperatures rise at maximum ve-

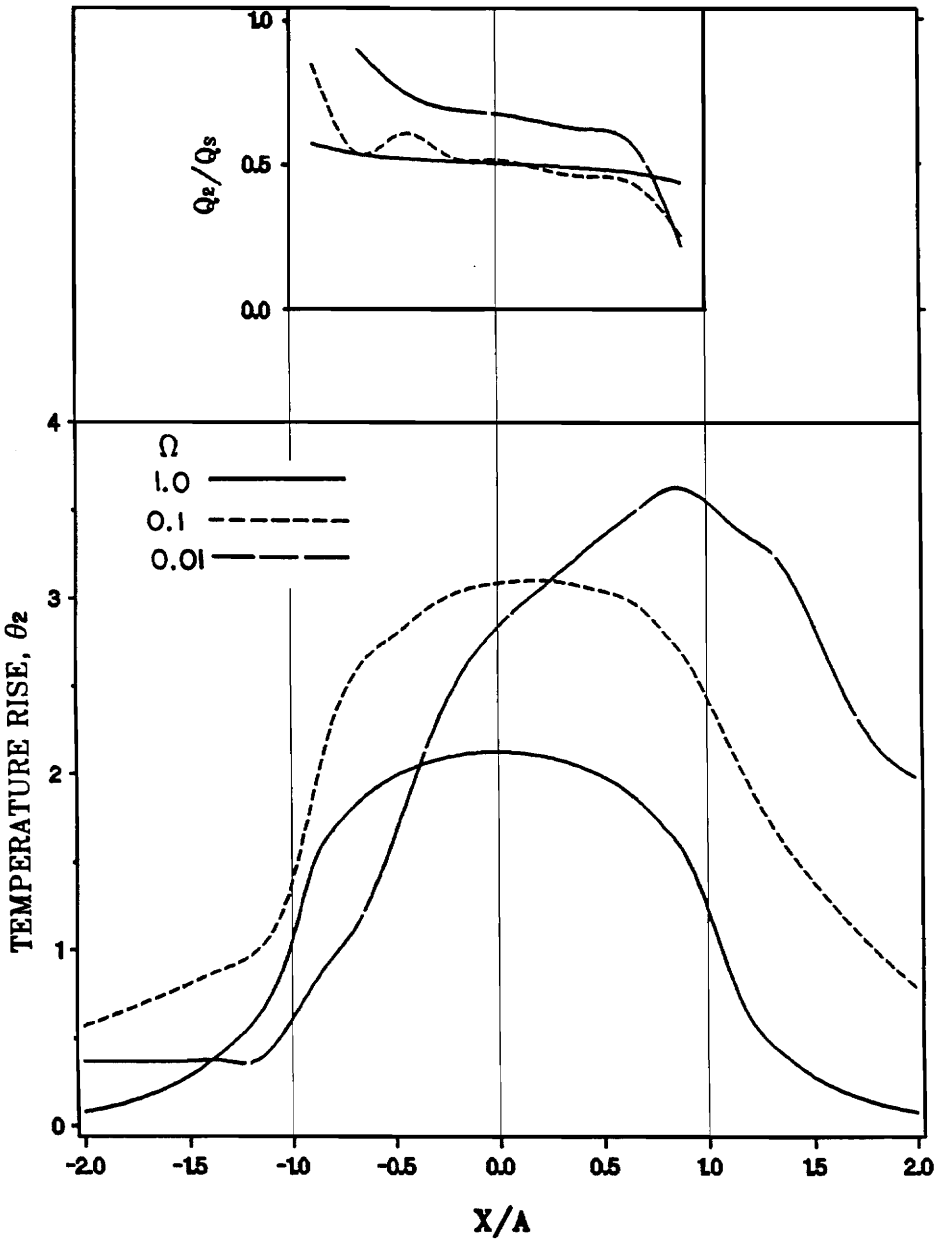

Figure 19. The effect of the omega on the quasi-steady state distribution of frictional heat and surface temperature rise for oscillating motion at the maximum velocity: $A = 10$, $K_1 = \Lambda_1 = 1.0$

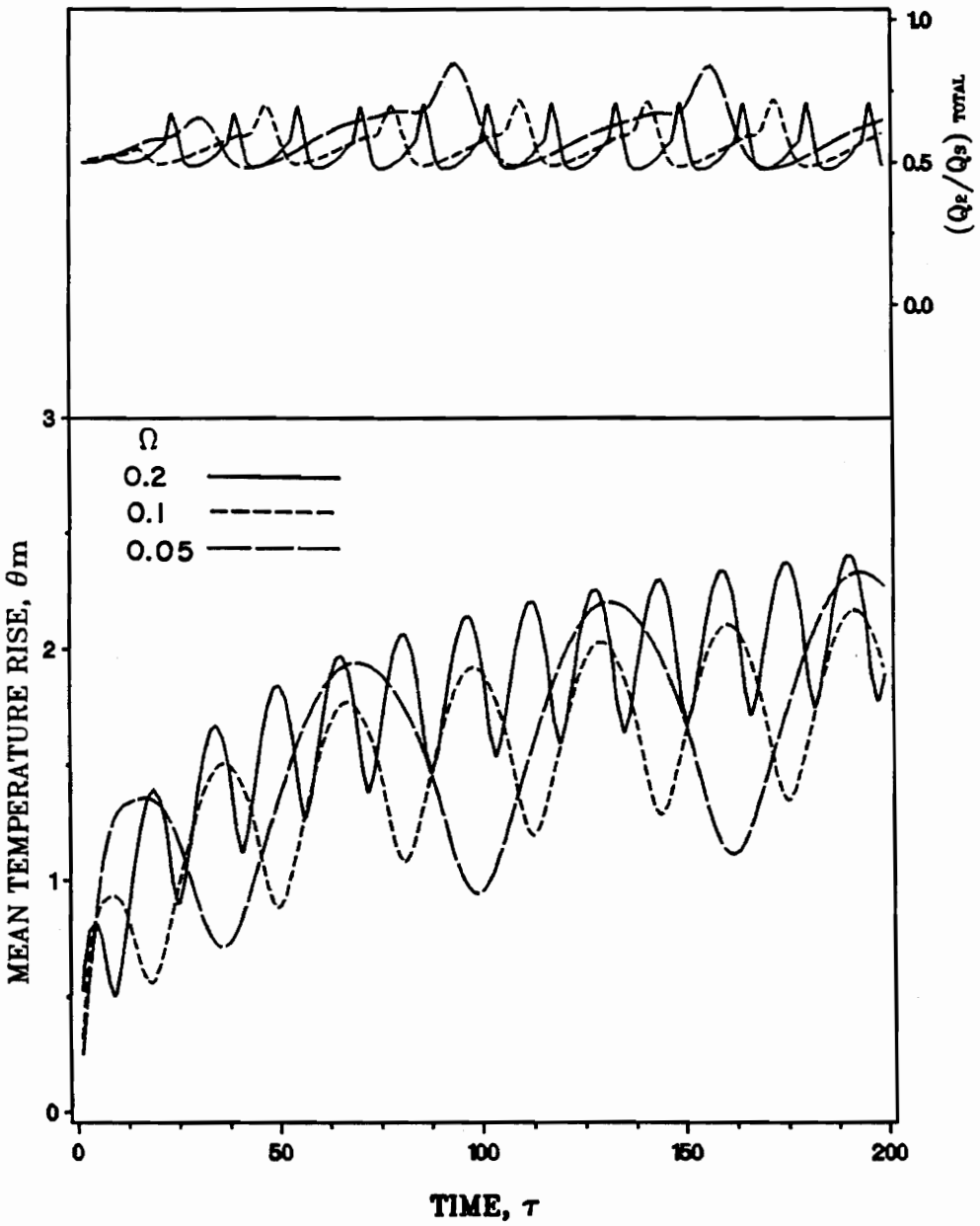

Figure 20. The effect of the omega on the distribution of frictional heat and mean surface temperature rise for oscillating motion: $A = 10$, $K_1 = \Lambda_1 = 1.0$

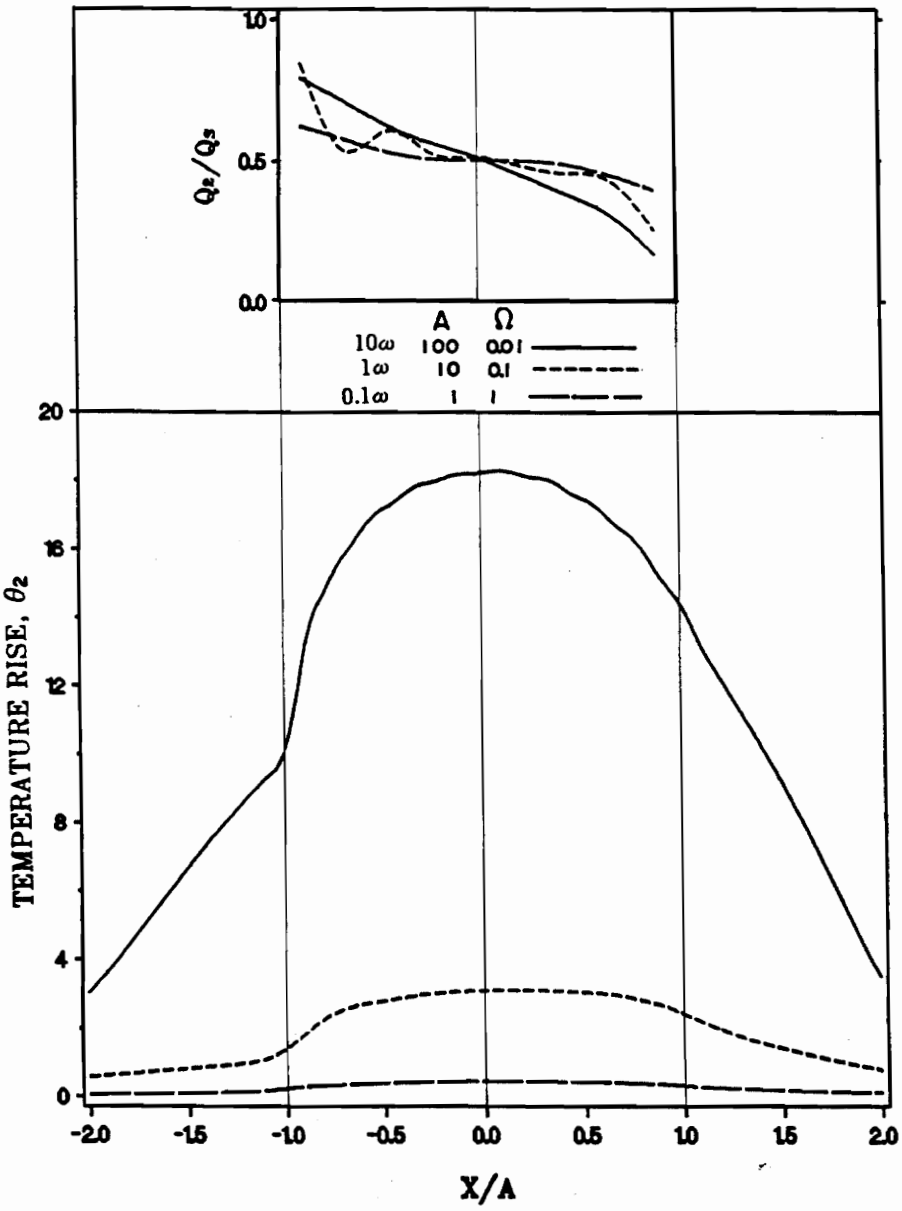

Figure 21. The effect of the real frequency on the quasi-steady state distribution of frictional heat and surface temperature rise for oscillating motion at the maximum velocity: $x_m/a = 1.0$, $K_1 = \Lambda_1 = 1.0$

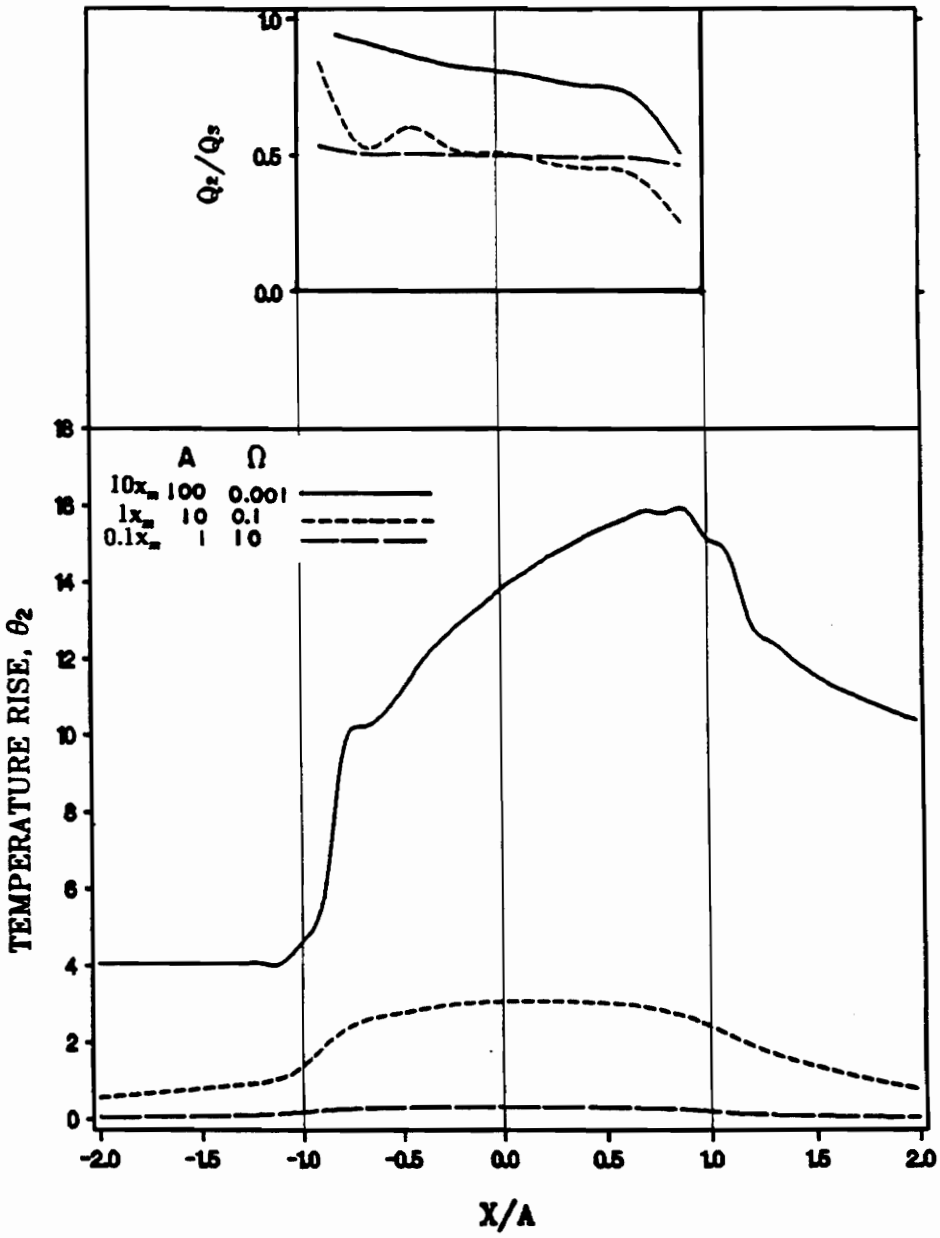

Figure 22. The effect of the real amplitude on the quasi-steady state distribution of frictional heat and surface temperature rise for oscillating motion at the maximum velocity: $K_1 = \Lambda_1 = 1.0$

locity. It shows the same phenomena as the constant velocity case in Figure 6 on page 52.

Figure 24 on page 77 and Figure 25 on page 78 are a study of multiple contact areas for oscillating motion at maximum velocity with an amplitude ratio of 1.0. The results display similar information to that shown on Figures 8 and 9 for the unidirectional case. Figure 24 displays the result of divided contact areas oriented in the direction of motion, and Figure 25 displays the results of areas oriented perpendicular to the direction of motion. Figures 24 and 25 show that the effect of orientation in the oscillating motion case is relatively small, which is not similar to the unidirectional motion cases. These two figures can be used for all the oscillating cases with an amplitude ratio of one and identical material properties for the regions. These figures can also be used in conjunction with a single area analysis to refine surface temperature estimates for multiple contacts.

Comparison of theory with experiments

In this section, a comparison of the theoretical calculations and experimental results are made. The experimental part of the theoretical and experimental project [3, 46] is done separately. This thesis and the thesis by Weick [47] are the results of the phase I project. A 1/4 in. diameter Zirconium Oxide (Ms grade), ZrO_2, ball and a sapphire disk are used in the fretting experiment conducted by Weick [47]. He used the Infrared Microscope System [48], developed by the Tribology research at VPI&SU, to measure the surface temperature rise in sliding contact, and provided all the experimental data

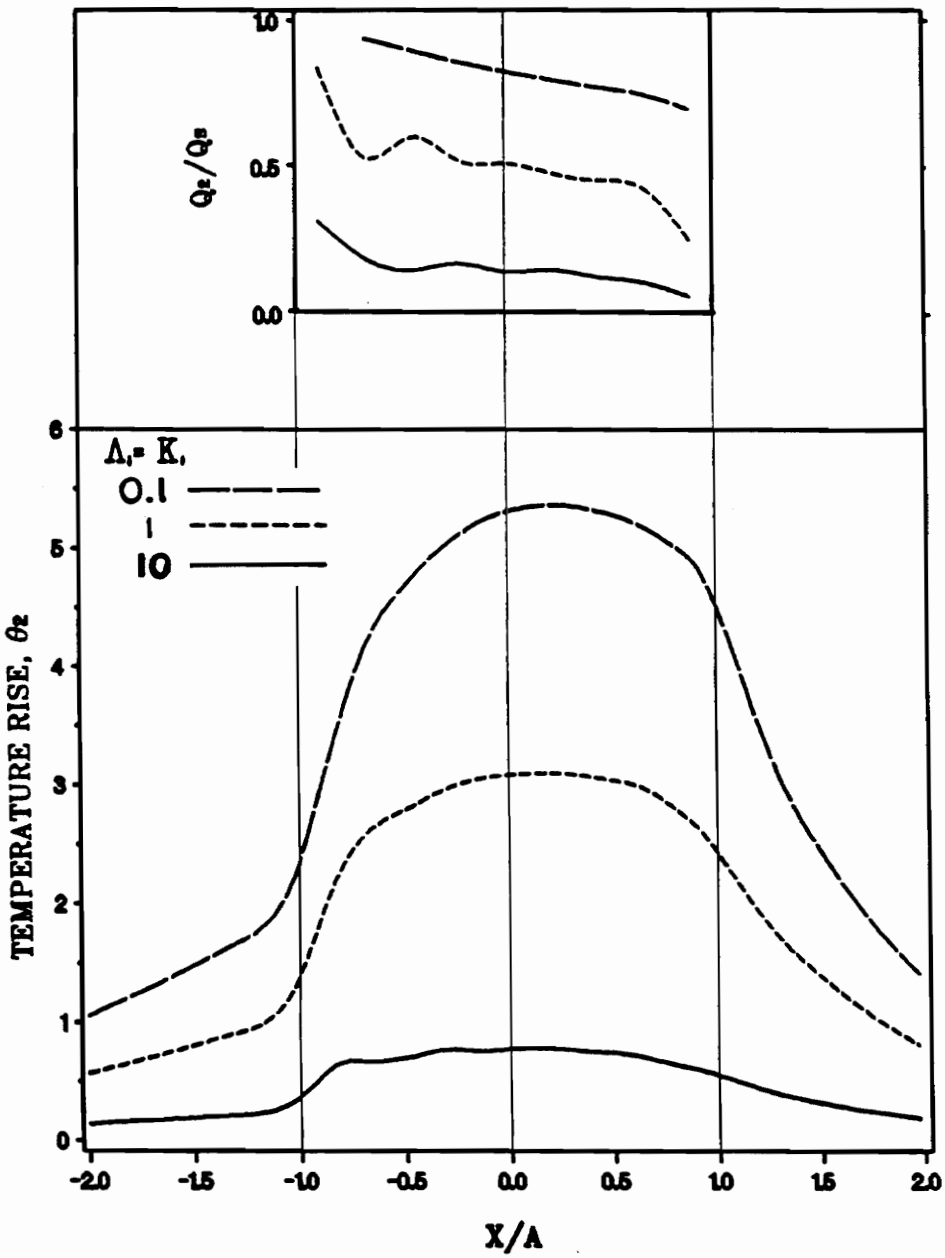

Figure 23. The effect of the thermal property ratio on the quasi-steady state distribution of frictional heat and surface temperature rise for oscillating motion at the maximum velocity: x_m/a = 1.0, A = 10, Ω = 0.1.

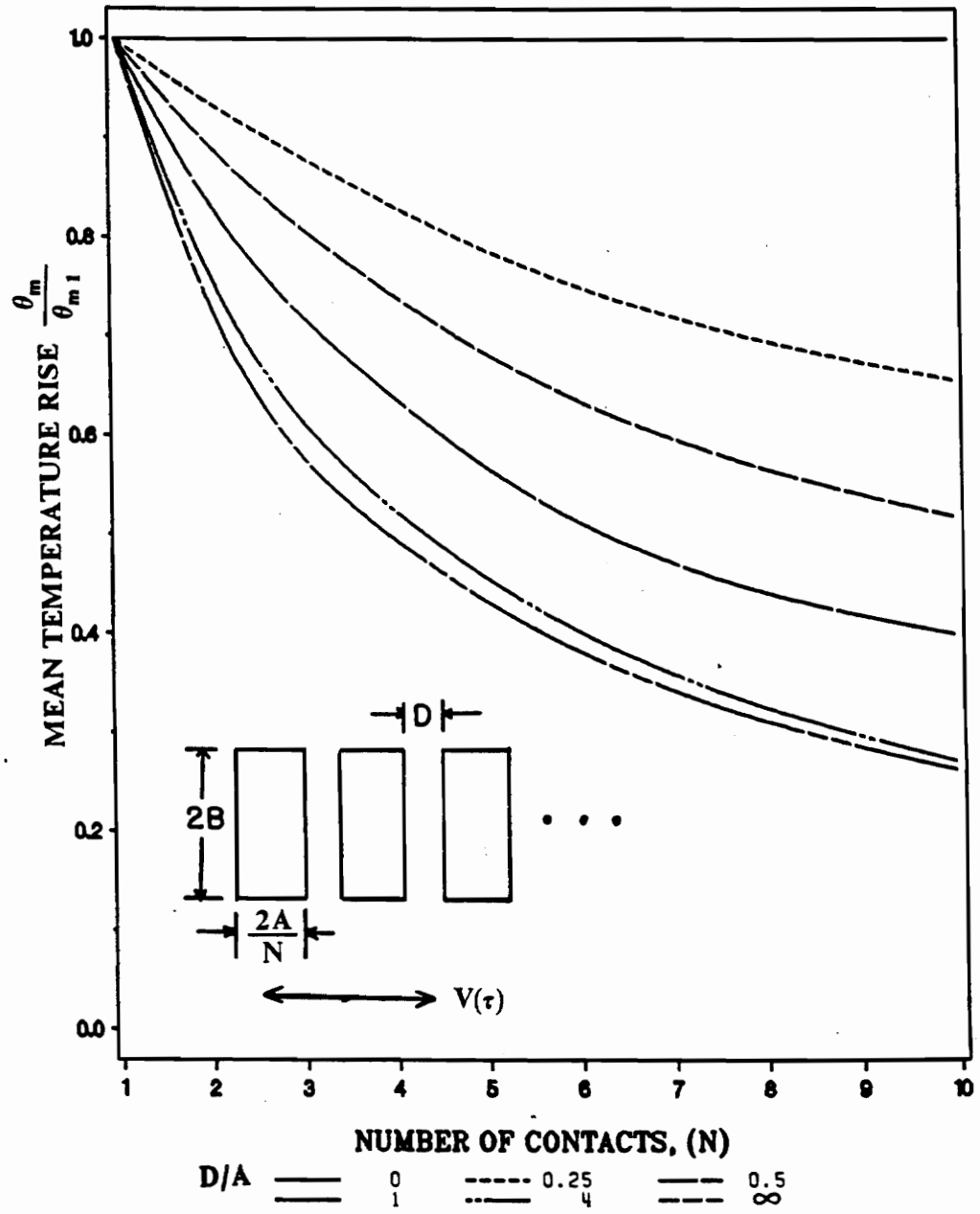

Figure 24. A study of the number and spacing of multiple contacts on the quasi-steady state normalized maximum mean surface temperature rise for oscillating motion with contacts oriented along with the direction of motion. : $x_m/a = 1.0$, $A = 10$, $B = 10$, $\Omega = 0.1$, $K_1 = \Lambda_1 = 1.0$

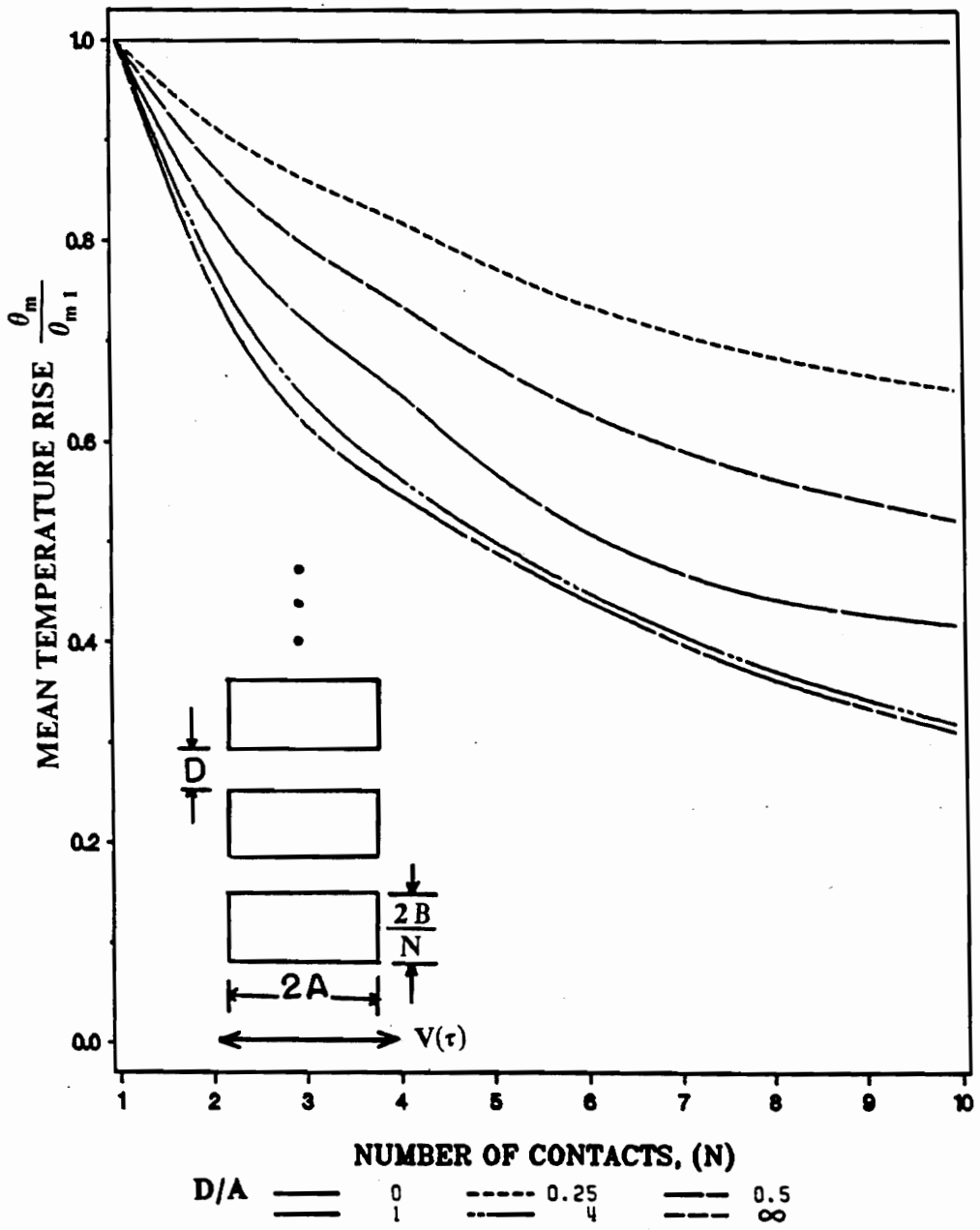

Figure 25. A study of the number and spacing of multiple contacts on the quasi-steady state normalized maximum mean surface temperature rise for oscillating motion with contacts oriented perpendicular to the direction of motion : $x_m/a = 1.0$, $A = 10$, $B = 10$, $\Omega = 0.1$, $K_1 = \Lambda_1 = 1.0$

necessary to preform the theoretical calculations. All data, such as frequency, amplitude, and friction force are measured during the experiment. The detailed discussion of the experimental work is documented in reference [47]. The calculated theoretical results and experimental data are shown in Table 6 on page 81, and the material properties used in the calculations are listed in Table 7 on page 82. As shown in previous figures, the theoretical temperatures for oscillating contact rise sharply during early times and eventually settle into a cyclic, repetitive pattern referred to as a quasi-steady state. Experimental measurements exhibit fluctuations and are by nature more random than purely theoretical predictions. However, the results [46, 47] displayed in the experiment rise in time and approach a quasi-steady state. Listed in Table 6 are average and maximum temperature rises measured at 5 and 90 seconds. This experiment [46, 47] shows that the temperature is still increasing at 5 seconds while at 90 seconds the temperature has reached a quasi-steady condition.

Theoretical results were calculated using four different assumptions for the contact area and the results listed in Table 6 are the long time or quasi-steady state solutions corresponding to the situation at 90 seconds. The plastic and elastic models show that the calculated temperature rise over-predicts the experimental data. Both models predicted a smaller area of contacts than the real area; therefore, the calculated temperatures are higher than the experimental temperature. The geometric area was taken as the area of the total apparent wear scar obtained by examining the photomacrograph of the ball shown in Figure 26 on page 83. Using the apparent geometric area, the calculated temperature rise underestimated the experimental results. This is because the real area of contact is not as large as the apparent area. From a picture taken after the experiment [47], approximately 5 small patches are evident within the apparent geometric area as shown on Figure 26 on page 83 [47]. The forth temperature rise calculations

of Table 6 are based on these 5 small patches, and gives the closest prediction to the experimental results. The total area of the 5 patches is smaller than the apparent area, which produces a higher temperature rise, but the spacing between the patches reduces the temperatures rise, which gives the best results of all.

Table 6 also compares results with the simple approximate analyses of Archard [5] , which is restricted to a constant velocity model. The total area for the 5 patches was used to calculate the temperature rise, for the forth case, as the Archard model cannot handle a multiple interacting contacts case. The results from the Archard model in Table 6 are simply not accurate.

Figure 27 on page 84 shows the effect of the real contact area and the number of multiple contacts for the above case. The real surface temperature rise calculation is based on the assumed real area of contact. The calculations are based on the parameters obtained after 90 second of the above experiment [47]. The smallest possible area is assumed to be plastic area and the largest possible area is considered to be the observed geometric area after the experiment. Also, the divided contacts (N = 5, 10), and the spacing between the contact patches ($d \rightarrow \infty$) are arbitrarily assumed. The divided area calculations are the results of the original area divided into a number of non-interacting square patches. The results in Figure 27 show that the temperature rise and the area are logarithmic functions. The temperature rise for a single area of contact varies from a maximum of 1200 K to a minimum of 70 K. With divided contacts, N = 5, the temperature rise ranges from 750 K to 35 K, and with N = 10, the temperature rise ranges from 670 K to 25 K. One can use this figure to back up an estimate of the real area of contact by using the knowledge of the surface temperature measured during experiment. For example, 93.5 K of maximum temperature rise was measured from the experiment

Table 6. **A comparison of the theoretical and experimental results for 1/4 in. diameter zirconium oxide (Ms grade) ball on sapphire disk: load = 40 N, $f = 195Hz$, (a) after 5 sec.: $x_m = 136\mu m$, $\mu = 0.86$; (b) after 90 sec.: $x_m = 145\mu m$, $\mu = 1.00$.**

		Theoretical			Experimental		
		Current analysis		Archard	Data		
Area type	Total area (m^2)	ΔT_{avg} (K)	ΔT_{max} (K)	ΔT (K)	Average ΔT_{avg} (K)	Average ΔT_{max} (K)	Time (sec)
Plastic Model	3.64×10^{-9}	808	1190	598	28.1	33.1	5
Elastic Model	2.41×10^{-8}	280	288	200			
Geometric Area	6.97×10^{-7}	64.3	71.8	39.8	82.3	93.5	90
Divided Area 5-Contacts	3.16×10^{-7}	77.7	90.7	64.9			

Note: the experimental data are obtained from [47]

Table 7. List of the material properties used in the experiment.

	Zirconium Oxide (Ms grade) ZrO_2	Sapphire disk Al_2O_3
α (m^2/s)	0.114×10^{-5}	0.25×10^{-4}
k $(\frac{W}{m\,C})$	3.08	41.8
E (N/m^2)	0.205×10^{12}	0.365×10^{12}
v	0.31	0.20
H (N/m^2)	0.11×10^{11}	0.177×10^{11}

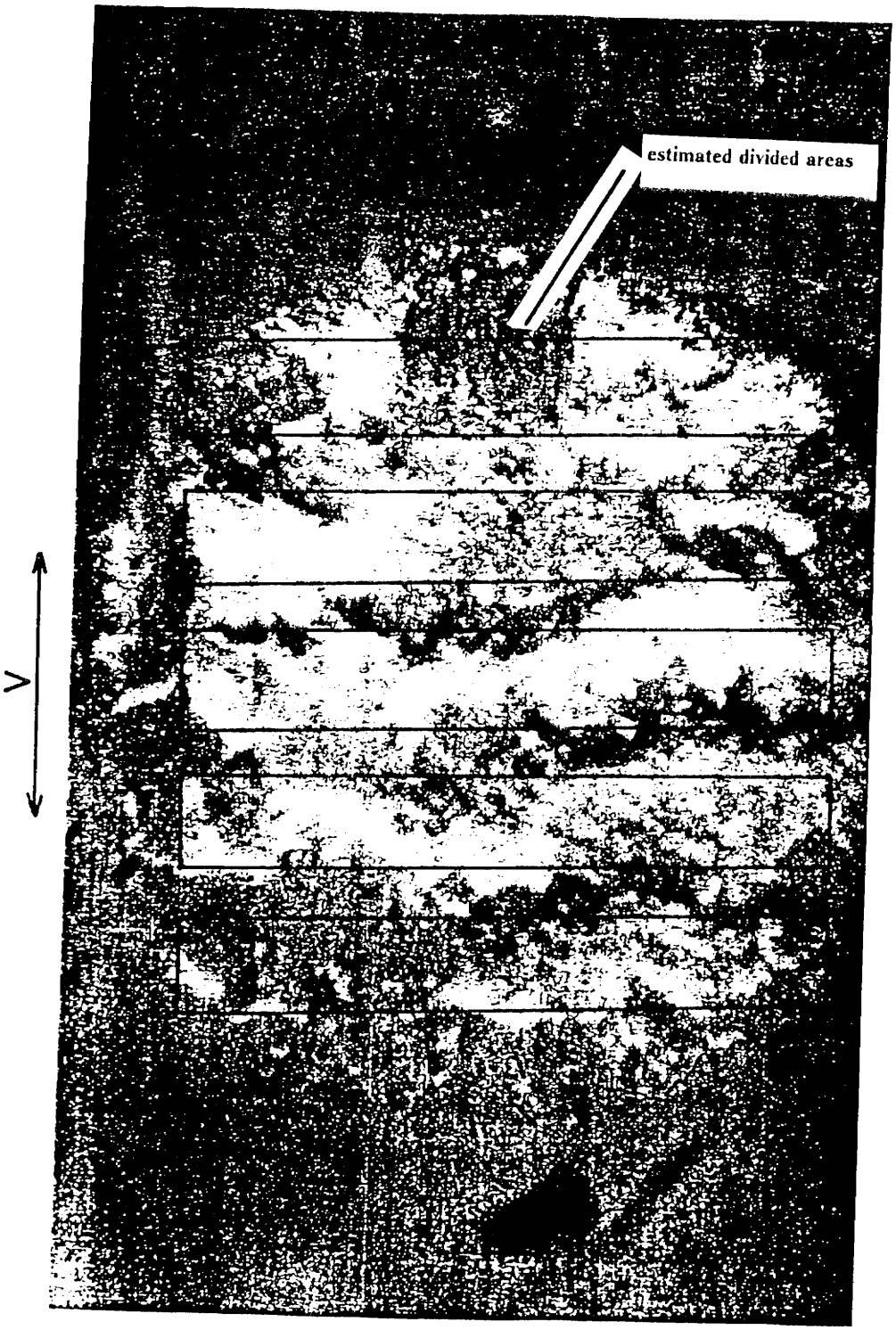

Figure 26. The apparent contact area for the zirconium oxide ball and the estimated divided areas.

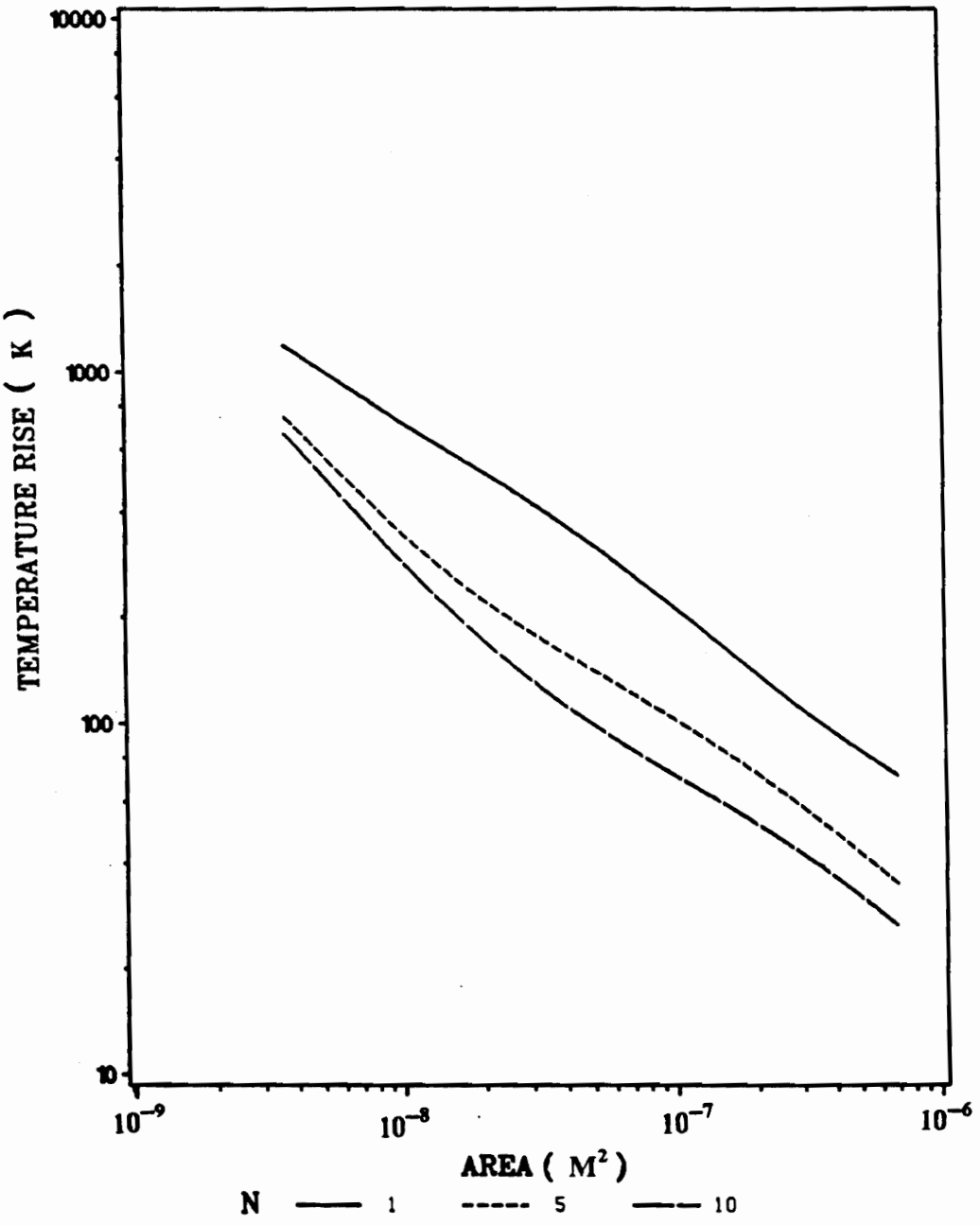

Figure 27. A study of the effect of the real contact area on the surface temperature rise.

[47]. By using Figure 27, the estimated total contact area is about 3.5×10^{-7} m^2. Similarly, for five and 10 divided non-interacting square contacts, the total area is about 1.0×10^{-7} m^2 and 5.0×10^{-8} m^2, respectively.

Chapter 6

CONCLUSIONS AND RECOMMENDATIONS

CONCLUSIONS

This study addresses various theoretical aspect of surface temperature rise and distribution of frictional heat in oscillating and unidirectional motion, and the numerical limitations and characteristics of the solution method. The following are the conclusions of this research study.

- The trapezoidal integration rule is unstable for the first kind integral equation. However, the midpoint rule is simple and does not exhibit numerical oscillation for high Peclet number.

- The analysis provides good agreement compared with existing theory for the single region case.

- Accurate numerical results are achieved by the following time steps,

$$\Delta\tau \leq \frac{\pi}{8} A, \quad \text{for unidirectional motion}$$

$$\Delta\tau \leq \frac{\pi}{2\,\Omega\,IDT}, \quad \text{for oscillating motion}$$

  where IDT > 4.

- Increasing the number of elements does not result in a significant improvement in accuracy but increases the computation cpu time significantly.

- This theoretical model allows the detailed study of the surface temperature rise for any arbitrary velocity (such as unidirectional and oscillating).

- This theoretical model has the flexibility to handle any arbitrary contact area.

- This model also has the flexibility to calculate the distribution of frictional heat and the surface temperature rise for any combination of material properties of the regions.

- The Peclet number for the unidirectional motion, and the combination of Peclet number and amplitude ratio for oscillating motion are extremely important factors that influence the characteristics of the distribution of frictional heat and surface temperature rise.

- For multiple contacts, the number, spacing, and orientation of the contacts are the most important factors that significantly affect the surface temperature rise in the sliding contacts.

- The results calculated using this theoretical model corresponding to the experimental data are found to be quite accurate. The existing Archard theory does not include interaction between contacts or oscillating velocity which underestimates the surface temperatures.

- This theoretical treatment (BIEM) is an advancement in numerical analysis for the surface temperature calculations compared to finite element technique [29, 31], finite difference [26 – 28] , and purely analytical methods [4, 5, 6].

RECOMMENDATIONS

By reviewing the theoretical study in this thesis, the following recommendations are made for future research.

- Develop a theoretical model that applies to a more general case and includes the following,

  - arbitrary, finite regions
  - changing contact area with time
  - volumetric heating
  - surface melting
  - composite materials

REFERENCES

1. Furey, M. J., "The Formation of Polymeric Films Directly on Rubbing Surfaces to Reduce Wear," *Wear*, Vol. 26, pp. 369-392. 1973.

2. Furey, M. J., "The 'in situ' Formation of Polymeric Films on Rubbing Surfaces," *Proceedings of International conference on Polymers and Lubrication (Brest)*, Published by Centre National de la Recherche Scientifique, Paris, No. 233, pp. 393-404, 1975.

3. Furey, M. J., and Vick, B., "Surface Temperature Generated in Oscillating Contact," *A Research Proposal Submitted to the National Science Foundation Tribology Program*, Virginia Polytechnic Institute and State University, Blacksburg, VA., September, 1987

4. Blok, H., "Theoretical Study of Temperature Rise at Surfaces of Actual Contact Under Oiliness Lubricating conditions," *Proc. Inst. of Mech. Engineers General Discuss of Lubrication*, Institute of Mechanical Engineers, London, Vol. 2, pp. 222-235, 1937.

5. Jaeger, J. C., "Moving Sources of Heat and the Temperature at Sliding Contact," *J. Royal Society of N.S. Wales*, Vol. 76, pp. 203-224. 1942.

6. Archard, J. F., "The Temperature of Rubbing Surfaces," *Wear* , Vol. 2, pp. 438-455, 1958/1959.

7. Archard, J. F., and Rowntree, R. A., "The Temperature of Rubbing Bodies: Part 2, The Distribution of temperatures," *Wear* Vol. 128, pp. 1-17, 1988.

8. Ling, F. F., *Surface Mechanics*, John Wiley and Sons, New York, 1973.

9. Ling, F. F., "A Quasi-Interactive Method for Computing Interface Temperature Distributions," *ZAMP*, Vol. 10, pp. 461-474, 1959.

10. Ling, F. F., and Ng, C. W., "On Temperatures at the Interfaces of Bodies in Sliding Contact," *Proc. 4th U.S. Natl. Congr. of Applied Mechanics*, ASME, New York, pp. 1343-1349, 1962.

11. Floquet, A., Play, D., and Godet, M., "Surface Temperatures in Distributed Contacts: Application to Bearing Design," *J. Lubrication Technology*, Vol. 99, pp. 277-283, 1977.

12. Floquet, A., and Play, D., "Contact Temperature in Dry Bearings: Three Dimensional Theory and Verification," *J. Lubrication Technology*, Vol. 103, pp. 243-251, 1981.

13. Ling, F. F., and Pu, S. L., "Probable Interface Temperatures of Solid in Sliding Contact," *Wear*, Vol. 7, pp. 23-34, 1964.

14. Ling, F. F., "On Temperature Transients at Sliding Surfaces," *J. Lubrication Technology*, Vol. 91, pp. 397-405, 1965.

15. Marscher, W. D., "A Critical Evaluation of the Flash-Temperature Concept," *ASLE Transactions*, Vol. 25, pp. 157-174, 1981

16. Barber, J. R., "The Conduction of Heat from Sliding Solids," *Int. J. Heat Mass Transfer*, Vol.13, pp 857-869, 1970

17. Lai, W. T., and Cheng, H. C., "Temperature Analysis in Lubricated Simple Sliding Rough Contact," *ASLE Transactions*, Vol. 28, pp 303-312, 1984.

18. Kennedy, F. E., "Single Pass Rub Phenomena--Analysis and Experiment," *J. Lubrication Technology*, Vol. 104, pp. 582-583, 1982.

19. McLean D., *Mechanical Properties of Metal*, Wiley, New York, pp. 141-144, 1962.

20. Rigney, D. A., and Heilmann, P., "An Energy-Based Model of Friction and Its Application to Coated Systems," *Wear*, Vol. 72, pp. 195-281, 1981.

21. Ryhming, I. L., "On the Temperature and Heat Source Distributions in Sliding Contact Problems," *Acta Mechanica* Vol. 32, pp. 261-274, 1979.

22. Furey, M. J., "Surface Temperatures in Sliding Contact," *ASLE Lubrication Conference*, Academic press., New York and London, Oct. 15-17, 1963.

23. Des Ruisseaux, N. R., Zerkle, R.D., "Temperature in Semi-Infinite and Cylindrical Bodies Subjected to Moving Heat Sources and Surface Cooling," *J. Heat Transfer*, Vol. 92, pp. 456-464, 1970.

24. Francis, H. A., "Interface Temperature Distribution within a Sliding Hertzian Contact," *ASLE Transactions*, Vol. 14, pp. 41-54, 1970.

25. Cameron, A., Gordon, A. N., and Symm, G. T., "Contact Temperatures in Rolling/Sliding Contact," *Proc. Royal Society*, Vol. A286, pp. 45-61, 1965.

26. Emery, A. F., Etemad, S., and Wolak, J., "Interfacial Temperatures and Surface Heat Flux for Blade-Seal Processes," *AIAA Paper 81-1165* , 1981.

27. Yanshin, A. A., Popov, Y. A., and Tseitlin, D., "Calculation of the Nonstationary Temperature Field in a Two-Layer Plate When Heated by a Moving Source in presence of Inhomogeneities on the Contact Surface of the Layers," *J. Engineering Physics*, Vol. 31, pp. 721-726, 1976.

28. Rashid, M., and Seireg, A., "Heat Partition and Transient Temperature Distribution in Layered Concentrated Contacts. Part I and Part II," *ASME/ASLE Joint Tribology Conference, Paper #86-Trib-11/12*, Pittsburg, PA, Oct. 20-11, 1986.

29. Kennedy, F. E., "Surface Temperatures in Sliding Systems--A Finite Element Analysis," *J. Lubrication Tech.*, Vol. 103, pp. 90-96, 1981.

30. Kennedy, F. E., and Ling, F. F., "A Thermal, Thermoelastic, and Wear Simulation of a High-Energy Sliding Contact Problem," *J. Lubrication Technology*, Vol. 96, pp. 497-507, 1974.

31. Kennedy, F. E., Colin, A., Floquet, A., and Glovsky, R., "Improved Techniques for Finite Element Analysis of Sliding Surface Temperatures," *Proceedings 10th Leeds-Lyon Symposium on Tribology*, Butterworths, London, 1983.

32. Kennedy, F. E., Cullen, S. C., and Leroy, J. M., " Contact Temperature and Its Effects in an Oscillating Sliding Contact," *ASME, Journal of Tribology, Paper #88-Trib-32* , 1988

33. Colin, F., and Floquet, A., "Combination of Finite Element and Integral Transform Techniques in a Heat Conduction Quasi-Static Problem," *Int. J. Num. Meth. Eng.*, Vol. 23, pp. 13-23, 1986.

34. Floquet, A., "Comparison Between Analytical and Numerical Methods in Heat Transfer Analysis in Tribology," *Proceedings of the 6th Leeds-Lyons Symposium on Tribology*, Mechanical Engineering Publications limited, London, 1979.

35. Rizzo, F. J., and Shippy, D. J., "A Method of Solution for Certain Problems of Transient Heat Conduction," *AIAA J.*, Vol. 8(11), 1970, pp 2004-2009.

36. Chang, Y. P., Kang, C. S., and Chen, D. J., "The Use of Fundamental Green's Functions for the Solution of Problems of Heat Conduction in Anisotropic Media," *Int. J. Heat Mass Transfer*, Vol.16, 1973, pp 1905-1918.

37. Shaw, R. P., "An Integral Equation Approach to Diffusion," *Int. J. Heat Mass Transfer*, Vol. 17, 1974, pp 693-699.

38. Brebbia, C. A., and Wrobel, L. C., "The Boundary Element Method for Steady State and Transient Heat Conduction," In: *Proc. 1st Int. Conf. on Numerical Methods in Thermal Problems*,, Pineridge Press., Swansea, 1979.

39. Brebbia, C. A., and Wrobel, L. C., "Steady and Unsteady potential Problems Using the Boundary Element Method," Chapter 1 in: *Recent Advances in Numerical Methods in Fluids*,, eds. Taylar, C., and Morgan, K., Pineridge Press., Swansea, 1980.

40. Kuroki, T., Ohura, Y. Obata, K., and Onishi, K., "Boundary Element Solution of Heat Equation with Singularities and Nonlinearities," *Theor. Appl. Mech.*, Vol. 31, 1982, pp361-370.

41. Skerget, P., and Brebbia, C. A., "Non-linear Potential Problems." Chapter 1 in: *Progress in Boundary Element Methods*, Vol. 2, ed. Brebbia, C. A., Pentech Press, London, 1983.

42. Onishi, K., and Kuroki, T., "On Non-linear Heat Transfer Problems," Chapter 6 in: *Development in Boundary Element Methods - 4*, ed. Banerjee, P. K., and Watson, J. O., Elsevier Applied Science Publishers, New York, 1985.

43. Ozisik, M. N., *Heat Conduction* , John Wiley &Sons, Inc., New York, 1980.

44. Linz, P., *Analytical and Numerical Methods for Volterra Equations* ,Philadelphia, 1985.

45. Vick, B., and Ozisik, M. N., "Quasi-Steady-State Temperature Distribution in Periodically Contacting Finite Regions," *J. Heat Transfer*, Vol. 104, pp. 739-744, 1981.

46. Furey, M. J., Vick, B., Foo, S. J., and Weick B. L., "A Theoretical and Experimental Study of Surface Temperatures Generated during Fretting," *Japan International Tribology Conference*, Nagoya, Japan, Oct. 29- Nov. 1, 1990.

47. Weick B. L., *Measurement of Surface Temperature during Oscillating Contact - Ceramic Interfaces*, Virginia Polytechnic Institute and State University, Blacksburg, VA., 1990 (to be published).

48. Furey, M. J., "Infrared Measurements of Surface Temperatures Produced in Tribological Processes," *Proceedings, 3rd International Tribology Congress*, ("EUROTRIB-81"), Warsaw, 21-24 September 1981, Vol. I, Tribological Processes in Solid Body Contact Area, 1981, pp. 118-139.

APPENDIX A: Fourier Transform Method for Moving Green's Function

MOVING GREEN'S FUNCTION

The moving full space Green's function is governing by equations (4.1), which are re-stated here without sub script i as,

$$\Lambda\left(\frac{\partial^2 G}{\partial X^2}+\frac{\partial^2 G}{\partial Y^2}+\frac{\partial^2 G}{\partial Z^2}\right)+\delta\,(X-X_o)\,\delta\,(Y-Y_o)\,\delta\,(Z-Z_o)\,\delta\,(\tau-\tau_o)$$

$$=\frac{\partial G}{\partial \tau}+V_x(\tau)\frac{\partial G}{\partial X} \qquad (A1.a)$$

$$G\to 0, \qquad X, Y, Z\to \pm\infty \qquad (A1.b)$$

$$G = 0, \qquad \tau < \tau_o \qquad (A1.c)$$

FOURIER TRANSFORM METHOD

Apply full range Fourier transforms to equation (A1.a)

$$\text{X-transform} : \overline{G}(\lambda_1, Y, Z, \tau) = \int_{X=-\infty}^{\infty} G e^{i\lambda_1 X} dX \qquad (A2.a)$$

$$\text{X-inversion} : G = \frac{1}{2\pi} \int_{\lambda_1=-\infty}^{\infty} \overline{G}(\lambda_1, Y, Z, \tau) e^{-i\lambda_1 X} d\lambda_1 \qquad (A2.b)$$

$$\text{Y-transform} : \overline{\overline{G}}(\lambda_1, \lambda_2, Z, \tau) = \int_{Y=-\infty}^{\infty} \overline{G} e^{i\lambda_2 Y} dY \qquad (A3.a)$$

$$\text{Y-inversion} : \overline{G} = \frac{1}{2\pi} \int_{\lambda_2=-\infty}^{\infty} \overline{\overline{G}}(\lambda_1, \lambda_2, Z, \tau) e^{-i\lambda_2 Y} d\lambda_2 \qquad (A3.b)$$

$$\text{Z-transform} : \overline{\overline{\overline{G}}}(\lambda_1, \lambda_2, \lambda_3, \tau) = \int_{Z=-\infty}^{\infty} \overline{\overline{G}} e^{i\lambda_3 Z} dZ \qquad (A4.a)$$

$$\text{Z-inversion} : \overline{\overline{G}} = \frac{1}{2\pi} \int_{\lambda_3=-\infty}^{\infty} \overline{\overline{\overline{G}}}(\lambda_1, \lambda_2, \lambda_3, \tau) e^{-i\lambda_3 Z} d\lambda_3 \qquad (A4.b)$$

Take the X-transform by operating on equation (A1.a) with

$$\int_{X=-\infty}^{\infty} e^{i\lambda_1 X} dX$$

The X-transform of equation (A1.a) becomes

$$\Lambda(-\lambda_1^2\overline{G}+\frac{\partial^2\overline{G}}{\partial Y^2}+\frac{\partial^2\overline{G}}{\partial Z^2})+e^{i\lambda_1 X_o}\delta(Y-Y_o)\delta(Z-Z_o)\delta(\tau-\tau_o)$$

$$=\frac{\partial\overline{G}}{\partial\tau}-iV_x(\tau)\lambda_1\overline{G}$$

Similarly, take the Y-transform of equation (A1.a) with

$$\int_{Y=-\infty}^{\infty}e^{i\lambda_2 Y}dY$$

Y-transform of equation (A1.a) becomes

$$\Lambda(-\lambda_1^2\overline{\overline{G}}-\lambda_2^2\overline{\overline{G}}+\frac{\partial^2\overline{\overline{G}}}{\partial Z^2})+e^{i(\lambda_1 X_o+\lambda_2 Y_o)}\delta(Z-Z_o)\delta(\tau-\tau_o)$$

$$=\frac{\partial\overline{\overline{G}}}{\partial\tau}-iV_x(\tau)\lambda_1\overline{\overline{G}}$$

And take Z-transform of equation (A1.a) with

$$\int_{Z=-\infty}^{\infty}e^{i\lambda_3 Z}dZ$$

Z-transform of equation (A1.a) becomes

$$\Lambda(-\lambda_1^2-\lambda_2^2-\lambda_3^2)\overline{\overline{\overline{G}}}+e^{i(\lambda_1 X_o+\lambda_2 Y_o+\lambda_3 Z_o)}\delta(\tau-\tau_o)$$

$$=\frac{\partial\overline{\overline{\overline{G}}}}{\partial\tau}-iV_x(\tau)\lambda_1\overline{\overline{\overline{G}}}$$

Rearrange the above expression as,

$$\frac{\mathrm{d}\overline{\overline{\overline{G}}}}{\mathrm{d}\tau} + \left[(\lambda_1^2 + \lambda_2^2 + \lambda_3^2)\Lambda - iV_x(\tau)\lambda_1\right]\overline{\overline{\overline{G}}}$$

$$= \mathrm{EXP}\left[i(\lambda_1 X_o + \lambda_2 Y_o + \lambda_3 Z_o)\right]\delta(\tau - \tau_o) \qquad (A5.a)$$

$$\overline{\overline{\overline{G}}} = 0, \qquad \tau < \tau_o \qquad (A5.b)$$

Let,

$$P(\tau) = (\lambda_1^2 + \lambda_2^2 + \lambda_3^2)\Lambda - iV_x(\tau)\lambda_1$$

Use an integrating factor

$$\mathrm{EXP}\left[\int_{\tau'=0}^{\tau} P(\tau')\mathrm{d}\tau'\right] = \mathrm{EXP}\left[\lambda_1^2\Lambda\tau - i\lambda_1\Lambda\int_{\tau'=0}^{\tau} V_x(\tau')\mathrm{d}\tau'\right]$$
$$\times\mathrm{EXP}\left[\lambda_2^2\Lambda\tau + \lambda_3^2\Lambda\tau\right]$$

Thus, express equation (A5.a) as

$$\frac{\mathrm{d}}{\mathrm{d}\tau}\left[\overline{\overline{\overline{G}}}\ \mathrm{EXP}\left(\int_{\tau'=0}^{\tau} P(\tau')\mathrm{d}\tau'\right)\right]$$

$$= \mathrm{EXP}\left[i(\lambda_1^2 X_o + \lambda_2^2 Y_o + \lambda_3^2 Z_o)\right]\delta(\tau - \tau_o)\ \times\mathrm{EXP}\left[\int_{\tau'=0}^{\tau} P(\tau')\mathrm{d}\tau'\right] \qquad (A6)$$

Integrate equation (A6) from $\tau = \tau < \tau_o$, to $\tau > \tau_o$,

$$\overline{\overline{\overline{G}}}(\lambda_1, \lambda_2, \lambda_3, \tau)\, \mathrm{EXP}\left[\int_{\tau'=0}^{\tau} P(\tau')d\tau'\right]$$

$$= \mathrm{EXP}[i(\lambda_1 X_o + \lambda_2 Y_o + \lambda_3 Z_o)] \times \mathrm{EXP}\left[\int_{\tau'=0}^{\tau_o} P(\tau')d\tau'\right]$$

$$\therefore \quad \overline{\overline{\overline{G}}}(\lambda_1, \lambda_2, \lambda_3, \tau)$$

$$= \mathrm{EXP}[i(\lambda_1 X_o + \lambda_2 Y_o + \lambda_3 Z_o)] \times \mathrm{EXP}\left(-\int_{\tau'=\tau_o}^{\tau} P(\tau')d\tau'\right)$$

$$= \mathrm{EXP}\left[i\lambda_1 X_o - \lambda_1^2 \Lambda(\tau - \tau_o) + i\lambda_1 \int_{\tau'=\tau_o}^{\tau} V_x(\tau')d\tau'\right]$$

$$\times \mathrm{EXP}[i\lambda_2 Y_o - \lambda_2^2 \Lambda(\tau - \tau_o)]$$

$$\times \mathrm{EXP}[i\lambda_3 Z_o - \lambda_3^2 \Lambda(\tau - \tau_o)]$$

$$= \bar{f}_1(\lambda_1)\ \bar{f}_2(\lambda_2)\ \bar{f}_2(\lambda_3)$$

Apply inversion formulas given by equations (A2.b), (A3.b), and (A4.b)

$$G = \{\frac{1}{2\pi}\int_{\lambda_1=-\infty}^{\infty} EXP\left[i\lambda_1(X_o - X) - \lambda_1^2\Lambda(\tau - \tau_o) + i\lambda_1\int_{\tau'=\tau_o}^{\tau} V_x(\tau')d\tau' \right] d\lambda_1\}$$

$$\times\{\frac{1}{2\pi}\int_{\lambda_2=-\infty}^{\infty} EXP\left[i\lambda_2(Y_o - Y) - \lambda_2^2\Lambda(\tau - \tau_o)\right] d\lambda_2\}$$

$$\times\{\frac{1}{2\pi}\int_{\lambda_3=-\infty}^{\infty} EXP\left[i\lambda_3(Z_o - Z) - \lambda_3^2\Lambda(\tau - \tau_o)\right] d\lambda_3\} \qquad (A7)$$

$$= f_1(X)\ f_2(Y)\ f_3(Z)$$

Where the integrals $f_1(X)$, $f_2(Y)$, $f_3(Z)$ can be evaluated analytically as,

$$f_1(X) = \frac{1}{2\pi}\int_{\lambda_1=-\infty}^{\infty} EXP\left[-\lambda_1^2\Lambda(\tau - \tau_o) - i\lambda_1\left[(X - X_o) - \int_{\tau'=\tau_o}^{\tau} V_x(\tau')d\tau' \right] \right] d\lambda_1$$

$$= \frac{1}{2\pi} EXP\left[-\frac{\left[(X - X_o)^2 - \int_{\tau'=\tau_o}^{\tau} V_x(\tau')d\tau' \right]^2}{4\Lambda(\tau - \tau_o)} \right] \left[\frac{\pi}{\Lambda(\tau - \tau_o)} \right]^{1/2} \qquad (A8.a)$$

Similarly,

$$f_2(Y) = \frac{1}{2\pi} \text{EXP}\left[-\frac{[(Y - Y_o)]^2}{4\Lambda(\tau - \tau_o)} \right] \left[\frac{\pi}{\Lambda(\tau - \tau_o)} \right]^{1/2} \qquad (A8.b)$$

$$f_3(Z) = \frac{1}{2\pi} \text{EXP}\left[-\frac{[(Z - Z_o)]^2}{4\Lambda(\tau - \tau_o)} \right] \left[\frac{\pi}{\Lambda(\tau - \tau_o)} \right]^{1/2} \qquad (A8.c)$$

Put equations (A8) into equation (A7),

$$G(X,Y,Z,\tau \mid X_o, Y_o, Z_o, \tau_o)$$

$$= \frac{1}{[4\pi\Lambda(\tau - \tau_o)]^{3/2}} \text{EXP}\left[-\frac{(X - X_o - X_c)^2 + (Y - Y_o)^2 + (Z - Z_o)^2}{4\Lambda(\tau - \tau_o)} \right] \qquad (A9)$$

Where,

$$X_c = \int_{\tau' = \tau_o}^{\tau} V_x(\tau')d\tau'$$

Equation (A9) is the solution of the three-dimensional moving Green's function for equation (4.1a) or (A1.a).

APPENDIX B: Integral of Moving Green's Function

The full space moving Green's function is governing by equation (4.1a)

$$\frac{\partial G_i}{\partial \tau} + V_i(\tau)\frac{\partial G_i}{\partial X} = \Lambda_i \nabla^2 G_i + \delta(X - X_o)\,\delta(Y - Y_o)\,\delta(Z - Z_o)\,\delta(\tau - \tau_o) \qquad \text{for all } X,Y,Z,\tau \tag{B1.a}$$

$$G_i \to 0, \qquad X, Y, Z \to \pm\infty \tag{B1.b}$$

$$G_i = 0, \qquad \tau < \tau_o \tag{B1.c}$$

The solution of Green's function (For detail derivation see "APPENDIX A: Fourier Transform Method for Moving Green's Function" on page 94) is

$$G_i = \frac{1}{[4\pi\Lambda_i(\tau - \tau_o)]^{3/2}} \times \mathrm{EXP}\left[-\frac{(X - X_o - X_c)^2 + (Y - Y_o)^2 + (Z - Z_o)^2}{4\Lambda_i(\tau - \tau_o)} \right] \tag{B2}$$

Where,

$$X_c = \int_{\tau' = \tau_o}^{\tau} V_i(\tau')d\tau'$$

As defined by equation (4.12a)

$$G(X, Y, \tau \mid X_o, Y_o, \tau_o) = \frac{\Lambda_1}{K_1}(G_1)_{Z=Z_o=0} + (G_2)_{Z=Z_o=0}$$

$$= \sum_{i=1}^{2} \frac{\Lambda_i}{K_i}(G_i)_{Z=Z_o=0}$$

The spatial integral of the Green's function, as defined in equation (4.12a), is

$$GI^p_{m\,n}(X, Y, \tau)$$

$$= \int_{\tau_o=\tau_p}^{\tau_{p+1}} \int_{X_o=X_m}^{X_{m+1}} \int_{Y_o=Y_n}^{Y_{n+1}} G(X, Y, \tau \mid X_o, Y_o, \tau_o)dX_o dY_o d\tau_o$$

$$= \int_{\tau_o=\tau_p}^{\tau_{p+1}} \sum_{i=1}^{2} \frac{\Lambda_i}{K_i} \int_{X_o=X_m}^{X_{m+1}} \int_{Y_o=Y_n}^{Y_{n+1}} [(G_i)_{Z=Z_o=0}]dX_o dY_o d\tau_o \qquad (B3)$$

Rewrite G as the product of one-dimensional Green's functions,

$$(G_l)_{Z=Z_o=0} = \{\frac{1}{[4\pi\Lambda_i(\tau-\tau_o)]^{1/2}}\,\mathrm{EXP}\left[-\frac{(X-X_o-X_c)^2}{4\Lambda_i(\tau-\tau_o)}\right]\}$$
$$\times\{\frac{1}{[4\pi\Lambda_i(\tau-\tau_o)]^{1/2}}\,\mathrm{EXP}\left[-\frac{(Y-Y_o)^2}{4\Lambda_i(\tau-\tau_o)}\right]\}$$
$$\times\{\frac{1}{[4\pi\Lambda_i(\tau-\tau_o)]^{1/2}}\}$$

$$= G_x(X, \tau, |X_o, \tau_o)$$
$$\times G_y(Y, \tau, |Y_o, \tau_o) \qquad (B4)$$
$$\times\{\frac{1}{[4\pi\Lambda_i(\tau-\tau_o)]^{1/2}}\}$$

Thus, spatial integral of equation (B3) over a rectangle using 'G' as defined above becomes,

$$GI^p_{m,n} = \int_{\tau_o=\tau_p}^{\tau_{p+1}} \sum_{i=1}^{2} \frac{\Lambda_i}{K_i} \int_{X_o=X_m}^{X_{m+1}} \int_{Y_o=Y_n}^{Y_{n+1}} (G_l)_{Z=Z_o=0} dX_o dY_o d\tau_o$$

$$= \int_{\tau_o=\tau_p}^{\tau_{p+1}} \sum_{i=1}^{2} \frac{\Lambda_i}{K_i} \left[\int_{X_o=X_m}^{X_{m+1}} G_x(X, \tau|X_o, \tau_o) dX_o\right]$$
$$\times\left[\int_{Y_o=Y_n}^{Y_{n+1}} G_y(Y, \tau|Y_o, \tau_o) dY_o\right] \qquad (B5)$$
$$\times \frac{1}{[4\pi\Lambda_i(\tau-\tau_o)]^{1/2}} d\tau_o$$

Perform the integral of one-dimensional Green's function individually,

$$\int_{X_o=X_m}^{X_{m+1}} G_x dX_o = \int_{X_o=X_m}^{X_{m+1}} \frac{1}{[4\pi\Lambda_i(\tau-\tau_o)]^{1/2}} EXP\left[-\frac{(X-X_o-X_c)^2}{4\Lambda_i(\tau-\tau_o)} \right] dX_o$$

make the following variables change

$$\zeta = \frac{X-X_o-X_c}{[4\Lambda_i(\tau-\tau_o)]^{1/2}}$$

$$\zeta_m = \frac{X-X_m-X_c}{[4\Lambda_i(\tau-\tau_o)]^{1/2}}$$

$$\zeta_{m+1} = \frac{X-X_{m+1}-X_c}{[4\Lambda_i(\tau-\tau_o)]^{1/2}}$$

$$X_o = X - X_c - [4\Lambda_i(\tau-\tau_o)]^{1/2}\zeta$$

$$dX_o = -[4\Lambda_i(\tau-\tau_o)]^{1/2} d\zeta$$

$$\therefore \int_{X_o=X_m}^{X_{m+1}} G_x dX_o = -\frac{1}{\pi^{1/2}} \int_{\zeta=\xi_m}^{\zeta_{m+1}} EXP[-\zeta^2] d\zeta$$

$$= -\frac{1}{2}[\text{erf}(\zeta_{m+1}) - \text{erf}(\zeta_m)]$$

$$\int_{X_o=X_m}^{X_{m+1}} G_x dX_o = -\frac{1}{2}\left[\text{erf}\left(\frac{X-X_{m+1}-X_c}{[4\Lambda_i(\tau-\tau_o)]^{1/2}} \right) - \text{erf}\left(\frac{X-X_m-X_c}{[4\Lambda_i(\tau-\tau_o)]^{1/2}} \right) \right] \quad (B6)$$

Similarly,

$$\int_{Y_o=Y_n}^{Y_{n+1}} G_y dY_o = -\frac{1}{2}\left[\operatorname{erf}\left(\frac{Y-Y_{n+1}}{[4\Lambda_i(\tau-\tau_o)]^{1/2}}\right)-\operatorname{erf}\left(\frac{Y-Y_n}{[4\Lambda_i(\tau-\tau_o)]^{1/2}}\right)\right] \qquad (B7)$$

Putting equations (B6) and (B7) into (B3) gives

$$\begin{aligned} &GI^p_{m\,n}(X, Y, \tau) \\ &= \int_{\tau_o=\tau_p}^{\tau_{p+1}} \sum_{i=1}^{2} \frac{\Lambda_i}{K_i} \times \frac{1}{4}\left[\operatorname{erf}\left(\frac{X-X_{m+1}-X_c}{[4\Lambda_i(\tau-\tau_o)]^{1/2}}\right)-\operatorname{erf}\left(\frac{X-X_m-X_c}{[4\Lambda_i(\tau-\tau_o)]^{1/2}}\right)\right] \\ &\qquad \times\left[\operatorname{erf}\left(\frac{Y-Y_{n+1}}{[4\Lambda_i(\tau-\tau_o)]^{1/2}}\right)-\operatorname{erf}\left(\frac{Y-Y_n}{[4\Lambda_i(\tau-\tau_o)]^{1/2}}\right)\right] \\ &\qquad \times \frac{1}{[4\pi\Lambda_i(\tau-\tau_o)]^{1/2}}\, d\tau_o \end{aligned} \qquad (B8)$$

Let,

$$\xi = [4(\tau-\tau_o)]^{1/2}$$

$$\xi_p = [4(\tau-\tau_p)]^{1/2}$$

$$\tau_o = \tau - \frac{\xi^2}{4}$$

$$d\tau_o = -\frac{\xi}{2}\, d\xi$$

Thus, equation (B8) can be rewritten using above new defined variables,

$$GI^{p}_{m,n} = -\int_{\xi=\xi_p}^{\xi_{p+1}} \sum_{i=1}^{2} \frac{\Lambda_i}{K_i} \frac{1}{8} \frac{1}{(\pi\Lambda_i)^{1/2}}$$

$$\left[\operatorname{erf}\left(\frac{X - X_{m+1} - X_c}{\Lambda_i^{1/2}\xi} \right) - \operatorname{erf}\left(\frac{X - X_m - X_c}{\Lambda_i^{1/2}\xi} \right) \right] \qquad (B9)$$

$$\times \left[\operatorname{erf}\left(\frac{Y - Y_{n+1}}{\Lambda_i^{1/2}\xi} \right) - \operatorname{erf}\left(\frac{Y - Y_n}{\Lambda_i^{1/2}\xi} \right) \right] d\xi$$

Where,

$$X_c = \int_{\tau' = \tau - \frac{\xi^2}{4}}^{\tau} V_x(\tau') d\tau'$$

$$i = 1,\ 2$$

The ξ integration for the above expression can be done by using Simpson's rule.

APPENDIX C: Oscillating contact: Velocity, Position, and Heat Source

VELOCITY AND POSITION

The oscillating velocity is considered as

$$v_2(t) = v_x(t) = v_m \cos \omega t \tag{C1}$$

Choose the reference velocity as

$$v_r = v_m = x_m \omega$$

and the dimensionless velocity becomes

$$V_x(\tau) = \frac{v_x(t)}{v_m} = (\cos\ \Omega\tau) \tag{C2}$$

Where,

$$\Omega = \frac{\omega \alpha_2}{v_m^2}$$

$$\tau = \frac{v_m^2 t}{\alpha_2}$$

The distance traveled by the moving region in the time period t_o to t is

$$x_c(t) = \int_{t'=t_o}^{t} v_x(t')dt'$$

$$= \int_{t'=t_o}^{t} v_m \cos \omega t' dt'$$

$$x_c(t) = \frac{v_m}{\omega} [\sin(\omega t) - \sin(\omega t_o)]$$

The dimensionless form of the position, needed

in the GF of equation (4.2), becomes

$$X_c(\tau) = x_c(t) \frac{v_m}{\alpha_2}$$

$$= \frac{v_m^2}{\alpha_2 \omega} [\sin(\omega t) - \sin(\omega t_o)]$$

$$X_c(\tau) = \frac{1}{\Omega} [\sin(\Omega \tau) - \sin(\Omega \tau_o)] \qquad (C3)$$

For special case of unidirectional motion the velocity is simply

$$v_2(t) = v_x(t) = v \qquad (C4)$$

The reference velocity is chosen as

$$v_r(t) = v$$

Thus, the dimensionless velocity becomes

$$V_x(t) = 1$$

and the dimensionless position of heat source is

$$X_c = \tau - \tau_o \tag{C5}$$

HEAT SOURCE

The heat flux is defined as

$$q''_s(x, y, t) = \mu P(x, y, t) | v_x(t) | \tag{C6}$$

where,

$\mu =$ coefficient of friction

$P(x, y, t) =$ pressure

For oscillating contact,

$$q''_s(x, y, t) = \mu P(x, y, t) | v_m \cos(\omega t) | \tag{C7}$$

choose the following as the reference heat flux

$$q''_r = \mu P_r v_r = \mu P_m v_m$$

Thus, the dimensionless form of frictional heat is defined as,

$$\begin{aligned} Q''_s(X, Y, \tau) &= \frac{q''_s(x, y, t)}{q''_r} \\ &= \frac{P}{P_m} \left|\cos(\Omega\tau)\right| \\ &= \left|\cos(\Omega\tau)\right| \end{aligned} \tag{C8}$$

Where P_m is chosen as P.

APPENDIX D: Listing of the Program: FRHMID FORTRAN

MAIN PROGRAM

```
C
C     ************************************************************************
C     *                                                                      *
C     *    FILENAME       : FRHMID FORTRAN                                   *
C     *    PROGRAMMER     : FOO, S.J.                                        *
C     *    DATE WRITTEN   : 6/13/89                                          *
C     *    DATE REVISION  : 11/14/89                                         *
C     *                                                                      *
C     *----------------------------------------------------------------------*
C     *    THIS PROGRAM COMPUTES THE DISTRIBUTION OF FRICTIONAL              *
C     *    HEAT AND RESULTING TEMPERATURE DISTRIBUTION FOR DRY               *
C     *    SLIDING CONTACT    DUE TO:                                        *
C     *                                                                      *
C     *         A) OSCILLATING MOTION                                        *
C     *         B) UNIDIRECTIONAL MOTION                                     *
C     *                                                                      *
C     *    SOLUTION USING A BIEM WITH MOVING GF'S ,                          *
C     *    SURFACE HEATING , GENERAL CONTACT AREA ,                          *
C     *    HALF-SPACE REGIONS                                                *
C     *                                                                      *
C     *----------------------------------------------------------------------*
C     *        INPUT AND OUTPUT UNITS                                        *
C     *      ============================                                    *
C     *    THE READ INPUT UNIT NUMBER = 5                                    *
C     *    THE PRINT OUTPUT UNIT NUMBER = 6                                  *
C     *    THE WRITE OUTPUT UNIT NUMBER = 10                                 *
C     *                                                                      *
C     *----------------------------------------------------------------------*
C     *    LIST OF SUBPROGRAM:                                               *
C     *                                                                      *
```

```
C     *    1) SUBROUTINE DLSARG (ELEMTS,GIMAT,LDA,FMAT,1,QMAT)          *
C     *    2) SUBROUTINE THETA1 (PP,XMM,YNN,TAUPP,T1)                   *
C     *    3) SUBROUTINE THETA2 (PP,XMM,YNN,TAUPP,T2)                   *
C     *    4) DOUBLE PRECISION FUNCTION GI (XMM,YNN,TAUPP,XM,YN,TAUP)   *
C     *    5) DOUBLE PRECISION FUNCTION GFINT (XMM,YNN,XM,YN,XCEN,S)    *
C     *    6) DOUBLE PRECISION FUNCTION G1I (XMM,YNN,TAUPP,XM,YN,TAUP)  *
C     *    7) DOUBLE PRECISION FUNCTION GF1INT (XMM,YNN,XM,YN,XCEN,S)   *
C     *    8) DOUBLE PRECISION FUNCTION G2I (XMM,YNN,TAUPP,XM,YN,TAUP)  *
C     *    9) DOUBLE PRECISION FUNCTION GF2INT (XMM,YNN,XM,YN,XCEN,S)   *
C     *   10) DOUBLE PRECISION FUNCTION  XC (TAUPP, TAUP)               *
C     *   11) DOUBLE PRECISION FUNCTION QS (ICON,M,N,P)                 *
C     *   12) SUBROUTINE VALUES (MAXPP,IDT)                             *
C     *   13) SUBROUTINE  VELOCITY (VTYPE,W,C)                          *
C     *   14) SUBROUTINE OUTQ1 (PP,TAUPP)                               *
C     *                                                                 *
C     *   NOTE THAT :                                                   *
C     *    SUBROUTINE DLSARG IS IMSL SUBROUTINE TO SOLVE MATRIX         *
C     *              ==> [GIMAT] [QMAT] = [FMAT]                        *
C     *    WHERE THE UNKNOWN MATRIX IS [QMAT].                          *
C     *                                                                 *
C     *******************************************************************
C
C
C     ------------------------------------------------------------------
C           PARAMETER LIST
C        ========================
C     A      = DIMENSIONLESS HALF LENGTH IN X; (INPUT)
C     AL1    = THERMAL DIFFUSIVITIES RATIO  (INPUT)
C     AVET1  = AVERAGE OF T1 OVER NUMBER OF POINTS CALCULATED
C     AVET2  = AVERAGE OF T2 OVER NUMBER OF POINTS CALCULATED
C     B      = DIMENSIONLESS HALF LENGTH IN Y; (INPUT)
C     C      = MAGNITUDE OF VELOCITY, UNIDIRECTIONAL (INPUT)
C     CX     = CENTER OF HEAT SOURCE IN X (INPUT)
C     CY     = CENTER OF HEAT SOURCE IN Y (INPUT)
C     DX     = DELTA X, STEP SIZE OF X (2A/MA)
C     DY     = DELTA Y, STEP SIZE OF Y (2B/NB)
C     DT     = DELTA T, STEP SIZE OF T (INPUT OR PI/2/W/IDT)
C     ELEMTS = NUMBER OF ELEMENTS FOR CONTACT AREA (NCON*MA*NA)
C     FMAT   = F MATRIX (KNOWN)
C     GIMAT  = G INTEGRAL MATRIX (KNOWN)
C     ICON   = NUMBER OF MULTIPLE CONTACT COUNTER
C     IDT    = NUMBER OF STEP IN 1/4 CYCLE; FOR OSCILLATING CASE (INPUT)
C     J,JJ   = NUMBER OF MULTIPLE CONTACT COUNTER
C     K1     = THERMAL CONDUCTIVITY RATIO (INPUT)
C     LDA    = THE DIMENSION OF GIMAT (CONSTANT)
C     MA     = TOTAL NUMBER OF ELEMENTS PER CONTACT ALONG X (INPUT)
C     MAXPP  = MAX # OF TIME STEP, (IDT*MAXQC, OSCILLATING) (INPUT)
C     MAXQC  = MAX. # OF 1/4 CYCLE (FOR OSCILLATING) (INPUT)
C     M,MM   = NUMBER OF ELEMENTS COUNTER ALONG X
C     NB     = TOTAL NUMBER OF ELEMENTS PER CONTACT ALONG Y (INPUT)
C     N,NN   = NUMBER OF ELEMENTS COUNTER ALONG Y
C     NCON   = # OF CONTACTS (INPUT)
C     PP     = TIME STEP COUNTER
C     Q1     = HEAT FLUX DISTRIBUTED TO BODY 1, STATIONARY REGION (OUTPUT)
C     QMAT   = Q MATRIX (UNKNOWN)
C     QTYPE  = MAGNITUDE OF HEAT FLUX INPUT FOR ZERO VELOCITY CASE (INPUT)
C     S      = CHANGE VARIABLE OF TIME  (TAUP, TAUPP)
C     T1     = DIMENSIONLESS TEMPERATURE RISE OF STATIONARY REGION (OUTPUT)
C     T2     = DIMENSIONLESS TEMPERATURE RISE OF MOVING REGION (OUTPUT)
C     TAUP   = DIMENSIONLESS TIME OF IMPULSE
C     TAUPP  = DIMENSIONLESS TIME OF RESPONSE DUE TO IMPULSE
C     VTYPE  = 1, OSCILLATING
C              2, CONSTANT
C              3, ZERO
C     W      = DIMENSIONLESS FREQUENCE (INPUT)
C     XCEN   = CENTER LOCATION OF CONTACT AREA DURING MOTION
C     XM     = X LOCATION OF IMPULSE OF HEAT FLUX
C     XMM    = X LOCATION OF RESPONSE DUE TO IMPULSE
C     YN     = Y LOCATION OF IMPULSE OF HEAT FLUX
C     YNN    = Y LOCATION OF RESPONSE DUE TO IMPULSE
C
```

```
C     ---------------------------------------------------------------
C
      IMPLICIT REAL*8 (A-H,O-Z)
      REAL*8 K1
      REAL RWKSP (45472)
      INTEGER VTYPE,PP,P,ELEMTS
      DIMENSION Q1(10,10,10,0:410),CX(10), CY(10),XL(20),YL(20),
     >          GIMAT(1000,1000), FMAT(1000), QMAT(1000)
      COMMON /L1/ A,B,NCON, VTYPE, CX,CY
      COMMON /L3/ DX,DY,DZ,DT
      COMMON /L4/ MA, NB
      COMMON /L5/ W,C
      COMMON /L6/ AL1,K1
      COMMON /L7/ QTYPE
      COMMON /L8/ PI
      COMMON /L9/ Q1
      COMMON /WORKSP/ RWKSP
C
      DATA LDA /1000/
C
C
C     ----- SYSTEM SUBROUTINE AND ERROR SET ROUTINE
C
C
      CALL TIMEON
      CALL ERRSET (208,256,-1,0,0)
      CALL ERRSET (209,256,-1,0,0)
      CALL ERRSET (261,256,-1,0,0)
      CALL IWKIN (45472)
C
      WRITE (10,*) 'PROGRAM: FRHMID FORTRAN'
      WRITE (10,*)
      PI = 4.D0 * DATAN(1.D0)
C
C
C     ------- INPUT VELOCITY TYPE ---------
C
C
      CALL VELOCITY (VTYPE, W, C)
C
C
C     ------- INPUT ALL OTHER VALUES ------------
C     ------- MOST DATA PASS THRU COMMON BLOCKS ---
C
      CALL VALUES(MAXPP,IDT)
C
C
C     --------- FOLLOWING DATA IS  FOR IMSL SUBROUTINE LSARG ----
C
C
      ELEMTS = NCON * MA * NB
C
C
C     ------- READ DATA TO CALCULATE THETA.-------
C
C
 10   PRINT *, 'ENTER 1, 2, 3, OR 4 FOR OUTPUT SELECTION'
      PRINT *, '       1)  THETA VS X/A AT Y LOCATION (YL)'
      PRINT *, '       2)  THETA VS Y/B AT X LOCATION (XL)'
      PRINT *, '       3)  THETA AT SPECIFIED LOCATION (XL,YL)'
      PRINT *, '       4)  NONE OF THE ABOVE'
      READ (5,*)  IOUT
      IF ((IOUT .LT. 1) .OR. (IOUT .GT. 4)) GOTO 10
      IF (IOUT .EQ. 3) THEN
 15        PRINT *, 'NUMBER OF POINTS AT WHICH TEMP IS CALCULATED '
           READ (5,*) NOPS
           IF (NOPS .GT. 20) GOTO 15
           DO 20 I = 1,NOPS
                PRINT *, 'ENTER X,Y LOCATIONS'
                READ (5,*) XL(I), YL(I)
 20        CONTINUE
      ELSEIF (IOUT .EQ. 1) THEN
```

```
            PRINT *, 'NUMBER OF Y LOCATIONS OF INTEREST'
            READ (5,*) NOPS
            DO 25 I = 1,NOPS
                 PRINT *, 'ENTER Y LOCATION'
25          READ (5,*) YL(I)
            PRINT *, 'ENTER XMIN,XMAX ,AND # OF POINTS '
            READ(5,*) XMIN,XMAX,IX
            DELTAX=(XMAX-XMIN)/(IX-1)
      ELSEIF (IOUT .EQ. 2) THEN
            PRINT *, 'NUMBER OF X LOCATIONS OF INTEREST'
            READ (5,*) NOPS
            DO 27 I = 1,NOPS
                 PRINT *, 'ENTER X LOCATION'
27          READ (5,*) XL(I)
            PRINT *, 'ENTER YMIN,YMAX ,AND # OF POINTS '
            READ(5,*) YMIN,YMAX,IY
            DELTAY=(YMAX-YMIN)/(IY-1)
      ENDIF
      IF (IOUT .NE. 4 ) THEN
         PRINT *, 'MAXPP =',MAXPP
         PRINT *, 'ENTER FIRST TIME STEP , LAST STEP , AND STEP SIZE '
         READ (5,*) MINPP,MPP,ISTEP
      ENDIF
C
C
C
C     -------- PRINT TITLE HEADING FOR Q1 ----------
C
C
      WRITE (10,1050)
C
C
C     ------- SET UP GIMAT AND FMAT TO SOLVE QMAT ------------
C     ------- CALCULATION FOR FLUX ----------
C
C
      DO 90 PP= 1,MAXPP
         PRINT *,'PP =',PP
         I = 0
         TAUPP = DFLOAT(PP) * DT
      DO 75 JJ = 1, NCON
      DO 75 MM= 1,MA
            XMM = CX(JJ) - A + (DFLOAT(MM)-.5D0) * DX
      DO 75 NN = 1 ,NB
            YNN = CY(JJ) - B + (DFLOAT(NN)-.5D0) * DY
            I = I + 1
            FMAT(I) = 0.D0
            K = 0
            P = PP-1
            TAUP = DFLOAT(P) * DT
         DO 80 J = 1, NCON
         DO 80 M = 1,MA
            XM = CX(J) - A + DFLOAT(M-1) * DX
         DO 80 N = 1 ,NB
            YN = CY(J) - B + DFLOAT(N-1) * DY
            K  = K + 1
            GIMAT(I,K) = GI (XMM,YNN,TAUPP,XM,YN,TAUP)
            FMAT(I)    = FMAT(I) + QS(J,M,N,P) *
     >                    G2I(XMM,YNN,TAUPP,XM,YN,TAUP)
80       CONTINUE

         DO 70 P = PP-2,0,-1
            TAUP = DFLOAT(P) * DT
         DO 70 J = 1, NCON
         DO 70 M = 1,MA
            XM = CX(J) - A + DFLOAT(M-1) * DX
         DO 70 N = 1 ,NB
            YN = CY(J) - B + DFLOAT(N-1) * DY
            FMAT(I)    = FMAT(I) +
     >       QS(J,M,N,P) * G2I(XMM,YNN,TAUPP,XM,YN,TAUP) -
     >       Q1(J,M,N,P) * GI (XMM,YNN,TAUPP,XM,YN,TAUP)
70       CONTINUE
```

```
 75      CONTINUE
C
C
C     CALL IMSL SUBROUTINE TO SOLVE MATRIX ==> [GIMAT] [QMAT] = [FMAT]
C
C
      CALL DLSARG (ELEMTS,GIMAT,LDA,FMAT,1,QMAT)
         I=0
         DO 60 J = 1, NCON
         DO 60 M = 1, MA
         DO 60 N = 1, NB
              I = I + 1
 60      Q1(J,M,N,PP-1) = QMAT(I)
C
C
C     ----------------- PRINT Q1 -----------------
C
C
      CALL OUTQ1 (PP,TAUPP)
      WRITE (10,*)
 90   CONTINUE

      PRINT *,'' FLUX ENDED
C
C
C     ----- SYSTEM SUBROUTINE FOR CPU TIME CHECK
C
C
      CALL TIMECK (NTF)
      CPUTME = NTF/100.D0
      WRITE (10,1000) CPUTME
         WRITE (10,*)
         WRITE (10,*)
         WRITE (10,*)
         WRITE (10,*)
C
C
C     ------- CALCULATION FOR THETA ------------
C     ------- AND AVERAGE THETA FOR NOPS*IX (OR IY) POINTS -----------
C
C
      IF (IOUT .EQ. 3) THEN
         WRITE (10,1300)
         DO 110 PP= MINPP,MPP,ISTEP
                  WRITE(10,*)
                  PRINT *,'PP =',PP
                  TAUPP = DFLOAT(PP) * DT
         DO 110 I = 1,NOPS
                  YNN = YL(I)
                  XMM = XL(I)
                  CALL THETA1(PP,XMM,YNN,TAUPP,T1)
                  CALL THETA2(PP,XMM,YNN,TAUPP,T2)
                  WRITE (10, 1400) PP,TAUPP,XMM,YNN,T1,T2
 110     CONTINUE
      ELSEIF (IOUT .EQ. 1) THEN
         WRITE (10,1200)
         DO 105 PP= MINPP,MPP,ISTEP
                  PRINT *,'PP =',PP
                  WRITE (10,*)
                  TAUPP = DFLOAT(PP) * DT
                  AVET1 = 0.D0
                  AVET2 = 0.D0
         DO 100 I = 1,NOPS
                  YNN = YL(I)
         DO 100 MX = 1,IX
                  XMM = XMIN+(MX-1)*DELTAX
                  CALL THETA1(PP,XMM,YNN,TAUPP,T1)
                  CALL THETA2(PP,XMM,YNN,TAUPP,T2)
                  WRITE (10, 1100) PP,TAUPP,XMM/A,YNN/B,T1,T2
                  AVET1 = T1+AVET1
                  AVET2 = T2+AVET2
 100     CONTINUE
```

```
          WRITE (10,1500) TAUPP,AVET1/(NOPS*IX), AVET2/(NOPS*IX)
 105      CONTINUE
      ELSEIF (IOUT .EQ. 2) THEN
         WRITE (10,1200)
         DO 205 PP= MINPP,MPP,ISTEP
                  PRINT *,'PP =',PP
                  WRITE (10,*)
                  TAUPP = DFLOAT(PP) * DT
                  AVET1 = 0.D0
                  AVET2 = 0.D0
         DO 200 I = 1,NOPS
                  XMM = XL(I)
         DO 200 MY = 1,IY
                  YNN = YMIN+(MY-1)*DELTAY
                  CALL THETA1(PP,XMM,YNN,TAUPP,T1)
                  CALL THETA2(PP,XMM,YNN,TAUPP,T2)
                  WRITE (10, 1100) PP,TAUPP,XMM/A,YNN/B,T1,T2
                  AVET1 = T1+AVET1
                  AVET2 = T2+AVET2
 200      CONTINUE
          WRITE (10,1500) TAUPP,AVET1/(NOPS*IY), AVET2/(NOPS*IY)
 205      CONTINUE
      ENDIF


      CALL TIMECK (NTF)
      CPUTME = NTF/100.D0
      WRITE (10,1000) CPUTME
      WRITE ( 6,1000) CPUTME
      STOP
C
C
C     ----- FORMAT STATEMENT
C
C
 1000 FORMAT (9X,' CPU TIME  = ',F8.2, ' SECONDS')
 1050 FORMAT (/,4X,'PP',3X,'NCON',3X,'MM',3X,'NN',4X,'TAU',
     >          5X,'X',7X,'Y',11X,'QS',12X,'Q1/QS',9X,'Q2/QS',
     >          9X,'THETA')

 1100 FORMAT (1X,I5,1X,3F8.3,2X,2F14.7)
 1200 FORMAT (1H1,4X,'PP',3X,'TAU',5X,'X/A',7X,'Y/B',
     >          9X,'THETA1',9X,'THETA2')
 1300 FORMAT (///,4X,'PP',3X,'TAU',5X,'X',5X,'Y',
     >         11X,'THETA1',9X,'THETA2')
 1400 FORMAT (1X,I5,1X,3F8.3,2X,2F14.7)
 1500 FORMAT (1X,'TAU = ',F8.3,3X,'AVERAGE THETA1 = ',F12.7,
     >                        1X,'AVERAGE THETA2 = ',F12.7)
      END
```

SUBROUTINE THETA1

```
C     ******************************************************************

      SUBROUTINE THETA1 (PP,XMM,YNN,TAUPP,T1)

C     //////////////////////////////////////////////////////////////////
C
C     CALCULATE THE DIMENSIONLESS TEMPERATURE (THETA) FOR STATIONARY
C     REGION
C
C     //////////////////////////////////////////////////////////////////

      IMPLICIT REAL*8 (A-H,O-Z)
      REAL*8 K1
      INTEGER VTYPE,PP,P
      DIMENSION Q1(10,10,10,0:410),CX(10), CY(10)
      COMMON /L1/ A,B,NCON, VTYPE, CX,CY
```

```
      COMMON /L3/ DX,DY,DZ,DT
      COMMON /L4/ MA, NB
      COMMON /L6/ AL1,K1
      COMMON /L9/ Q1

      T1 = 0.D0

      DO 10 P = 0, PP-1
         TAUP = DFLOAT(P) * DT
      DO 10 J = 1, NCON
      DO 10 M = 1, MA
         XM = CX(J) - A + DFLOAT(M-1) * DX
      DO 10 N = 1, NB
         YN = CY(J) - B + DFLOAT(N-1) * DY
C
C
C        -------SINCE P START WITH ZERO ==> Q1(J,M,N,P) IS CORRECT.
C
C
 10      T1 = T1 + Q1(J,M,N,P) * G1I(XMM,YNN,TAUPP,XM,YN,TAUP)

      T1 = T1 * 2.D0 * AL1/K1

      RETURN
      END
```

SUBROUTINE THETA2

```
C     ***********************************************************************

      SUBROUTINE THETA2 (PP,XMM,YNN,TAUPP,T2)

C     ///////////////////////////////////////////////////////////////////////
C
C     CALCULATE THE DIMENSIONLESS TEMPERATURE (THETA) FOR MOVING
C     REGION
C
C     ///////////////////////////////////////////////////////////////////////

      IMPLICIT REAL*8 (A-H,O-Z)
      REAL*8 K1
      INTEGER VTYPE,PP,P
      DIMENSION Q1(10,10,10,0:410),CX(10), CY(10)
      COMMON /L1/ A,B,NCON, VTYPE, CX,CY
      COMMON /L3/ DX,DY,DZ,DT
      COMMON /L4/ MA, NB
      COMMON /L9/ Q1

      T2 = 0.D0

      DO 10 P = 0, PP-1
         TAUP = DFLOAT(P) * DT
      DO 10 J = 1, NCON
      DO 10 M = 1, MA
         XM = CX(J) - A + DFLOAT(M-1) * DX
      DO 10 N = 1, NB
         YN = CY(J) - B + DFLOAT(N-1) * DY
C
C
C        -------SINCE P START WITH ZERO ==> Q1(J,M,N,P) IS CORRECT.
C
C
 10      T2 = T2 + (QS(J,M,N,P) - Q1(J,M,N,P) ) *
     >             G2I(XMM,YNN,TAUPP,XM,YN,TAUP)

      T2 = T2 * 2.D0

      RETURN
```

```
      END
```

FUNCTION GI

```
C     ***********************************************************************

      DOUBLE PRECISION FUNCTION GI (XMM,YNN,TAUPP,XM,YN,TAUP)

C     ///////////////////////////////////////////////////////////////////////
C
C     USING SIMPSON'S RULE FOR TIME (NEW VARIABLE) INTEGRATION
C
C     ///////////////////////////////////////////////////////////////////////

      IMPLICIT REAL*8 (A-H,O-Z)
      COMMON /L3/ DX,DY,DZ,DT

      S1  = 2.DO * DSQRT(TAUPP-TAUP)
      XC1 = XC(TAUPP, TAUP)
       TAUP1 = TAUP + DT
      S2  = 2.DO * DSQRT(TAUPP-TAUP1)
      XC2 = XC(TAUPP, TAUP1)
      S3  = (S1 + S2 ) / 2.DO
       TAUP2 = (TAUP + TAUP1) / 2.DO
      XC3 = XC(TAUPP, TAUP2)

      GI = (S2-S1) / 6.DO * (GFINT(XMM,YNN,XM,YN,XC1,S1) +
     >                 4.DO *  GFINT(XMM,YNN,XM,YN,XC3,S3) +
     >                         GFINT(XMM,YNN,XM,YN,XC2,S2) )

      RETURN
      END
```

FUNCTION GFINT

```
C     ***********************************************************************

      DOUBLE PRECISION FUNCTION GFINT (XMM,YNN,XM,YN,XCEN,S)

C     ///////////////////////////////////////////////////////////////////////
C
C     INTEGRAL OF GREEN'S FUNCTION
C
C     ///////////////////////////////////////////////////////////////////////
C
C     USING SIMPSON'S RULE FOR TIME (NEW VARIABLE) INTEGRATION
C
C     ///////////////////////////////////////////////////////////////////////

      IMPLICIT REAL*8 (A-H,O-Z)
      REAL*8 K1
      INTEGER PP, P
      COMMON /L3/ DX,DY,DZ,DT
      COMMON /L6/ AL1,K1
      COMMON /L8/ PI

      GFINT = 0.DO
      S1    = DSQRT(AL1) * S
      X11   = (XMM -XM -DX)
      X12   = (XMM -XM)
      Y11   = (YNN -YN -DY)
      Y12   = (YNN -YN)
      X21   = X11-XCEN
      X22   = X12-XCEN
```

```
      IF (S .NE. 0.D0) THEN

      GFINT = DSQRT(AL1) / K1 * (DERF(X11/S1) -DERF(X12/S1))
     >                        * (DERF(Y11/S1) -DERF(Y12/S1))
      GFINT = -0.125D0/DSQRT(PI)*(GFINT + (DERF(X21/S) -DERF(X22/S))
     >                                  * (DERF(Y11/S) -DERF(Y12/S)) )

      ELSE

       ERFX11 = DSIGN (1.D0,X11)
       IF (DABS(X11) .LE. 0.1D-6) THEN
       ERFX11 =0.D0
       ENDIF
       ERFX12 = DSIGN (1.D0,X12)
       IF (DABS(X12) .LE. 0.1D-6) THEN
       ERFX12 =0.D0
       ENDIF

       ERFY11 = DSIGN (1.D0,Y11)
       IF (DABS(Y11) .LE. 0.1D-6) THEN
       ERFY11 =0.D0
       ENDIF
       ERFY12 = DSIGN (1.D0,Y12)
       IF (DABS(Y12) .LE. 0.1D-6) THEN
       ERFY12 =0.D0
       ENDIF

       ERFX21 = DSIGN (1.D0,X21)
       IF (DABS(X21) .LE. 0.1D-6) THEN
       ERFX21 =0.D0
       ENDIF
       ERFX22 = DSIGN (1.D0,X22)
       IF (DABS(X22) .LE. 0.1D-6) THEN
       ERFX22 =0.D0
       ENDIF

      GFINT = DSQRT(AL1) / K1 * (ERFX11 - ERFX12) * (ERFY11 - ERFY12)
      GFINT = -0.125D0/DSQRT(PI)*(GFINT + (ERFX21 - ERFX22)
     >                                  * (ERFY11 - ERFY12) )

      ENDIF
      RETURN
      END
```

FUNCTION G1I

```
C     ***********************************************************************

      DOUBLE PRECISION FUNCTION G1I (XMM,YNN,TAUPP,XM,YN,TAUP)

C     ///////////////////////////////////////////////////////////////
C
C     USING SIMPSON'S RULE FOR TIME (NEW VARIABLE) INTEGRATION
C
C     ///////////////////////////////////////////////////////////////

      IMPLICIT REAL*8 (A-H,O-Z)
      COMMON /L3/ DX,DY,DZ,DT

      S1  = 2.D0 * DSQRT(TAUPP-TAUP)
      XC1 = XC(TAUPP, TAUP)
           TAUP1 = TAUP + DT
      S2  = 2.D0 * DSQRT(TAUPP-TAUP1)
      XC2 = XC(TAUPP, TAUP1)
      S3  = (S1 + S2 ) / 2.D0
           TAUP2 = (TAUP + TAUP1) / 2.D0
      XC3 = XC(TAUPP, TAUP2)
```

```
      G1I = (S2-S1) / 6.D0 * (GF1INT(XMM,YNN,XM,YN,XC1,S1) +
     >                  4.D0 *  GF1INT(XMM,YNN,XM,YN,XC3,S3) +
     >                          GF1INT(XMM,YNN,XM,YN,XC2,S2) )

      RETURN
      END
```

FUNCTION GF1INT

```
C     ***********************************************************************

      DOUBLE PRECISION FUNCTION GF1INT (XMM,YNN,XM,YN,XCEN,S)

C     ///////////////////////////////////////////////////////////////////////
C
C     INTEGRAL OF GREEN'S FUNCTION (GF1) OF STATIONARY REGION
C
C     ///////////////////////////////////////////////////////////////////////

      IMPLICIT REAL*8 (A-H,O-Z)
      REAL*8 K1
      INTEGER PP, P
      COMMON /L3/ DX,DY,DZ,DT
      COMMON /L6/ AL1,K1
      COMMON /L8/ PI

      GF1NT = 0.D0
      S1    = DSQRT(AL1) * S
      X11   = (XMM -XM -DX)
      X12   = (XMM -XM)
      Y11   = (YNN -YN -DY)
      Y12   = (YNN -YN)

      IF (S .NE. 0.D0) THEN

      GF1INT =  (DERF(X11/S1) -DERF(X12/S1))
     >        * (DERF(Y11/S1) -DERF(Y12/S1))
      GF1INT = -0.125D0/DSQRT(PI*AL1) * GF1INT

      ELSE

       ERFX11 = DSIGN (1.D0,X11)
       IF (DABS(X11) .LE. 0.1D-6) THEN
       ERFX11 =0.D0
       ENDIF
       ERFX12 = DSIGN (1.D0,X12)
       IF (DABS(X12) .LE. 0.1D-6) THEN
       ERFX12 =0.D0
       ENDIF

       ERFY11 = DSIGN (1.D0,Y11)
       IF (DABS(Y11) .LE. 0.1D-6) THEN
       ERFY11 =0.D0
       ENDIF
       ERFY12 = DSIGN (1.D0,Y12)
       IF (DABS(Y12) .LE. 0.1D-6) THEN
       ERFY12 =0.D0
       ENDIF

      GF1INT = (ERFX11 - ERFX12) * (ERFY11 - ERFY12)
      GF1INT = -0.125D0/DSQRT(PI*AL1)* GF1INT

      ENDIF
      RETURN
      END
```

FUNCTION G2I

```
C     ***********************************************************************

      DOUBLE PRECISION FUNCTION G2I (XMM,YNN,TAUPP,XM,YN,TAUP)

C     ///////////////////////////////////////////////////////////////////////
C
C     USING SIMPSON'S RULE FOR TIME (NEW VARIABLE) INTEGRATION
C
C     ///////////////////////////////////////////////////////////////////////

      IMPLICIT REAL*8 (A-H,O-Z)
      COMMON /L3/ DX,DY,DZ,DT

      S1  = 2.DO * DSQRT(TAUPP-TAUP)
      XC1 = XC(TAUPP, TAUP)
      TAUP1 = TAUP + DT
      S2  = 2.DO * DSQRT(TAUPP-TAUP1)
      XC2 = XC(TAUPP, TAUP1)
      S3  = (S1 + S2 ) / 2.DO
      TAUP2 = (TAUP + TAUP1) / 2.DO
      XC3 = XC(TAUPP, TAUP2)

      G2I = (S2-S1) / 6.DO * (GF2INT(XMM,YNN,XM,YN,XC1,S1) +
     >                 4.DO *  GF2INT(XMM,YNN,XM,YN,XC3,S3) +
     >                         GF2INT(XMM,YNN,XM,YN,XC2,S2) )

      RETURN
      END
```

FUNCTION GF2INT

```
C     ***********************************************************************

      DOUBLE PRECISION FUNCTION GF2INT (XMM,YNN,XM,YN,XCEN,S)

C     ///////////////////////////////////////////////////////////////////////
C
C     INTEGRAL OF GREEN'S FUNCTION (GF2) OF MOVING REGION
C
C     ///////////////////////////////////////////////////////////////////////

      IMPLICIT REAL*8 (A-H,O-Z)
      REAL*8 K1
      INTEGER PP, P
      COMMON /L3/ DX,DY,DZ,DT
      COMMON /L8/ PI

      GF2INT = 0.DO
      X11   = (XMM -XM -DX) - XCEN
      X12   = (XMM -XM) - XCEN
      Y11   = (YNN -YN -DY)
      Y12   = (YNN -YN)

      IF (S .NE. 0.DO) THEN

      GF2INT = -0.125DO/DSQRT(PI)*((DERF(X11/S) -DERF(X12/S))
     >                           * (DERF(Y11/S) -DERF(Y12/S)) )

      ELSE

       ERFX11 = DSIGN (1.DO,X11)
       IF (DABS(X11) .LE. 0.1D-6) THEN
       ERFX11 =0.DO
```

```
      ENDIF
      ERFX12 = DSIGN (1.D0,X12)
      IF (DABS(X12) .LE. 0.1D-6) THEN
      ERFX12 =0.D0
      ENDIF

      ERFY11 = DSIGN (1.D0,Y11)
      IF (DABS(Y11) .LE. 0.1D-6) THEN
      ERFY11 =0.D0
      ENDIF
      ERFY12 = DSIGN (1.D0,Y12)
      IF (DABS(Y12) .LE. 0.1D-6) THEN
      ERFY12 =0.D0
      ENDIF

     GF2INT = -0.125D0/DSQRT(PI)*((ERFX11 - ERFX12)
     >                           * (ERFY11 - ERFY12) )

      ENDIF
      RETURN
      END
```

FUNCTION XC

```
C     ***********************************************************************

      DOUBLE PRECISION FUNCTION  XC (TAUPP, TAUP)

C     ///////////////////////////////////////////////////////////////////////
C
C     THIS FUNCTION IS TO CALCULATE THE CENTER OF HEAT SOURCE
C
C     ///////////////////////////////////////////////////////////////////////

      IMPLICIT REAL*8 (A-H,O-Z)
      INTEGER VTYPE
      DIMENSION CX(10),CY(10)
      COMMON /L1/ A,B,NCON, VTYPE, CX,CY
      COMMON /L3/ DX,DY,DZ,DT
      COMMON /L5/ W,C
C
      XC =0.D0
C
C
C     VTYPE EQUAL TO 1, IT IS OSCILLATING HEAT SOURCE(S)
C
C
      IF (VTYPE .EQ. 1) THEN
         XC = (DSIN(W*TAUPP) - DSIN(W*TAUP)) / W
C
C
C     ------- VTYPE EQUAL TO 2, IT IS CONSTANT MOVING HEAT SOURCE(S) --
C
C
         ELSE IF (VTYPE .EQ. 2) THEN
              XC  = C * (TAUPP-TAUP)
              ELSE
                   XC = 0.D0
      ENDIF
      RETURN
      END
```

FUNCTION QS

```
C     ****************************************************************
      DOUBLE PRECISION FUNCTION QS (ICON,M,N,P)
C     ////////////////////////////////////////////////////////////////
C
C     THIS FUNCTION IS TO CALCULATE THE TOTAL HEAT FLUX
C
C     ////////////////////////////////////////////////////////////////
      IMPLICIT REAL*8 (A-H,O-Z)
      REAL*8 KC
      INTEGER VTYPE,PP,P
      DIMENSION CX(10),CY(10)
C
      COMMON /L1/ A,B,NCON, VTYPE, CX,CY
      COMMON /L3/ DX,DY,DZ,DT
      COMMON /L5/ W,C
      COMMON /L7/ QTYPE
      COMMON /L8/ PI
C
      IF (VTYPE .EQ. 1) THEN
            QS = DABS(DCOS(W*DFLOAT(2*P+1)*DT/2.D0))
         ELSE IF (VTYPE .EQ. 2) THEN
            QS = DABS(C)
         ELSE
            QS = QTYPE
      ENDIF
      RETURN
      END
```

SUBROUTINE VALUES

```
C     ****************************************************************
C
      SUBROUTINE VALUES (MAXPP,IDT)
C     ////////////////////////////////////////////////////////////////
C
C     THIS ROUTINE IS TO READ IN ALL THE VALUE NEEDED TO RUN THIS
C     PROGRAM.
C
C     ////////////////////////////////////////////////////////////////
      IMPLICIT REAL*8 (A-H,O-Z)
      REAL*8 K1
      INTEGER VTYPE,PP
      DIMENSION CX(10), CY(10)
      COMMON /L1/ A,B,NCON, VTYPE, CX,CY
      COMMON /L3/ DX,DY,DZ,DT
      COMMON /L4/ MA, NB
      COMMON /L5/ W,C
      COMMON /L6/ AL1,K1
      COMMON /L8/ PI
C
C
C     ------- READ IN DATA ---------
C
C
C
C
C
```

```
C      -------- INPUT AL1 & K1 FOR DIMENSIONLESS PROPERTIES -------
C
C
       PRINT *,'ENTER DIMENSIONLESS AL1'
       READ (5,*) AL1
       WRITE (10,120) AL1
       PRINT *,'ENTER DIMENSIONLESS K1'
       READ (5,*) K1
       WRITE (10,130) K1
C
C
C      -------- INPUT A & B FOR DIMENSIONLESS CONTACT ------
C
C
       PRINT *,'ENTER HALF LENGTH OF CONTACT IN X-DIRECTION, A'
       READ (5,*) A
       WRITE (10,111) A
C
C
       PRINT *,'ENTER HALF LENGTH OF CONTACT IN Y-DIRECTION, B'
       READ (5,*) B
       WRITE (10,112) B
C
C
C      -------- THE AMPLITUDE RATIO (Xm/a)----------
C
C
       AMPR = 1.D0 / W/ A
       WRITE (10, 113) AMPR
C
C
C      -------- NUMBER OF HEAT SOURCE(S) ----------
C
C
 20    PRINT *,' NUMBER OF CONTACTS (1-10)'
       READ (5,*) NCON
       IF ((NCON .GT. 10) .OR. (NCON .LT. 1)) GOTO 20
       WRITE (10,110)  NCON
C
C
       WRITE (10,*) 'CENTER LOCATION OF HEAT SOURCE(S)'
       WRITE (10,*) '         X           Y '
C
C
C      -------- INPUT CENTER OF HEAT SOURCE ----------
C
C
       DO 100 I=1,NCON
          PRINT *,'CENTER LOCATION OF HEAT SOURCE IN X, AND Y'
          READ (5,*) CX(I), CY(I)
          WRITE (10,500) CX(I), CY(I)
 100   CONTINUE
C
C
C      -------- INPUT SPACE STEPS (DX AND DY) AND IDT (DT) --------
C
C
       PRINT *,'NUMBER OF ELEMENT(S) PER CONTACT IN X, MA'
       PRINT *,'NUMBER OF ELEMENT(S) PER CONTACT IN Y, NB'
       READ (5,*) MA,NB
       WRITE (10,150) MA,NB
C
C      -------- CALCULATE DX, AND DY
C
       DX = 2.D0*A/DFLOAT(MA)
       DY = 2.D0*B/DFLOAT(NB)
       WRITE (10,200) DX,DY
C
C
C
       IF (VTYPE .EQ. 1) THEN
C
```

```
C
C       -------- OSCILLATING VELOCITY ----------
C
C
            PRINT *, ' ENTER IDT'
            READ (5,*) IDT
            DT = PI/2.D0/W/DFLOAT (IDT)
            WRITE (10,220) DT, IDT
C
C
C       -------- MAXIMUN 1/4 CYCLE ----------
C
C
            PRINT *,'ENTER =>  MAX. 1/4 CYCLE'
            READ (5,*) MAXQC
            WRITE (10,210) MAXQC
            MAXPP = MAXQC * IDT
        ELSE
C
C
C       -------- CONSTANT VELOCITY ----------
C
C
            PRINT *, ' ENTER  DT'
            READ (5,*)  DT
            WRITE (10,230) DT
            IDT =  1.D0
C
C       ------ MAXPP == MAX. # OF TIME STEP ------
            PRINT *,'ENTER =>  MAX. PP'
            READ (5,*) MAXPP
            WRITE (10,215) MAXPP
        ENDIF
C
        PRINT *, 'DT=',DT
C
C
C       -------- FORMAT STATEMENTS -----------
C
C
  110   FORMAT (/,1X,'NUMBER OF CONTACTS  = ', I5)
  111   FORMAT(1X,'HALF LENGTH OF CONTACT IN X-DIRECTION, A=',F12.5)
  112   FORMAT(1X,'HALF LENGTH OF CONTACT IN Y-DIRECTION, B=',F12.5)
  113   FORMAT(/,1X,'AMPLITUDE RATIO = 1 / (OMEGA * A) = Xm / a = ',F12.5)
  120   FORMAT(1X,'RATIO OF THERMAL DIFFUSIVITIES,  AL1 = ',F12.5)
  130   FORMAT(1X,'RATIO OF THERMAL CONDUCTIVITIES, K1  = ',F12.5)
  150   FORMAT (/,1X,'NUMBER ELEMENT(S) IN X=', I4,';  Y=', I4)
  200   FORMAT (/,1X,'DX = ',F12.7,5X,'DY = ',F12.7)
  210   FORMAT (1X, 'MAX. 1/4 CYCLE =',I4,/)
  215   FORMAT (1X, 'MAX. PP =',I4,/)
  220   FORMAT (1X,'DT = ',F19.10,5X,'IDT = ',I4 ,/)
  230   FORMAT (1X,'DT = ',F19.10,5X,/)
  500   FORMAT (3X, F9.3,3X,F9.3 )
        RETURN
        END
```

SUBROUTINE VELOCITY

```
C       ***********************************************************************

        SUBROUTINE  VELOCITY (VTYPE,W,C)

C       ///////////////////////////////////////////////////////////////
C
C       THIS SUBROUTINE IS FOR THE USER TO SELECT THE VELOCITY TYPE:
C       1) OSCILLATING
C       2) CONSTANT
C       3) STATIONARY.
```

```
C
C     ////////////////////////////////////////////////////////////////
      IMPLICIT REAL*8 (A-H,O-Z)
      INTEGER VTYPE

      COMMON /L7/ QTYPE
      COMMON /L8/ PI

      PI = 4.DO * DATAN(1.DO)
      WRITE (10,1200)
      WRITE (10,*) 'RECTANGULAR CONTACT
      WRITE (10,*)
C
C
      PRINT *,'ENTER VELOCITY TYPE:'
      PRINT *,'     1) OSCILLATING VELOCITY'
      PRINT *,'     2) CONSTANT VELOCITY, C'
      PRINT *,'     3) STATIONARY '
      READ (5,*) VTYPE
C
C
      IF (VTYPE .EQ. 1) THEN
C
C
C
C     -------- FOR OSCILLATING VELOCITY -----------
C
C
         PRINT *,'THE FREQUENCY, (W)=N*PI, ENTER N '
         READ (5,*) W
         W = W*PI
         WRITE (10,*) 'OSCILLATING VELOCITY'
         WRITE (10,1000)   W
      ELSE IF (VTYPE .EQ. 2) THEN
C
C
C     -------- FOR CONSTANT VELOCITY -------------
C
C
            PRINT *,'INPUT VALUE FOR C'
            READ (5,*) C
            WRITE (10,1100) C
      ELSE IF(VTYPE .EQ. 3) THEN
C
C
C     ------- STATIONARY -----------
C
C
            WRITE (10,*) 'VELOCITY = 0.000'
            PRINT *,'INPUT VALUE FOR QS'
            READ (5,*) QTYPE
      ENDIF
 1000 FORMAT (1X,'THE FREQUENCY, OMEGA =',F20.14)
 1100 FORMAT (1X,'CONSTANT VELOCITY, V =',F12.5)
 1200 FORMAT (1X,'SOLUTIONS FOR FRICTIONAL HEATING BETWEEN 2 ',
     >           'SEMI-INFINITE REGIONS.',/,
     >           ' USING MIDPOINT RULE IN TIME AND SPACE.')
      RETURN
      END
```

SUBROUTINE OUTQ1

```
C     ****************************************************************

      SUBROUTINE OUTQ1 (PP,TAUPP)
```

```
C     ////////////////////////////////////////////////////////////////
C
C     PRINT Q1
C
C     ////////////////////////////////////////////////////////////////

      IMPLICIT REAL*8 (A-H,O-Z)
      DIMENSION Q1(10,10,10,0:410),CX(10),CY(10)
      INTEGER PP, VTYPE

      COMMON /L1/ A,B,NCON, VTYPE, CX,CY
      COMMON /L3/ DX,DY,DZ,DT
      COMMON /L4/ MA, NB
      COMMON /L9/ Q1

      SUMQ2 = 0.D0
      SUMQS = 0.D0
      TOTALQ = QS(ICON,I,J,PP-1)
      DTIME = TAUPP - DT/2.D0
      T = TOTALQ
      IF (TOTALQ .LE. 0.1D-10) THEN
C        ---------- WHEN TOTALQ = 0.D0 THEN Q1 & Q2 SHOULD BE ZERO ---
         T=1.D0
      ENDIF
      DO 20 ICON=1,NCON
      SUMT2 = 0.D0
      DO 10 J =  1 ,NB
               YNN = CY(ICON) - B + (DFLOAT(J)-.5D0) * DY
      DO 10 I =  1 ,MA
               XMM = CX(ICON) - A + (DFLOAT(I)-.5D0) * DX
         CALL THETA2(PP,XMM,YNN,TAUPP,T2)
         Q2 = (TOTALQ-Q1(ICON,I,J,PP-1))
C
C
C     ------- CALCULATE T(MEAN) AND Q2(TOTAL) ----------
C
C

         SUMT2 = SUMT2+T2
         SUMQ2 = SUMQ2+Q2
         SUMQS = SUMQS+T

         Q2 = Q2/T
         WRITE (10, 100) PP,ICON,I,J,DTIME,XMM,YNN,TOTALQ,
     >   Q1(ICON,I,J,PP-1)/T,Q2,T2
 10   CONTINUE
      T2M = SUMT2 / DFLOAT(MA*NB)
      WRITE (10, 110) T2M
 20   CONTINUE
      Q2M = SUMQ2/SUMQS
      WRITE (10,120) Q2M
 100  FORMAT (1X,4I5,1X,3F8.3,2X,5F14.7)
 110  FORMAT (1X,'THETA2 MEAN = ',F14.7)
 120  FORMAT (1X,'Q2/QS TOTAL = ',F14.7)
      RETURN
      END
```

VITA

The author is the first of seven Children of Tong Soon and Lee Moi Lim Foo and was born on January 21, 1965, in Muar, Johor, Malaysia. He went to Kuala Lumpur, Malaysia for English intensive study after completing his high school education in his home town. He began to pursue his Bachelor of Science degree in Mechanical Engineering in August, 1984 at the University of Southwestern Louisiana, Lafayette, Louisiana. After receiving his bachelor's degree in May of 1988, he decided to further his education at VPI & SU pursuing his Master of Science degree, of which this thesis is a result.

Foo, Ser Jee